Supporting Information

Site selective template-directed synthesis of antibody Fc conjugates with concomitant ligand release

Viktoriia Postupalenko,[a] Léo Marx,[b] Mathilde Pantin[b], David Viertl,[c,d] Nadège Gsponer,[a] Natalia Gasilova,[e] Margret Schottelius,[c] Frédéric Lévy,[f] Patrick Garrouste,[b] Jean-Manuel Segura and Origène Nyanguile[a]*

[a]Institute of Life Technologies, HES-SO Valais-Wallis, Rue de l'Industrie 23, CH-1950 Sion, Switzerland. [b]Debiopharm Research & Manufacturing SA, Campus "après-demain", Rue du Levant 146, 1920 Martigny, Switzerland. [c]Department of Nuclear Medicine and Molecular Imaging, Lausanne University Hospital, CH-1011 Lausanne, Switzerland. [d]In Vivo Imaging Facility, Department of Research and Training, University of Lausanne, CH-1011 Lausanne. [e]EPFL Valais Wallis, MSEAP, ISIC-GE-VS, rue de l'Industrie 17, 1951 Sion, Switzerland. [f]Debiopharm International SA, Forum "après-demain", Chemin Messidor 5-7, Case postale 5911, 1002 Lausanne, Switzerland.

Table des matières

Abbreviations

ACN: acetonitrile

AF647-NHS: 2-((1E,3E)-5-((E)-3,3-dimethyl-5-sulfonato-1-(3-sulfonatopropyl)indolin-2-ylidene)penta-1,3-dien-1-yl)-3-(5-((2,5-dioxopyrrolidin-1-yl)oxy)-5-oxopentyl)-3-methyl-1-(3-sulfonatopropyl)-3H-indol-1-ium-5-sulfonate

BCN: bicyclo[6.1.0]nonyne

Boc: tert-butyloxycarbonyl

DBCO: dibenzocyclooctyne

DCM: dichloromethane

DFO: desferrioxamine B

DIC: N,N'-diisopropylcarbodiimide

DIEA: N,N-diisopropylethylamine

DMF: dimethyl formamide

DMSO: dimethyl sulfoxide

DOTA: 1,4,7,10-Tetraazacyclododecane-1,4,7,10-tetraacetic acid

FITC: fluorescein isothiocyanate

HATU: 1-[Bis(dimethylamino)methylene]-1H-1,2,3-triazolo[4,5-b]pyridinium 3-oxide hexafluorophosphate

HPLC: high-performance liquid chromatography

HRMS: high resolution mass spectrometry

HCD: higher energy collision-induced dissociation

LC-FTMS: liquid chromatography Orbitrap Fourier transform mass spectrometry

LC-FT-MS/MS: liquid chromatography Orbitrap Fourier transform tandem mass spectrometry

NCE: normalized collision energy

NHS: N-hydroxysuccinimide

NMR: nuclear magnetic resonance

NODAGA: α^1-[3-[(2,5-Dioxo-1-pyrrolidinyl)oxy]-3-oxopropyl]hexahydro-1H-1,4,7-triazonine-1,4,7-triacetic acidPBS: phosphate-buffered saline

PEG: polyethylene glycol

pH: potential for hydrogen

p-SCN-Bn-TCMC: 2-[4,7,10-tris(2-amino-2-oxoethyl)-6-[(4-isothiocyanatophenyl)methyl]-1,4,7,10-tetrazacyclododec-1-yl]acetamide

p-SCN-Bn-CHX-A"-DTPA: [(R)-2-Amino-3-(4-isothiocyanatophenyl)propyl]-trans-(S,S)-cyclohexane-1,2-diamine-pentaacetic acid

rt: room temperature

SMCC-DM1: N2'-deacetyl-N2'-[3-[[1-[[4-[[(2,5-dioxo-1-pyrrolidinyl)oxy]carbonyl]cyclohexyl]methyl]-2,5-dioxo-3-pyrrolidinyl]thio]-1-oxopropyl]-maytansine

SPDB-DM4: N2′-deacetyl-N2′-[4-[[4-[(2,5-dioxo-1-pyrrolidinyl)oxy]-4-oxobutyl]dithio]-4-methyl-1-oxopentyl]-maytansine

SPPS: solid-phase peptide synthesis

TCEP: tris (2-carboxyethyl) phosphine

TCO-NHS: (E)-Cyclooct-4-enyl 2,5-dioxopyrrolidin-1-yl carbonate

TFA: trifluoroacetic acid

TIS: triisopropylsilane

Tz-PEG_5-NHS ester: 2,5-Dioxo-1-pyrrolidinyl 19-oxo-21-[4-(1,2,4,5-tetrazin-3-yl)phenyl]-4,7,10,13,16-pentaoxa-20-azaheneicosanoate

UPLC: ultra-performance liquid chromatography

UV: ultraviolet

Reagents and Solvents

Fmoc-protected amino acids, N,N-diisopropylcarbodiimide (DIC), OxymaPure®, piperazine and Fmoc-Rink Amide AM resin were purchased from Merck KGaA (Darmstadt, Germany). Solvents for synthesis, deprotection reagents, and cleavage reagents used were of synthesis grade and purchased from Merck or Fisher Scientific AG (Reinach, Suisse). Amino acids were purchased from Bachem AG (Bubendorf, Switzerland), Merck KGaA and Aapptec (Louisville, U.S.A.). Solvents and other chemicals used for high-performance liquid chromatography (HPLC) and ultra-performance liquid chromatography mass spectrometry (UPLC-MS) were of HPLC reagent grade and purchased from Macherey-Nagel (Düren, Switzerland).

Fc-III peptide and fluorescently labeled Fc-III-FAM peptide were purchased from AmbioPharm (North Augusta, USA) and Genscript (Piscataway, NJ, USA), respectively. The DOTA, and fluorescein-carbonate derivatives were synthesized by Genochem (Grasse, France). The GingisKHAN™ and FabRICATOR™ proteases were purchased from Genovis (Lund, Sweden), EndoS protease was purchased from BioConcept (Allschwil, Switzerland). PEG linkers were purchased from BroadPharm (San Diego, U.S.A.). Herceptin® (trastuzumab), Rituxan® (rituximab) and Tecentriq® (atezolizumab) were purchased from Roche (Switzerland).Vertibix® (panitumumab) was purchased from Amgen. Keytruda® (pembrolizumab) was purchased from MSD Merck Sharp & Dohme.

T-DM1 was purchased from Roche. Vedotin was purchased from Enovation Chemicals. Trastuzumab-Vedotin was prepared using similar protocol as for ADCETRIS®.

General Experimental Details

UPLC-MS

Reactions were monitored by liquid chromatography-mass spectrometry (LC-MS). LC-MS was carried out by Reversed Phase-UPLC MS (Agilent InfinityLab LC/MSD XT) on a Kinetex 1.7 µm XB-C18 100 Å, LC Column 50 x 2.1 mm column (Phenomenex Helvetia) using a mixture of solvent B (acetonitrile with 0.1% TFA) and solvent A (water with 0.1% TFA), 2%–98% gradient, at a flow rate of 0.617 mL/min for 4 min. The peptide signal was monitored at 214 nm. The peptide purity stated in the following sections was determined by integration of the area under the curves of each peak observed in the chromatogram unless otherwise stated.

Concentration determination

Peptide samples were prepared by dissolving purified peptide or peptide conjugate in DMSO. The concentrations were determined in 1x PBS pH 7.4 using the absorbance of tryptophan (ε = 5500 M^{-1} cm^{-1}), tyrosine (ε = 1490 M^{-1} cm^{-1}), cysteine (ε = 125 M^{-1} cm^{-1}) residues, carbonate reactivity modulator (ε = 1510 M^{-1} cm^{-1}), p-SCN-Bn-CHX-A"-DTPA (ε = 13775 M^{-1} cm^{-1}), NODAGA-NHS (ε = 346 M^{-1} cm^{-1}), p-SCN-Bn-TCMC (24980 M^{-1} cm^{-1}) N_3-NHS (ε = 2430 M^{-1} cm^{-1}), DBCO-NHS ester (ε = 12560 M^{-1} cm^{-1}), BCN-NHS (ε = 3050 M^{-1} cm^{-1}), TCO-NHS ester (ε = 3300 M^{-1} cm^{-1}), Tz-PEG_5-NHS ester (ε = 16870 M^{-1} cm^{-1}), VC-PAB-MMAE (ε = 1870 M^{-1} cm^{-1}), SPDB-DM4 (ε = 11200 M^{-1} cm^{-1}), SMCC-DM1 (ε = 5700 M^{-1} cm^{-1}), PNU-159682 (7000 M^{-1} cm^{-1}) at 280 nm, FITC (ε = 73000 M^{-1} cm^{-1}) at 496 nm, AF647-NHS (270000 M^{-1} cm^{-1}) at 650nm.

Competitive binding FP assays

The fluorescence polarization measurements were performed on SpectraMax Paradigm Multi-Mode Detection Platform (Molecular Devices) in flat-bottom 384-well Corning microplates (Merck KGaA), using excitation and emission wavelengths of 485 nm and 535 nm, respectively. The acquisition time was 700 ms, and the read height was 1 mm. All reagents used in the assay were diluted in PBS containing 0.05% of Tween 20.

Increasing concentrations of peptide were mixed with the Fc-III-FAM tracer and added to the IgG1 in a total volume of 80µL. The final concentration of Fc-III-FAM was kept constant at 5 nM, the final concentration of IgG1 was of 10 - 30 nM and the final volume of sample was of 80 µl. The mixture was incubated at 27°C for 15 min and the fluorescence signal was measured on a Spectramax Paradigm. All sample preparations were done in PBS pH 7.4 or 7.0 containing 0.05% of Tween 20. Each experiment was performed in triplicate.

Table S1. Effect of Fc-III lysine and tyrosine scanning mutagenesis in the fluorescence polarization competition assay.

Fc-III substituent	IC_{50} (nM)[1]
Fc-III	58 ± 15
Fc-III-D1K	672 ± 94
Fc-III-A3K	1721 ± 263
Fc-III-W4K	7115 ± 2060
Fc-III-H5K	1506 ± 92
Fc-III-L6K	2359 ± 2
Fc-III-G7K	448 ± 89
Fc-III-E8K	293 ± 30
Fc-III-L9K	84 ± 17
Fc-III-V10K	3272 ± 439
Fc-III-W11K	12074 ± 944
Fc-III-T13K	300 ± 81
Fc-III-L6Y	241 ± 30
Fc-III-L6hY	1161 ± 182

[1]The fluorescence polarization competition assay was performed as described previously[1] using Fc-IIII-FAM as a probe, and the IC_{50} values were calculated using the Igor Pro software by fitting the curve with the Hill equation.

Peptide Synthesis

a) Synthesis. Peptides were synthesized by Fmoc/tBu solid-phase peptide chemistry on a Rink Amide AM resin (loading 0.57 mmol/g) using a Liberty Blue™ automated microwave peptide synthesizer (CEM Corp., Kamp-Lintfort, Germany) following a standard protocol. Each coupling was performed for 4 min at room temperature, using 0.2 M of Fmoc amino acid preactivated with 0.5 M DIC and 1 M OxymaPure® in DMF. Fmoc removal was performed with 10% v/v piperazine in DMF.

b) Cleavage. After completion of the synthesis, peptides were deprotected and cleaved from the resin manually with TFA under gentle agitation over a period of 1.5 h at RT in the presence of scavengers (standard cleavage solution: TFA/TIS/Water 90:5:5). After filtration and evaporation of most of the cleavage solution under a stream of nitrogen, the crude peptides were precipitated by addition of cold diethyl ether, centrifuged, and washed with cold diethyl ether. The resulting amorphous powder was dried, dissolved in ultrapure water/ACN, frozen, and lyophilized.

c) Disulfide bond formation. Crude lyophilized peptides (0.1 mmol) were resuspended in 10 ml of DMSO, then 100 µl of 2 mol/l NH_3 in methanol (2 eq) and 510 µl of 31.4% H_2O_2 (50 eq) were added. The progress of the oxidation was monitored via analytical UPLC-MS. After

completion of the reaction (usually 30 min), it was neutralized with 10 ml of 0.1% an aqueous solution of TFA and the peptides were purified by HPLC.

d) Purification. The peptide purifications were performed by Preparative Reversed Phase-HPLC on a Kinetex 5u XB-C18 100A, 100 x 21.2 mm column (Phenomenex Helvetia, Basel, Switzerland) by applying a 15%–55% gradient of solvent B (described in UPLC-MS section above), at a flow rate of 35 mL/min for 25 min. The peptide absorbance was monitored at 214 nm. Fractions were analyzed by UPLC-MS prior to the lyophilization step.

The purity of the peptides was determined on UPLC-MS systems:

- Method 1: Waters Acquity UPLC system coupled to a Micromass Quattro micro API mass spectrometer with a Kinetex® XB-C18 column (100Å, 1.7 µm, 50 x 2.1 mm; Phenomenex Helvetia) using solvent system using solvent system A (0.1% TFA in water) and B (0.1% TFA in ACN) at a flow rate of 0.6 mL/min and a 2-98% gradient of B over 4 min. Peptide elution was monitored at a wavelength of 214 nm.
- Method 2: Agilent InfinityLab Liquid Chromatography/Mass Selective Detector XT (LC/MSD XT) system with a Kinetex® XB-C18 column (100Å, 1.7 µm, 50 x 2.1 mm; Phenomenex Helvetia) using solvent system using solvent system A (0.03% TFA in water) and B (0.03% TFA in ACN) at a flow rate of 0.62 mL/min and a 5-95% gradient of B over 4 min. Peptide elution was monitored at wavelengths of 214 and 280 nm.
- Method 3: Waters Acquity UPLC System coupled to a Waters SQD mass spectrometer, BEH C18 1.7µm 50x2.1mm column heated at 40°C and fitted with 2µm insert filter pre-columns (available from Waters), and solvent systems A1 (water+0.1%FA) and B1 (ACN+0.1%FA) at a flow rate of 0.9 mL/min and a 5–100% gradient of B1 over 2.9 min.
- Method 4: Waters Acquity UPLC System coupled to a Waters SQD mass spectrometer with a CSH C18 column (130 Å, 1.7µm, 2.1 mm x 50 mm) heated at 40°C using solvent system A (water+0.1%FA) and B (ACN+0.1%FA) at a flow rate of 0.6 mL/min and a 5-85% gradient of B over 5 min.
- Method 5: Waters Acquity UPLC System coupled to a Waters SQD mass spectrometer with a CSH C18 column (130 Å, 1.7 µm, 2.1 mm x 50 mm) heated at 40 °C using solvent systems A (water+0.1% FA) and B (ACN+0.1% FA) at a flow rate of 0.9 mL/min and a 5–100% gradient of B over 2.7 min.

- Method 6: Waters Acquity UPLC System coupled to a Waters SQD mass spectrometer with a CSH Fluoro-phenyl column (130 Å, 1.7 µm, 2.1 mm x 50 mm) heated at 40 °C using solvent system A (water+0.1% FA) and B (ACN+0.1% FA) at a flow rate of 0.9 mL/min and a 5–100% gradient of B over 2.9 min.

Table S2. Characteristics of Fc-III peptide and its derivatives.

Compound	Calculated Exact Mass	Calculated $[M + 2H]^{2+}$	Found $[M + 2H]^{2+}$	Retention time (min)	Purity (%)	UPLC-MS method
Fc-III	1529.73	765.87	765.81	1.67	> 95	1
D1K	1584.87	793.44	793.10	1.67	98	1
A3K	1628.88	815.44	815.11	1.67	99	1
W4K	1513.74	757.87	757.40	2.159	99	2
H5K	1562.81	782.41	782.62	1.78	98	1
L6K	1586.80	794.40	794.00	2.125	100	2
G7K	1642.90	822.45	822.29	1.62	86	1
E8K	1570.84	786.42	786.02	1.61	99	1
L9K	1586.80	794.40	794.33	1.46	99	1
V10K	1600.82	801.41	801.00	2.335	100	2
W11K	1513.74	757.87	757.92	1.48	98	1
T13K	1598.85	800.43	799.81	1.64	99	1
A3Dap	1586.88	794.44	794.20	2.332	98	2
A3Orn	1614.88	808.44	808.10	2.31	98	2
A3hK	1642.88	822.44	822.20	2.286	94	2
L6Dap	1544.80	773.40	774.09	1.41	100	1
L6Dab	1558.80	780.40	780.00	2.115	90	2
L6Orn	1572.80	787.40	787.75	1.45	100	1
E8Dap	1528.84	765.42	765	2.267	98	2

E8Orn	1556.84	779.42	779	1.949	100	2
PEG_{20}-L6Orn	2525.94	1263.97	1263.3	1.09	88	5
PEG_{24}-L6Orn	2630.06	1316.03	1315.5	2.36	98	2
L6Y	1621.74	811.87	811.97	1.84	99	1
L6hY	1635.74	818.87	818.6	2.451	99	2
E8hY	2007.18	1004.59	1004.40	2.572	98	2

Chemical Synthesis

Synthesis of 2-[2-(tert-butoxycarbonylamino)ethoxy]ethyl (4-fluorocarbonylphenyl) carbonate (**compound 001**)**:**

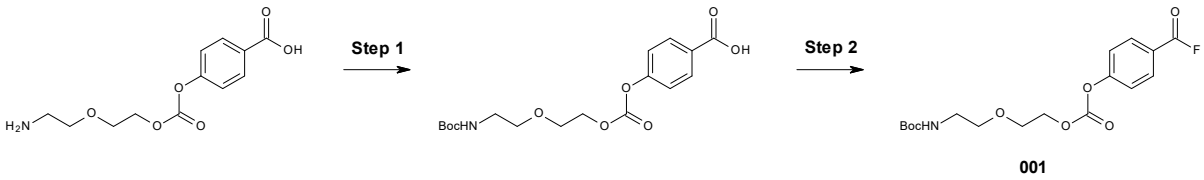

Step 1. 4-[2-(2-aminoethoxy)ethoxycarbonyloxy]benzoic acid; 2,2,2-trifluoroacetic acid, which was prepared according [1] (1.42 g, 2.22 mmol, 1.0 eq) and by di-tert-butyl dicarbonate (1.50 g, 6.69 mmol, 3 eq.) were dissolved in DCM (24 mL) and DMF (2.4 mL) at rt. Triethylamine (0.6 mL, 4.45 mmol, 2.0 eq.) was added to the reaction mixture at rt. After stirring at rt for 2 h, the reaction mixture was concentrated under vacuum. Purification by flash chromatography (50 g Cartridge, heptane:EA 8:2 to 3:7 over 12 CV followed by 98% EA over 2 CV) afforded 4-[2-[2-(tert-butoxycarbonylamino)ethoxy]ethoxycarbonyloxy]benzoic acid (1.17 g, 3.17 mmol, 70% purity, quantitative yield).

Step 2. Dicyclohexylmethanediimine (158 mg, 0.76 mmol, 1.0 eq.) followed by pyridine hydrofluoride (80 µL, 0.83 mmol, 1.1 eq.) were added to a mixture of 4-[2-[2-(tert-butoxycarbonylamino)ethoxy]ethoxycarbonyloxy]benzoic acid (400 mg, 0.76 mmol, 1.0 eq.) and pyridine (0.15 mL, 1.90 mmol, 2.5 eq.) in DCM (4 mL) in a plastic vessel at rt. After stirring at rt for 2 h, 0.5 equiv. of HF pyridine, 0.5 equiv. of DCC and 1 equiv. of pyridine were added to the reaction mixture. After stirring at rt for 4 h, 0.5 equiv. of HF pyridine, 0.5 equiv. of DCC and 1 equiv. of pyridine were added to the reaction mixture. After stirring at rt for 5 h, the reaction mixture was filtrated through a pad of Celite and concentrated in vacuo. Purification by flash chromatography (25 g Cartridge, heptane:EA 9:1 to 3:7 over 12 CV) afforded 2-[2-(tert-butoxycarbonylamino)ethoxy]ethyl (4-fluorocarbonylphenyl) carbonate (compound **001**)

(257.6 mg, 0.69 mmol, 92% yield) as a colourless oil. UPLC-MS (method 3): Rt = 1.86 min, m/z = 272 $[M+H]^+$, 394 $[M+Na]^+$; ^{1}H NMR (400 MHz, $CDCl_3$) d 8.05 – 7.99 (m, 2H), 7.36 – 7.28 (m, 2H), 4.83 (br s, 1H), 4.40 – 4.32 (m, 2H), 3.75 – 3.66 (m, 2H), 3.52 (t, *J* = 5.2 Hz, 2H), 3.28 (q, *J* = 5.1 Hz, 2H), 1.38 (s, 9H).

Synthesis of 3-[4-[3-(2-aminoethoxy)propanoylsulfanyl]phenyl]propanoic (**compound 002**)**:**

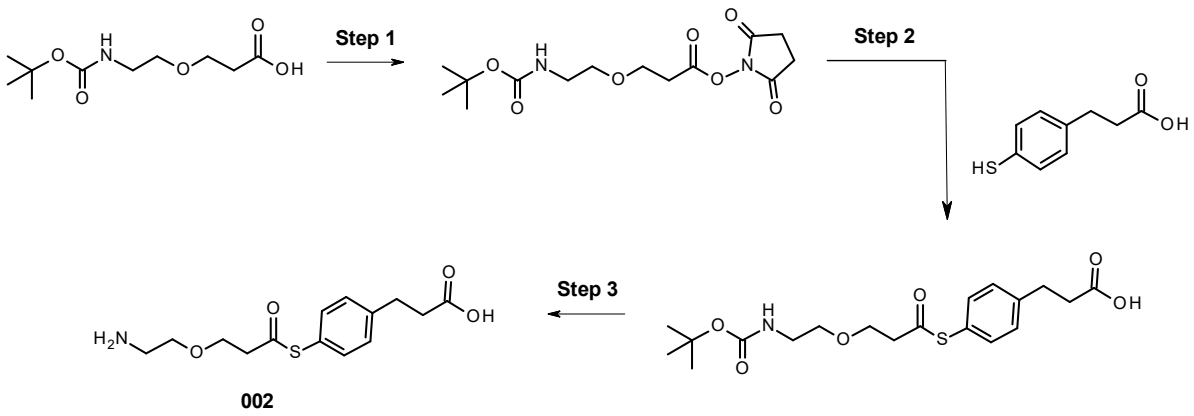

Step 1. To a solution of 3-(2-((tert-butoxycarbonyl)aminoethoxy)propanoic acid (1.50 g, 6.24 mmol, 1.0 eq.) in DCM (25 mL) at rt was added EDC.-HCl (4.78 g, 24.95 mmol, 4.0 eq.) followed by 1hydroxypyrrolidine-2,5-dione (2.87 g, 24.95 mmol, 4.0 eq.). After stirring at rt for 16 h, purification on C18 (60 g, 20 to 80% of ACN+0.1%TFA in water+0.1%TFA over 10 CV) afforded (2,5-dioxopyrrolidin-1-yl) 3-[2-(tertbutoxycarbonylamino-ethoxy]propanoate (1.77 g, 5.37 mmol, 94% UV purity, 81% yield) as a colorless oil after freeze-drying. UPLC-MS (method 3): Rt = 1.26 min, m/z = 331 $[M+H]^+$, 232 $[M-Boc+H]^+$, 375 $[M+FA-H]^-$; ^{1}H NMR ($CDCl_3$, 400 MHz): δ 5.24 (br s, 1H), 3.78 (t, *J* = 6.1 Hz, 2H), 3.51 (t, *J* = 5.0 Hz, 2H), 3.36 – 3.20 (m, 2H), 2.90 – 2.73 (m, 6H), 1.41 (s, 9H); ^{13}C NMR ($CDCl_3$, 100 MHz): δ 169.1, 166.6, 156.3, 79.2, 70.4, 65.6, 40.4, 32.4, 28.5, 25.7.

Step 2. DIEA (0.12 mL, 0.67 mmol, 1.0 eq.) was added to a mixture of (2,5-dioxopyrrolidin-1-yl) 3-[2-(tert-butoxycarbonylamino)ethoxy]propanoate (221 mg, 0.67 mmol, 1.0 eq.) and 3-(4-mercaptophenyl)propanoic acid (128 mg, 0.67 mmol, 1.0 eq.) in DMF (3 mL) at rt. After stirring at rt for 2 days, purification on C18 (30 g, 20 to 80% of ACN+0.1%TFA in water+0.1%TFA over 12 CV) afforded 3[4[3[2(tertbutoxycarbonylamino)ethoxy]propanoylsulfanyl]phenyl]propanoic acid (99.6 mg, 0.24 mmol, 95% UV purity, 36% yield) as a white solid after freeze-drying. UPLC-MS (method 3): Rt = 1.67 min, m/z = 298 $[M-Boc+H]^+$, 396 $[M-H]^-$; ^{1}H NMR ($CDCl_3$, 400 MHz): δ 7.36 (d, *J* = 7.9 Hz, 2H), 7.27 (d, *J* = 7.9 Hz, 2H), 3.75 (t, *J* =

6.2, 2H), 3.49 (t, *J* = 5.0, 2H), 3.36 – 3.24 (m, 2H), 2.99 (t, *J* = 7.6, 2H), 2.88 (t, *J* = 5.7, 2H), 2.69 (t, *J* = 7.6, 2H), 1.44 (s, 9H); ^{13}C NMR ($CDCl_3$, 100 MHz): δ 176.8, 142.1, 134.9, 133.2, 129.4, 125.4, 70.2, 66.3, 43.8, 35.0, 30.4, 28.6.

Step 3. TFA (1 mL) was added to 3-[4-[3-[2-(tert-butoxycarbonylamino)ethoxy]propanoylsulfanyl]phenyl]propanoic acid (75.6 mg, 0.19 mmol, 1.0 eq.) at rt. The reaction mixture was stirred at rt for 10 min then concentrated in vacuo affording 3-[4-[3-(2-aminoethoxy)propanoylsulfanyl]phenyl]propanoic acid (compound **002**) (51.4 mg, 0.17 mmol, 98% UV purity, 89% yield) as a white solid. UPLC-MS (method 3): Rt = 0.81 min, m/z = 299 $[M+H]^+$, 296 $[M-H]^-$. ^{1}H NMR (DMSO-d_6, 400 MHz): δ 5.14 (d, J = 8.4, 2H), 5.12 (d, J = 8.8 Hz, 2H), 1.60 (t, J = 5.8 Hz, 2H), 1.47 (t, J = 5.1 Hz, 2H), 0.92 (t, J = 4.8 Hz, 2H), 0.78 (t, J = 5.7 Hz, 2H), 0.72 (t, J = 7.4 Hz, 2H), 0.47 (t, J = 7.4 Hz, 2H); ^{13}C NMR (DMSO-d_6, 100 MHz): δ 199.7, 175.5, 140.9, 132.6, 127.4, 121.8, 64.1, 40.6, 36.7, 32.7, 27.7.

Synthesis of compound 3-(4-((3-(2-(2-(4,7,10-tris(2-(tert-butoxy)-2-oxoethyl)-1,4,7,10-tetraazacyclododecan-1-yl)acetamido)ethoxy)propanoyl)thio)phenyl)propanoic acid (**compound 003)**:

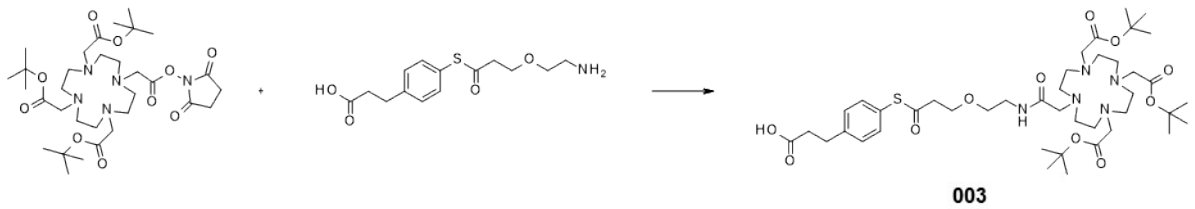

tert-butyl 2-[4,10-bis(2-tert-butoxy-2-oxo-ethyl)-7-[2-(2,5-dioxopyrrolidin-1-yl)oxy-2-oxo-ethyl]-1,4,7,10-tetrazacyclododec-1-yl]acetate;hexafluorophosphate (103.3 mg, 0.13 mmol, 1.0 eq.) followed by DIEA (90 µL, 0.51 mmol, 4.0 eq.) were added to a solution of 3-[4-[3-(2-aminoethoxy)propanoylsulfanyl]phenyl]propanoic acid (37.7 mg, 0.13 mmol, 1.0 eq.) in DMF (0.6 mL) at rt. After stirring at rt for 1.5 h, TFA was added until acidic pH was reached. Purification by preparative HPLC (5-50% ACN+0.1%FA in water+0.1%FA) was achieved yielding compound **003** (3-(4-((3-(2-(2-(4,7,10-tris(2-(tert-butoxy)-2-oxoethyl)-1,4,7,10-tetraazacyclododecan-1-yl)acetamido)ethoxy)propanoyl)thio)phenyl)propanoic acid) (64.3 mg, 60.4 mmol, 80% UV purity, 48% yield) as white powder after freeze-drying. UPLC-MS (method 4): Rt = 2.61 min, m/z = 852 $[M+H]^+$, 850 $[M-H]^-$.

Synthesis of tri-tert-butyl 2,2',2''-(10-(1-((2,5-dioxopyrrolidin-1-yl)oxy)-1,12,17-trioxo-2,5,8,11-tetraoxa-13,16-diazaoctadecan-18-yl)-1,4,7,10-tetraazacyclododecane-1,4,7-triyl)triacetate (**compound 004**):

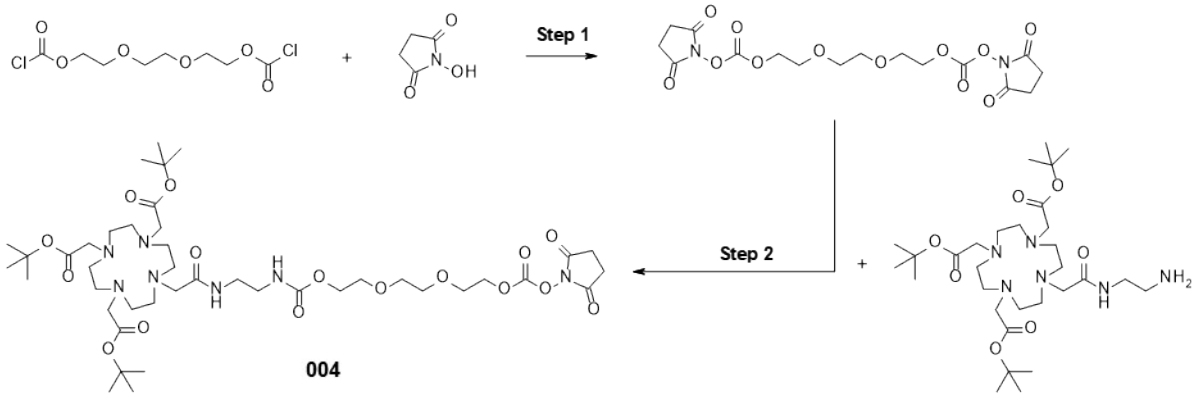

Step 1. To a stirring solution of N-hydroxysuccinimide (1.29 g, 11 mmol) in THF (20 mL) was added tri(ethylene glycol) bis(chloroformate) (0.5 g, 1.8 mmol), and the solution was cooled in an ice bath. Triethylamine (1.866 mL, 1.41 g, 11 mmol) was added over 10 minutes, and, after 30 minutes, the reaction mixture was allowed to warm to room temperature and stir overnight. The reaction mixture was cooled in an ice bath. The precipitate was filtered, washed with EA and dried over anhydrous Na_2SO_4. The product was dissolved in 10 ml of THF and used without further purification. UPLC-MS (method 1): Rt = 1.43, m/z = 433.24 $[M+H]^+$.

Step 2. To a solution of tri(ethylene glycol) bis(N-hydroxysuccinimide) (0.532 g, 1.2 mmol) in THF (16 mL) was added 2-aminoethyl-mono-amide-DOTA-tris(t-Bu ester) (311.4 mg, 0.448 mmol) in several steps, and the solution was stirred at room temperature until the conversion reached ~80%. Then, the reaction mixture was neutralized with 16 mL of aqueous TFA and purified by HPLC, yielding compound **004** (tri-tert-butyl 2,2',2''-(10-(1-((2,5-dioxopyrrolidin-1-yl)oxy)-1,12,17-trioxo-2,5,8,11-tetraoxa-13,16-diazaoctadecan-18-yl)-1,4,7,10-tetraazacyclododecane-1,4,7-triyl)triacetate) (71 mg, 76 µmol, UV purity 91%, 15 % yield). UPLC-MS (method 2): Rt = 2.611, m/z = 932.5 $[M+H]^+$.

Synthesis of NHS-suc-VC-PAB-MMAE **(compound 005)**:

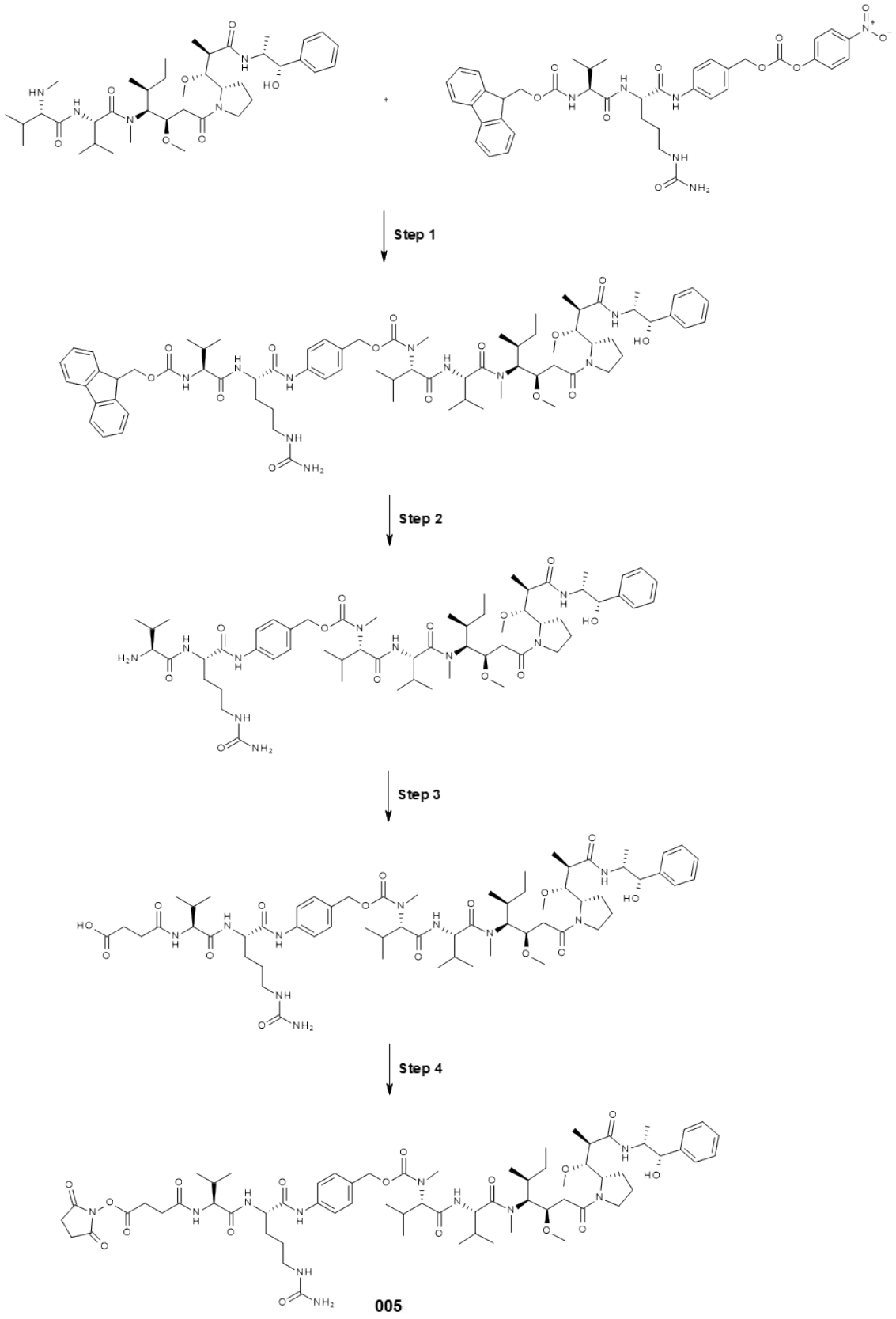

Step 1. HOBt (8.80 mg, 65.1 µmol, 0.5 eq.) followed by pyridine (0.3 mL, 3.7 mmol, 31.2 eq.) were added to a solution of MMAE (129.00 mg, 176.1 µmol, 1.5 eq.) and Fmoc-VC-PAB-OPNP (91.40 mg, 119.2 µmol, 1.0 eq.) in DMF (4 mL). After stirring at rt for 24 h, the mixture was poured into ethyl acetate (25 mL) and washed two times with water (20 mL). The aqueous phase was extracted two times with ethyl acetate (20 mL). The pooled organic phase was washed one time with citric acid 10% (10 mL), two times with water (15 mL) and one time with brine (15 mL). The organic layer was dried over $MgSO_4$, filtered, and concentrated under vacuo. Purification by silica gel flash chromatography (25 g, 1% of MeOH in DCM over 7 CV followed by 10% of MeOH in DCM over 7 CV) afforded Fmoc-VC-PAB-MMAE (94.50 mg, 70.2 µmol, 100% UV purity, 59% yield) as a white solid after concentration in vacuo. UPLC-MS (method 5): Rt = 1.97 min, 1345 $[M+H]^+$, 1389 $[M+FA-H]^-$, 1165 $[M-Fmoc+CO_2-H]^-$.

Step 2. Piperidine (1.0 mL, 10.0 mmol, 107.1 eq.) was added to a solution of Fmoc-VC-PAB-MMAE (157.40 mg, 93.6 µmol, 1.0 eq.) in ACN (4 mL). After stirring at rt for 12 h, the reaction mixture was concentrated in vacuo. The resulting residue was diluted with DCM and then diethylether was added. The mixture was filtered, the cake was dissolved in DCM then concentrated in vacuo to afford VC-PAB-MMAE (138.70 mg, 102.5 µmol, 70% UV purity, 92 % yield) as a yellow oil. UPLC-MS (method 5): Rt = 1.42 min, m/z = 1123 $[M+H]^+$, 1121 $[M-H]^-$.

Step 3. dihydrofuran-2,5-dione (15.10 mg, 149.4 µmol, 1.2 eq.) followed by DIEA (0.2 mL, 1.2 mmol, 9.3 eq.) were added to a solution of VC-PAB-MMAE (138.70 mg, 123.5 µmol, 1.0 eq.) in DMF (5 mL). After stirring at rt for 30 min, TFA was added until acidic pH was reached. Purification by preparative HPLC (20 to 80% of ACN+0.1% TFA in water+0.1% TFA) afforded suc-VC-PAB-MMAE (100.00 mg, 81.7 µmol, 100% UV purity, 66% yield) as a white powder after freeze-drying. UPLC-MS (method 5): Rt = 1.56 min, m/z = 1223 $[M+H]^+$, 1221 $[M-H]^-$.

Step 4. DIEA (56.6 µL, 326.9 µmol, 4.0 eq.) was added to a mixture of suc-VC-PAB-MMAE (100.00 mg, 81.7 µmol, 1.0 eq.) and HATU (31.08 mg, 81.7 µmol, 1.0 eq.) in DMF (4 mL) at rt. after stirring at rt for 5 min, 1-hydroxypyrrolidine-2,5-dione (9.41 mg, 81.7 µmol, 1.0 eq.)

was added to the reaction mixture. After stirring at rt for 10 min, TFA was added until acidic pH was reached. Purification by preparative HPLC (20 to 80% of ACN+0.1% TFA in water+0.1% TFA) afforded NHS-suc-VC-PAB-MMAE (compound **005**), (93.70 mg, 66.7 µmol, 94% UV purity, 82% yield) as a white powder after freeze-drying. UPLC-MS (method 5): 1.60 min, m/z = 1320 $[M+H]^+$, 1364 $[M+FA-H]^-$.

Synthesis of PNU-OPFP **(compound 006)**:

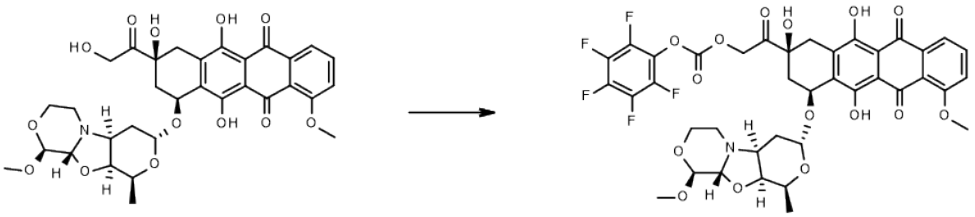

006

Five drops of TEA were added to a mixture of PNU-159682 (85.0 mg, 132.5 µmol, 1.0 eq.) and bis(perfluorophenyl) carbonate (242.2 mg, 59.6 µmol, 4.5 eq.) in a mixture of DCM (1.7 mL) and THF (1.7 mL) at rt. After stirring at rt for 1 h, four drops of TFA were added to the reaction mixture at rt. The reaction mixture was concentrated in vacuo (bath at 30 °C). The residue was dissolved in DMF (6 mL) then purified by preparative HPLC (40 to 100% of ACN in water) to afford PNU-OPFP (compound **006**), (87.2 mg, 102.4 µmol, 100% UV purity, 77% yield) as an orange powder after freeze-drying. UPLC-MS (method 3): Rt = 2.39 min, m/z = 852 $[M+H]^+$, 850 $[M-H]^-$.

General procedure for the synthesis of Fc-III-carbonate DOTA reactive conjugates

To prepare the Fc-III carbonate-DOTA reactive conjugates listed in table 1 and 2, a solution of $(tBu)_3$DOTA-carbonate reported previously (compound 12[1], 1.5 eq) in DMF was added to HATU.HPF_6 (1.4 eq) and stirred for 1 min, followed by the addition of DIEA (2 eq). After 3 min, the pre-activated $(tBu)_3$DOTA-carbonate was added to the Fc-binding vector and the reaction mixture was stirred for 1 to 4 hours at rt. Completion of the reaction was monitored by UPLC-MS. If the reaction did not go to completion, an additional amount of pre-activated carbonate derivative (about 1 eq) was added, and the mixture was further stirred for 1 to 2 hours. The reactive conjugate was precipitated with cold diethyl ether.

tBu deprotection. A cleavage cocktail consisting of TFA/TIS/Water 95/2.5/2.5 was added to the pellet of $(tBu)_3$DOTA-carbonate-Fc-III derivatives. The reaction mixture was stirred for 1-3h at RT, followed by precipitation with cold diethyl ether.

Purification. The purification of peptide conjugates was carried out by Preparative Reversed Phase-HPLC (Waters) on a Kinetex 5 µm C18 100 Å, LC Column 150 x 10.0 mm column (Phenomenex Helvetia) by applying a 15%–55% gradient of solvent B, at a flow rate of 8 mL/min for 25 min. The peptide signal was monitored at 214 nm. Fractions were analyzed by UPLC-MS prior to lyophilization.

Table S3. Characteristics of Fc-III X-carbonate DOTA reactive conjugates.

X	Calculated Exact Mass	Calculated $[M + 2H]^{2+}$	Found $[M + 2H]^{2+}$	Retention time (min)	Purity (%)	UPLC-MS method
D1K	2221.87	1111.94	1112.00	2.394	97	2
A3K	2265.88	1133.94	1134.00	2.362	98	2
W4K	2150.74	1076.37	1076.40	2.219	93	2
H5K	2199.81	1100.91	1101.00	2.491	97	2
L6K	2223.80	1112.90	1113.34	1.53	93	1
G7K	2279.90	1140.95	1141.00	2.403	97	2
E8K	2207.84	1104.92	1104.90	2.4	96	2
L9K	2223.80	1112.90	1112.90	2.229	98	2
V10K	2237.82	1119.91	1119.90	2.351	86	2
T13K	2235.85	1118.93	1119.00	2.373	90	2
A3Dap	2226.16	1113.08	1112.8	2.36	>90	2
A3Orn	2254.16	1128.08	1126.8	2.34	>90	2
A3hK	2282.16	1142.08	1140.8	2.34	>90	2
L6Dap	2181.86	1091.93	1091.90	2.181	68	2
L6Dab	2193.83	1097.92	1099.00	2.183	85	2
L6Orn	2209.83	1105.92	1106.00	2.193	98	2
E8Dap	2168.12	1085.06	1083.8	2.385	>90	2

E8Orn	2196.12	1099.06	1097.8	2.34	>90	2

Synthesis of **L6Orn-carbonate-NH_2**:

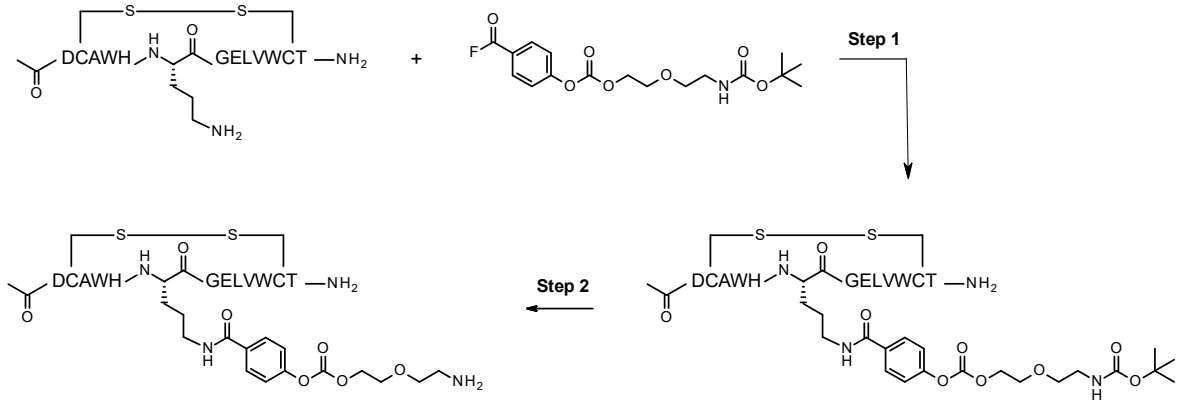

Step 1. 2-[2-(tert-butoxycarbonylamino)ethoxy]ethyl (4-fluorocarbonylphenyl) carbonate (71 mg, 0.19 mmol, 2.0 eq.) in solution in DMF (stock solution 1mg/40µL) was added to L6Orn-NH_2 (150 mg, 1.0 eq.) at rt. After stirring at rt for 1 min, DIEA (30 µL, 0.19 mmol, 2.0 eq.) was added to the reaction mixture. After stirring at rt for 10 min, the reaction mixture was concentrated in vacuo. Purification by preparative HPLC (5% to 95% of ACN+0.1%FA of in water+0.1%FA over 24 min) afforded L6Orn-carbonate-NHBoc (117 mg, 61 µmol, 90% UV purity, 57% yield). UPLC-MS (method 4): Rt = 2.48 min, m/z = 962 $[M+2H]^{2+}$, 960 $[M-2H]^{2}$.

Step 2. TFA (2.1 mL) was added to L6Orn-carbonate-NHBoc (117 mg, 61 µmol, 1.0 eq.) at rt. After stirring at rt for 5 min, the reaction mixture was concentrated in vacuo. The residue was dissolved in a mixture of ACN (2 mL) and H_2O (2 mL) and freeze-dried to afford L6Orn-carbonate-NH_2 (131 mg, 90% UV purity) as a white powder. UPLC-MS (method 4): Rt = 1.77 min, m/z = 913 $[M+2H]^{2+}$, 911 $[M-2H]^{2-}$.

Synthesis of **PEG_{20}-L6Orn-carbonate-NH_2:**

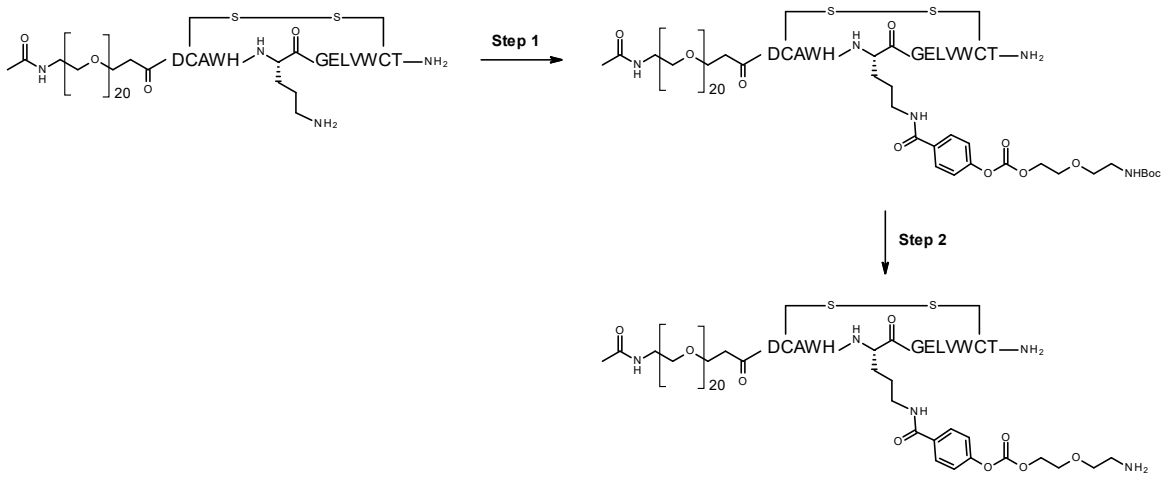

Step 1. HATU (3.97 mg, 10.5 µmol, 1.1 eq.) follower by DIEA (10 µL, 57.0 µmol, 6.0 eq.) were added to a solution of 4-[2-[2-(tert-butoxycarbonateonylamino)ethoxy]ethoxycarbonateonyloxy]benzoic acid (4.21 mg, 11.4 µmol, 1.2 eq.) in DMF (0.8 mL) at rt. After stirring at rt for 5 min, PEG_{20}-L6Orn (24.0 mg, 9.5 µmol, 1.0 eq.) was added to the reaction mixture. After stirring at rt for 10 min, TFA was added until acidic pH was reached. Purification by preparative HPLC (5 to 100% of ACN+0.1%TFA in water+0.1%TFA) afforded PEG_{20}-L6Orn-carbonate-NHBoc (19.2 mg, 6.6 µmol, 99% UV purity, 70% yield) as a white powder after freeze-drying. UPLC-MS (method 4): Rt = 2.44 min, m/z = 1439 $[M+2H]^{2+}$, 1437 $[M-2H]^{2-}$.

Step 2. Trifluoroacetic acid (1 mL) was added to a solution of PEG_{20}-L6Orn-carbonate-NHBoc (19.2 mg, 6.6 µmol, 1.0 eq.) in DCM (1 mL) at rt. After stirring at rt for 30 min, the reaction mixture was concentrated in vacuo. A mixture of ACN/water (10 mL, 1:1) was added and the mixture was freeze-dried to afford PEG_{20}-L6Orn-carbonate-NH_2 (20.1 mg, 6.6 µmol, 100% UV purity, quant.) as a white powder. UPLC-MS (method 4): Rt = 1.92 min, m/z = 1389 $[M+2H]^{2+}$, 1387 $[M-2H]^{2-}$.

Synthesis of **PEG_{24}-L6Orn-carbonate-NH_2**:

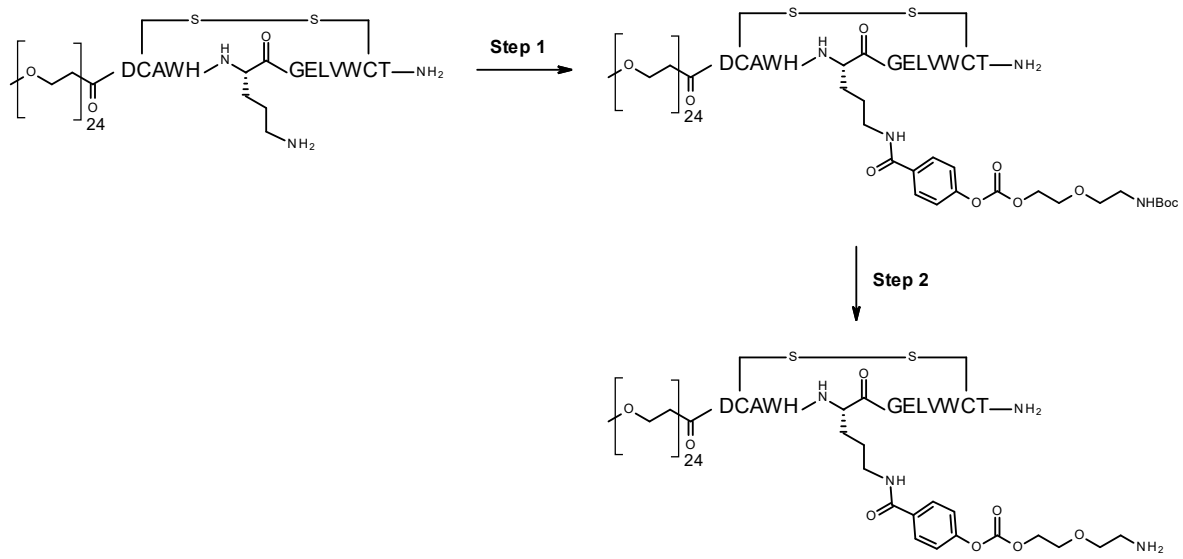

Step 1. 2-(2-aminoethoxy)ethyl (4-fluorocarbonylphenyl) carbonate (14.4 mg, 38.7 µmol, 2.0 eq.) and DIEA (19.0 µL, 38.1 µmol, 2.0 eq.) were added to a solution of PEG_{24}-L6Orn (50.9 mg, 19.0 µmol, 1.0 eq.) in 0.4 mL DMF. After stirring at rt for 4 h, the reaction mixture was precipitated with 9.0 mL of cold ether. UPLC-MS (method: 2): Rt = 2.82 min, m/z = 1514 $[M+2H]^{2+}$.

Step 2. TFA/TIS/H_2O (570/15/15 µL) was added to a pellet of PEG_{24}-L6Orn-carbonate-NHBoc (57.6 mg, 19.0 µmol, 1.0 eq.) at rt. The reaction mixture was stirred at rt for 1 h, then precipitated with 5.4 mL of cold ether. UPLC-MS (method 2): Rt = 2.39, m/z = 976 $[M+3H]^{3+}$.

Synthesis of **L6Dap/L6Dab/L6Orn/L6K-thioester-DOTA**:

HATU.HPF6 (1.3 eq.) was added to a solution of compound 003 (1.4 eq.) and stirred for 1 min, followed by the addition of DIEA (3.0 eq.) at rt. After 3 min stirring at rt, the pre-activated compound 003 was added to L6Dap/L6Dab/L6Orn/L6K peptides (1.0 eq.) and stirred at rt for 1-3 h. Completion of the reaction was monitored by UPLC-MS. The reactive conjugates were precipitated with cold diethyl ether.

Subsequently, the tert-butyl protecting groups of the DOTA moiety were removed by treatment with TFA/TIS/water (95/2.5/2.5, v/v/v) over 1-3 hours at rt, followed by precipitation with cold diethyl ether and purification by HPLC (as described for Fc-III-carbonate-DOTA).

Synthesis of **L6Orn-carbonate-DTPA**:

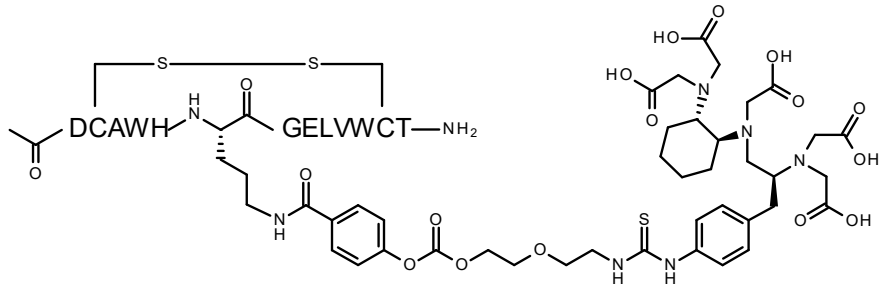

p-SCN-Bn-CHX-A"-DTPA.3HCl (19.1 mg, 27.2 µmol, 1.0 eq) was added to a solution of L6Orn-carbonate-NH_2 (49.6 mg, 27.2 µmol, 1.0 eq.) and TEA (22 µL, 160 mmol, 6.0 eq.) in DMF (0.4 mL) at rt. After stirring at rt for 3 h, TFA was added until acidic pH was reached. Purification by reversed phase automated flash chromatography on a C_{18} biotage column (30 g, 25 to 60% ACN+0.1%TFA in H_2O+0.1%TFA over 12 CV) afforded L6Orn-carbonate-DTPA (45.2 mg, 10.6 µmol, 90% UV purity, 62% yield). UPLC-MS (method 4): Rt = 2.11 min, m/z = 1210 $[M+2H]^{2+}$, 1208 $[M-2H]^{2-}$.

Synthesis of **L6Orn-carbonate-Bn-TCMC**:

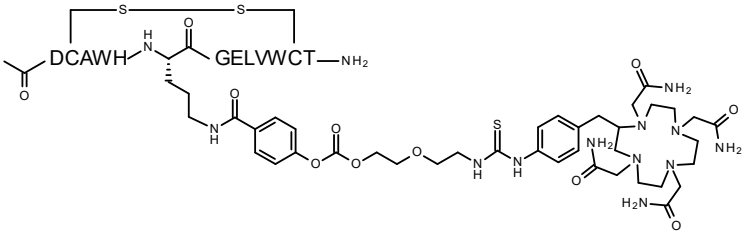

DIEA (30.12 µL, 60.2 µmol, 11.0 eq.) was added to a solution of L6Orn-carbonate-NH_2 (10.00 mg, 5.48 µmol, 1.0 eq.) and p-SCN-Bn-TCMC (5.70 mg, 8.22 µmol, 1.5 eq.) in DMF (0.13 mL). After stirring at rt for 1 h, HCl was added until acidic pH was reached. Purification by preparative HPLC (18 to 32% of ACN+0.1% TFA in water+0.1% TFA) afforded L6Orn-

carbonate-Bn-TCMC (3.91 mg, 1.5 µmol, 98% UV purity, 28% yield) as a white powder after freeze-drying. UPLC-MS (method 2): Rt = 2.17 min, m/z = 1186 $[M+2H]^{2+}$, 791.5 $[M+3H]^{3+}$.

Synthesis of **L6Orn-carbonate-NODAGA**:

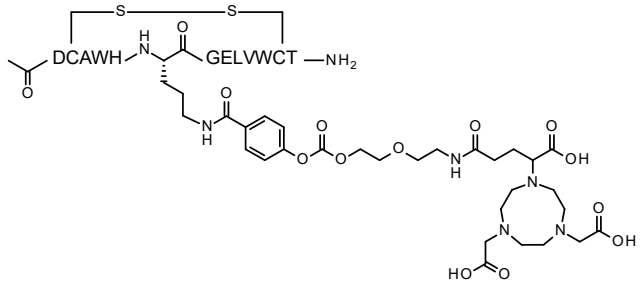

DIEA (1.9 µL, 10.8 µmol, 4.0 eq.) was added to a solution of NODAGA-NHS ester.TFA.HPF_6 (1.97 mg, 2.7 µmol, 1.0 eq.) and L6Orn-carbonate-NH_2 (5.0 mg, 2.7 µmol, 1.0 eq.) in DMF (0.1 mL) at rt. After stirring at rt for 3.5 h, NODAGA-NHS ester.TFA.HPF_6 (1.97 mg, 2.7 µmol, 1.0 eq.) was added to the reaction mixture at rt. After stirring at rt for 1 h, TFA (4 µL) was added to the reaction mixture. Purification by preparative HPLC on C_{18} (21 to 33% ACN+0.1%TFA in water+0.1%TFA) afforded L6Orn-carbonate-NODAGA (1.44 mg, 0.66 µmol, 87% UV purity, 21% yield). UPLC-MS (method 2): Rt = 2.303 min, m/z = 1091.4 $[M+2H]^{2+}$.

Synthesis of **L6Orn-carbonate-FITC:**

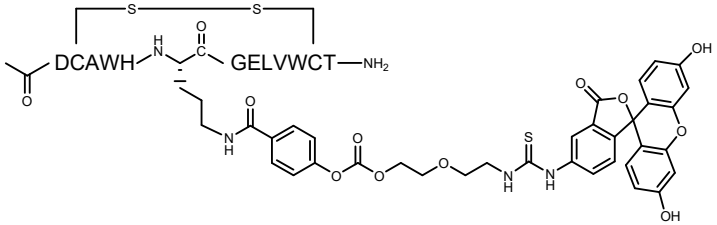

A solution of compound 009 reported previously[1] (4.82 mg, 7.4 µmol, 2.4 eq) in DMF was added to HATU.HPF6 (6.8 µmol, 2.2 eq) and stirred for 1 min, followed by the addition of DIEA (6.8 µmol, 2.2 eq). After 3 min, the pre-activated carbonate-FITC was added to the L6Orn peptide (4.8 mg, 3.05 µmol, 50 µL) and the reaction mixture was stirred for 5 hours at rt.

Completion of the reaction was monitored by UPLC-MS. The reactive conjugate was precipitated with cold diethyl ether and dried. Purification by preparative HPLC on C_{18} (28 to 40% ACN+0.1%TFA in water+0.1%TFA) afforded L6Orn-carbonate-FITC (4.79 mg, 2.16 µmol, 100% UV purity, 71% yield). UPLC-MS (method 2): Rt = 2.73 min, m/z = 1107.4 $[M+2H]^{2+}$.

Synthesis of **L6Orn-carbonate-AF647:**

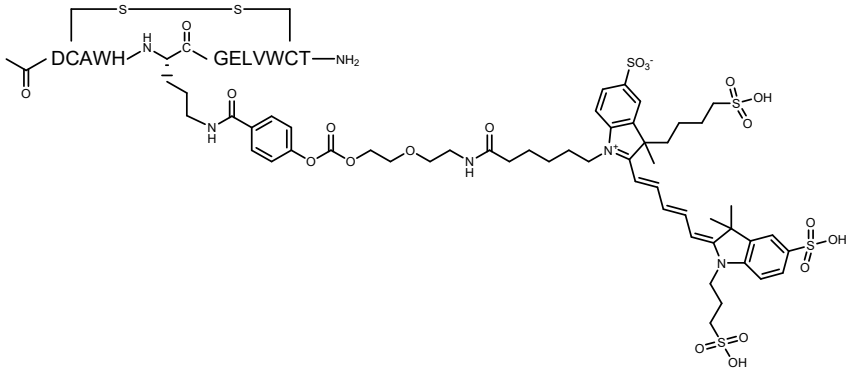

DIEA (25.7 µmol, 6.52 eq) was added to a solution of AF647-NHS ester (4.6 mg, 4.7 µmol, 1.18 eq) in DMF and L6Orn-carbonate-NH_2 (7.2 mg, 3.9 µmol, 100 µL). After stirring at rt for 5h, TFA was added until acidic pH is reached. Purification by preparative HPLC (Eluent: 22 to 70% of MeCN+0.1% TFA in water+0.1% TFA) afforded FcIII-L6Orn-carbonate-AF647 (3.3 mg, 0.001 mmol, 86% UV purity, 26.1 % yield) as a blue powder after freeze-drying. UPLC-MS (method 5): Rt = 1.09 min, m/z = 1341.0 $[M+2H]^{2+}$.

Synthesis of **L6Orn-carbonate-Tz**:

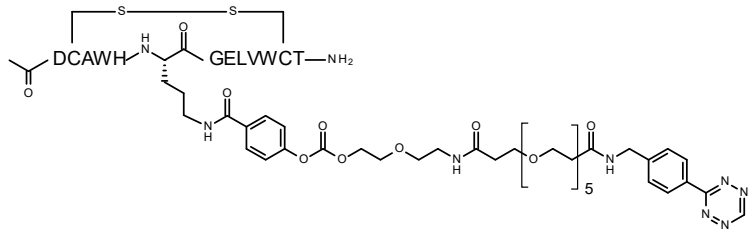

DIEA (1.9 µL, 11.0 µmol, 4.0 eq.) was added to a solution of L6Orn-carbonate-NH_2 (5.0 mg, 2.7 µmol, 1.0 eq.) and Tz-PEG_5-NHS ester (1.66 mg, 2.7 µmol, 1.0 eq.) in DMF (0.1 mL) at rt. After stirring at rt for 2 h, more of Tz-PEG_5-NHS ester (1.66 mg, 2.7 µmol, 1.0 eq.) in DMF

(50 µL) was added to the reaction mixture. After stirring at rt for 3h, TFA was added until acidic pH was reached. Purification by reversed phase automated flash chromatography on a C_{18} biotage column (12 g, 20 to 80% of ACN+0.1%TFA in water+0.1%TFA over 12 CV) afforded L6Orn-carbonate-Tz (6.2 mg, 2.4 µmol, UV purity 91%, 89% yield) as a pale pink powder after freeze-drying. UPLC-MS (method 4): Rt = 2.29 min, m/z = 1157 $[M+2H]^{2+}$, 1155 $[M-2H]^{2-}$.

Synthesis of **L6Orn-carbonate-TCO**:

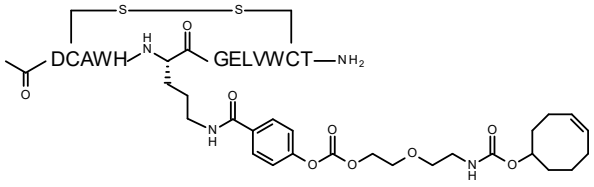

DIEA (1.9 µL, 10.8 µmol, 4.0 eq.) was added to a solution of TCO-NHS ester (0.72 mg, 2.7 µmol, 1.0 eq.) and L6Orn-carbonate-NH_2 (5.0 mg, 2.7 µmol, 1.0 eq.) in DMF (0.1 mL) at rt. After stirring at rt for 1.5 h, TFA (4 µL) was added to the reaction mixture. Purification on C_{18} (12 g, 10 to 50% of ACN+0.1%TFA in water+0.1%TFA over 12 CV) afforded L6Orn-carbonate-TCO (2.8 mg, 1.10 µmol, UV purity 80%, 41% yield) as a white powder after freeze-drying. UPLC-MS (method 4): Rt = 2.75 min, m/z = 988 $[M+2H]^{2+}$, 986 $[M-2H]^{2-}$.

Synthesis of **L6Orn-carbonate-N_3**:

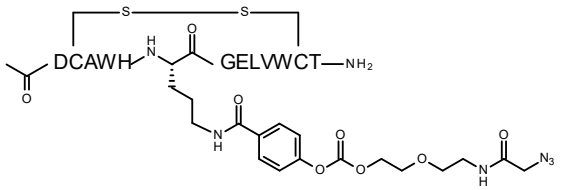

DIEA (1.9 µL, 10.8 µmol, 4.0 eq.) was added to a solution of (2,5-dioxopyrrolidin-1-yl) 2-azidoacetate (0.53 mg, 2.7 µmol, 1.0 eq.) and L6Orn-carbonate-NH_2 (5.0 mg, 2.7 µmol, 1.0 eq.) in DMF (0.1 mL) at rt. After stirring at rt for 3 h, TFA (4 µL) was added to the reaction mixture. Purification by reversed phase automated flash chromatography on a C_{18} biotage column (12 g, 10 to 50% of ACN+0.1%TFA in water+0.1%TFA over 12 CV) afforded L6Orn-carbonate-

N_3 (2.7 mg, 1.3 µmol, UV purity 94%, 49% yield) as a white powder after freeze-drying. UPLC-MS (method 4): Rt = 2.16 min, m/z = 954 $[M+2H]^{2+}$, 952 $[M-2H]^{2-}$.

Synthesis of **L6Orn-carbonate-DBCO**:

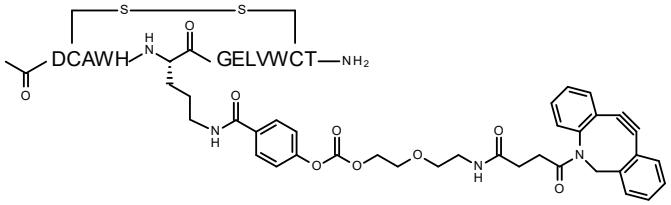

DIEA (1.9 µL, 10.8 µmol, 4.0 eq.) was added to a solution of DBCO-NHS ester (1.12 mg, 2.7 µmol, 1.0 eq.) and L6Orn-carbonate-NH_2 (5.0 mg, 2.7 µmol, 1.0 eq.) in DMF (0.1 mL) at rt. After stirring at rt for 1.5 h, TFA (4 µL) was added to the reaction mixture. Purification on C_{18} (32 to 44% of ACN+0.1%TFA in water+0.1%TFA) afforded L6Orn-carbonate-DBCO (2.27 mg, 1.07 µmol, UV purity 97%, 38% yield) as a white powder after freeze-drying. UPLC-MS (method 4): Rt = 2.79 min, m/z = 1056 $[M+2H]^{2+}$, 1055 $[M-2H]^{2-}$.

Synthesis of **L6Orn-carbonate-BCN**:

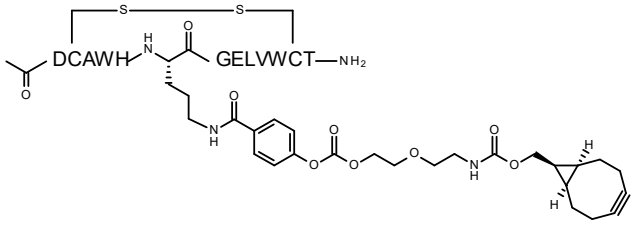

DIEA (1.9 µL, 10.8 µmol, 4.0 eq.) was added to a solution of BCN-NHS ester (0.83 mg, 2.7 µmol, 1.0 eq.) and L6Orn-carbonate-NH_2 (5.0 mg, 2.7 µmol, 1.0 eq.) in DMF (0.1 mL) at rt. After stirring at rt for 2.5 h, TFA (4 µL) was added to the reaction mixture. Purification on C_{18} (34 to 46% of ACN+0.1%TFA in water+0.1%TFA) afforded L6Orn-carbonate-BCN (2.03 mg, 1.01 µmol, UV purity 95%, 35% yield) as a white powder after freeze-drying. UPLC-MS (method 2): Rt = 2.903 min, m/z = 1000.8 $[M+2H]^{2+}$.

Synthesis of **L6Orn-carbonate-SMCC-DM1**:

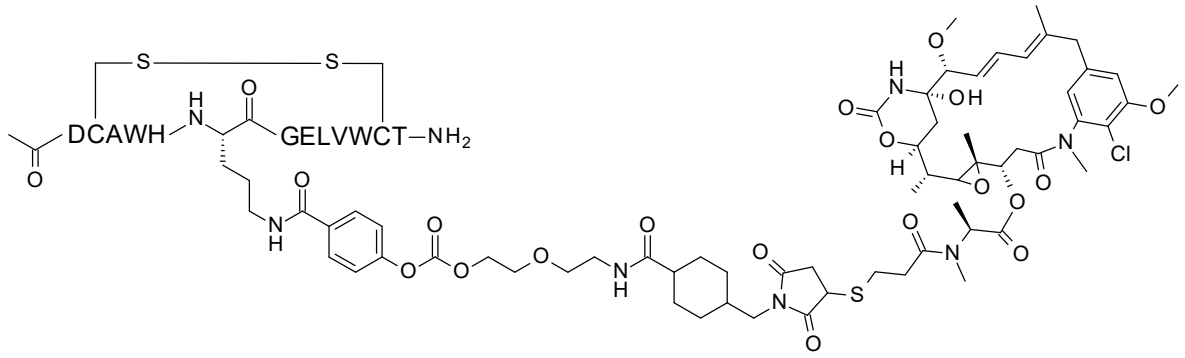

DIEA (1.9 µL, 10.8 µmol, 4.0 eq.) was added to a solution of DM1-SMCC (2.79 mg, 2.7 µmol, 1.0 eq.) and L6Orn-carbonate-NH_2 (5.0 mg, 2.7 µmol, 1.0 eq.) in DMF (0.2 mL) at rt. After stirring at rt for 70 min, TFA (4 µL) was added to the reaction mixture. Purification by reversed phase automated flash chromatography on a C_{18} biotage column (12 g, 20 to 80% of ACN+0.1%TFA in water+0.1%TFA over 12 CV) afforded L6Orn-carbonate-SMCC-DM1 (5.23 mg, 1.80 µmol, UV purity 96%, 69% yield) as a white powder after freeze-drying. UPLC-MS (method 4): Rt = 2.80 min, 1390 $[M-2H]^{2-}$.

Synthesis of **L6Orn-carbonate-SPDB-DM4**:

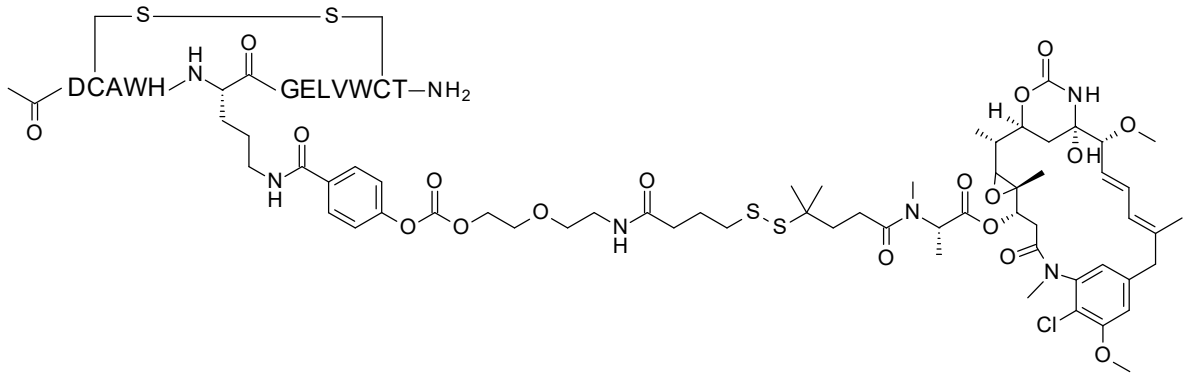

A saturated aqueous $NaHCO_3$ solution (83 µL) was added to a mixture of DM4 (4.28 mg, 5.5 µmol, 1.0 eq.) and SPDB (0.89 mg, 2.7 µmol, 0.5 eq.) in DMA (0.75 mL) at rt. After stirring at rt for 110 min, SPDB (0.89 mg, 2.7 µmol, 0.5 eq.) in DMA (0.2 mL) was added to the reaction mixture at rt. After stirring at rt for 10 min, the reaction mixture was added to L6Orn-carbonate-NH_2 (10.0 mg, 5.5 µmol, 1.0 eq.) at rt. After stirring at rt for 1 h, TFA was added until acidic pH was reached. Purification on C_{18} (30 g, 20 to 80% of ACN+0.1%TFA in water+0.1%TFA over 12 CV) afforded L6Orn-carbonate-SPDB-DM4 (10.7 mg, 3.9 µmol, UV purity 99%, 71%

yield) as a white product after freeze-drying. UPLC-MS (method 4): Rt = 2.99 min, m/z = 1351 $[M-2H]^{2-}$.

Synthesis of **L6Orn-carbonate-suc-VC-PAB-MMAE**:

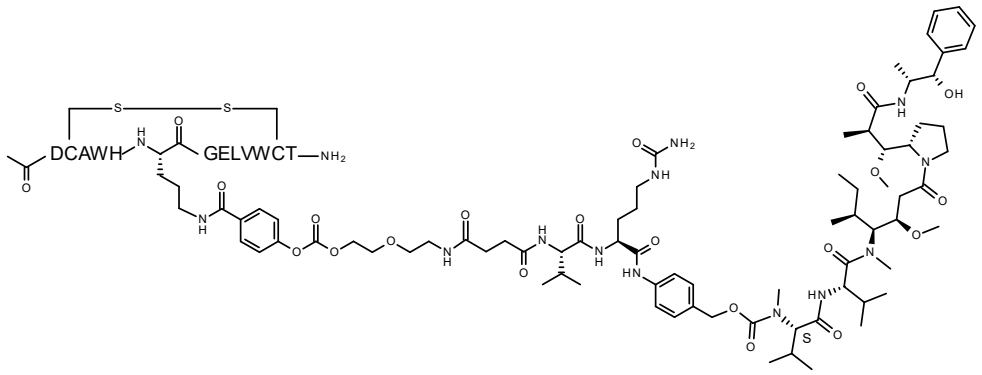

DIEA (13 µL, 26.0 µmol, 3.0 eq.) was added to a solution of NHS-suc-NH-VC-PAB-MMAE (12.6 mg, 9.5 µmol, 1.1 eq.) in 450 µL DMF and L6Orn-carbonate-NH_2 (15.8 mg, 8.7 µmol, 1.0 eq.) in 86 µL DMF. After stirring at rt for 2 h, TFA was added until acidic pH was reached. Purification by preparative HPLC (34 to 50% of ACN in water with 0.1% TFA) afforded L6Orn-carbonate-suc-VC-PAB-MMAE (17.1 mg, 5.6 µmol, 99% UV purity, 65% yield) as a white powder after freeze-drying. UPLC-MS (method 2): Rt = 2.98 min, m/z = 1516 $[M+2H]^{2+}$.

Synthesis of **L6Orn-carbonate-PNU**:

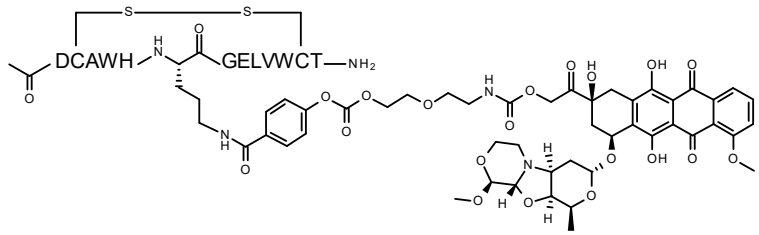

DIEA (11.5 µL, 65.8 µmol, 4.0 eq.) was added to a solution of L6Orn-carbonate-NH_2 (30.0 mg, 16.4 µmol, 1.0 eq.) and PNU-OPFP (compound **027**) (14.0 mg, 16.4 µmol, 1.0 eq.) in DMF (1 mL) at rt. After stirring at rt for 2.5 h, TFA (5 µL) was added to the reaction mixture at rt. Purification by preparative HPLC (20 to 60% of ACN in water) afforded L6Orn-carbonate-PNU (18.9 mg, 5.8 µmol, 77% UV purity, 35% yield) as an orange powder after freeze-drying. UPLC-MS (method 3): Rt = 1.47 min, m/z = 1247 $[M+2H]^{2+}$, 1244 $[M-2H]^{2-}$.

Synthesis of **PEG20-L6Orn-carbonate-PDB-DM4**:

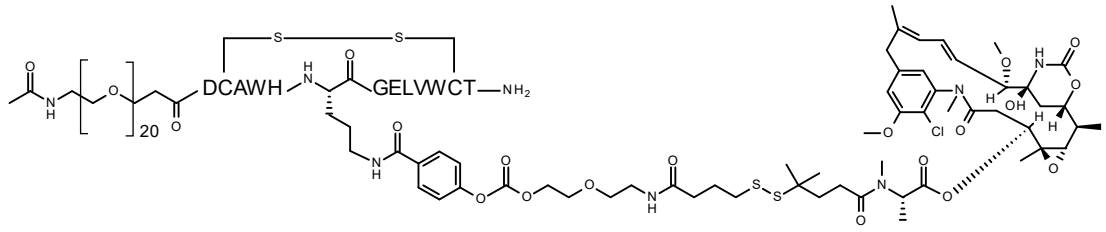

A saturated aqueous $NaHCO_3$ solution (83 µL) was added to a mixture of DM4 (1.28 mg, 1.6 µmol, 1.0 eq.) and SPDB (0.53 mg, 1.6 µmol, 1.0 eq.) in DMA (0.75 mL) at rt. After stirring at rt for 10 min, the reaction mixture was added to PEG20-L6Orn-carbonate-NH_2 (5.00 mg, 1.6 µmol, 1.0 eq.) at rt. After stirring at rt for 1 h, TFA was added until acidic pH was reached. Purification by preparative HPLC (5 to 100% of ACN+0.1%TFA in water+0.1%TFA) afforded PEG20-L6Orn-carbonate-PDB-DM4 (3.45 mg, 0.9 µmol, 100% UV purity, 58% yield) as a white product after freeze-drying. UPLC-MS (method 4): Rt = 2.83 min, m/z = 1826 $[M-2H]^{2-}$.

General procedure for the synthesis of Fc-III-Y-carbonate-DOTA variants:

To prepare the Tyr variants reactive conjugates, 2 eq. of DMAP were added to a solution of compound 004 (2 eq.) in DMF and stirred for 1 min, followed by the addition of the Fc-binding vector (1 eq.) and DIEA (4 eq.). The reaction mixture was stirred for 1 to 4 hours at room temperature. Completion of the reaction was monitored by UPLC-MS. The reactive conjugate was precipitated with cold diethyl ether.

Subsequently, the tert-butyl protecting groups of the DOTA moiety were removed by treatment with TFA/TIS/water (95/2.5/2.5, v/v/v) over 1-3 hours at room temperature, followed by precipitation with cold diethyl ether and purification by HPLC (as described for Fc-III-carbonate DOTA conjugates).

Compound	Structure
L6Y-DOTA	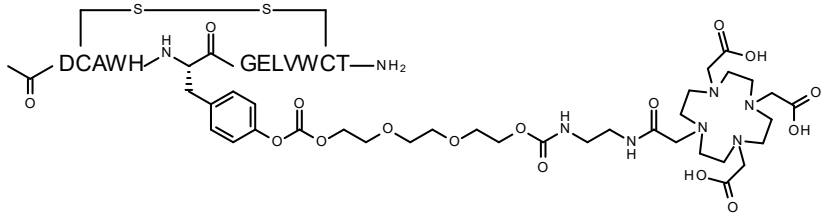
L6hY-DOTA	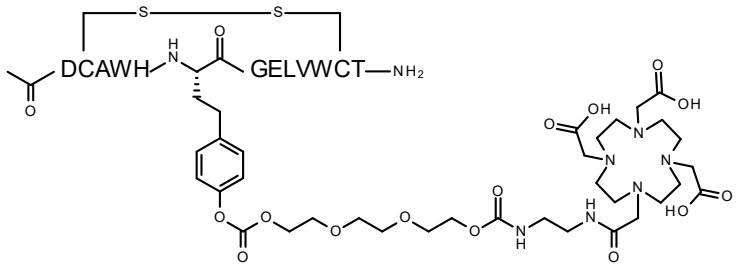
E8hY-DOTA	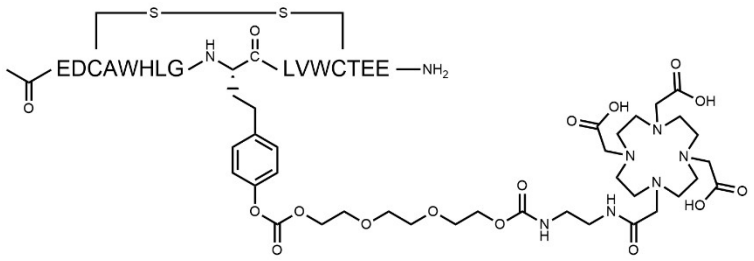

The MS characterization of DOTA-peptide conjugates is shown in table S4 below.

Table S4: Characterization of Fc-III-Y-carbonate DOTA -reactive conjugates

Compound	Calculated Exact Mass	Calculated $[M + 2H]^{2+}$	Found $[M + 2H]^{2+}$	Retention time (min)	Purity[1] (%)	UPLC-MS method
L6Y-DOTA	2269.74	1135.87	1136.12	1.58	54	1
L6hY-DOTA	2283.74	1142.87	1142.97	1.6	60	1
E8hY-DOTA	2655.18	1328.59	1328.14	1.72	80	1

[1]The purity of tyrosine carbonates was low because of partial hydrolysis of the carbonate during the HPLC purification step.

Antibody conjugation

General procedure for the preparation of antibody conjugates in solution

To prepare the trastuzumab-payload conjugates, 2 eq of reactive conjugate (2.4 nmol, if not specified otherwise) in DMSO (2-7% v/v in final reaction mixture) was added to a solution of an antibody (1 eq, 1.2 nmol; antibody was buffer-exchanged into phosphate-buffered saline (PBS) prior to the conjugation) diluted in 50 mM $NaHCO_3$ pH 9.0 (20-28µL) and the reaction mixture (36 µL) was stirred at room temperature for 2 hours.

Peptide release from antibody conjugates

Following the payload conjugation to the antibody, the reaction mixture was quenched with 64 µl of 0.1M glycine pH 2.5 and incubated 5 min. The antibody conjugate was then purified by gel filtration chromatography using a pre-equilibrated BioRad P-30 column (bed height: 3.7 cm; overall length: 5 cm, Bio-Rad, Hercules, U.S.A.) and then eluted with 100 µl of 0.1M glycine pH 2.5. The purified antibody conjugate fractions were neutralized with 10 µl of 1M PBS pH 8.5. The buffer was exchanged for PBS (pH 7.4) using a Vivaspin® 500 centrifugal concentrator and then analyzed by HRMS.

Cell viability assay

The human breast carcinoma cell line SK-BR-3 (HER-2 positive) and the epithelial, human breast adenocarcinoma MDA-MB-231 (HER-2 negative) cell lines were purchased from ATCC. They were maintained in high-glucose Dulbecco's Modified Eagle's Medium (DMEM) supplemented with 10% fetal bovine serum at 37°C under 5% CO_2 until ready for use. SK-BR-3 or MDA-MB-231 (5'000 cells/well) were treated with serially diluted ADCs. The samples were added at the corresponding concentrations in triplicates. After incubation for 72h at 37°C, cell viability of the ADCs was assessed using the CellTiter-Glo 2.0 (G7570, Promega, Madison, WI, USA).

Enzymatic cleavage of antibody conjugates

Cleavage of antibody conjugates into Fab and Fc fragments was achieved by digestion with GingisKHAN™ protease (50 units per 50 µg of antibody conjugate in 0.1 M Tris pH 8.0 in the presence of 2.8 µl of GingisKHAN™ reducing agent in a total volume of 28 µl, for 1 hour at 37 °C). The cleavage of antibody conjugates into $F(ab')_2$ and Fc/2 fragments was achieved by digestion with FabRICATOR™ from Genovis (67 units per 50 µg of antibody conjugates in PBS, pH 7.4 for 30 min at 37 °C).

Samples preparation for LC-FTMS analysis

The deglycosylation of antibody conjugates was achieved by incubating units 200 units of Endo S with 50 µg of antibody conjugate (10 µl) with 1.2 µl of the formulation buffer in a total volume of 12.2 µl for 1h at 37°C.

Samples preparation for middle-down analysis

Trastuzumab conjugates were digested into $F(ab')_2$ and Fc/2 subunits with FabRICATOR™ from Genovis (67 units per 50 µg of antibody conjugates in PBS, pH 7.4 for 30 min at 37 °C). TCEP was then added to 30 mM final concentration and reaction mixture was incubated for 30 min at 50 °C to achieve complete reduction of all disulfide bonds for Lc, Fd', and Fc/2 subunits.

High-resolution mass spectrometry analysis

Direct injection HRMS for peptide analysis was performed on a QExactive HF-HT-Orbitrap-FT-MS instrument, (Thermo Fisher Scientific, Bremen, Germany) coupled to an automated chip-based nanoelectrospray device (Triversa Nanomate, Advion, Ithaca, U.S.A.). Electrospray ionization was conducted at a capillary voltage of 1.4 kV and nitrogen nanoflow of 0.15 psi. MS experiments were performed with a nominal resolution of 45000 and in the positive ion mode. Data deconvolution was performed with Protein Deconvolution (Thermo Fischer Scientific, Sunnyvale, CA, U.S.A.) using the Xtract algorithm with a 90% fit factor.

LC-FTMS and middle-down analysis

For both intact mass measurement (LC-MS) and middle-down analysis (LC-FT-MS/MS, conjugation site localization), samples were separated onto an Acquity UPLC Protein column BEH C4 (300 Å, 1.7 µm, 1 x 150 mm, Waters, Milford, MA, U.S.A.) using a Dionex Ultimate 3000 analytical RSLC system (Dionex, Germering, Germany) coupled to a HESI source (Thermo Fisher Scientific, Bremen, Germany). The separation was performed with a flow rate of 90 µl/min by applying a gradient of solvent B from 15 to 25 % in 2 min, then from 25 to 40 % within 12 or 20 min, followed by column washing and re-equilibration steps. Solvent A was composed of water with 0.1 % formic acid, while solvent B consisted of acetonitrile with 0.1 % TFA.

Eluting proteoforms were analyzed on a QExactive HF-HT-Orbitrap-FT-MS benchtop instrument (Thermo Fisher Scientific, Bremen, Germany). For intact mass measurements MS1, the scan was performed in protein mode with 15 000 resolution and averaging 10 µscans. Middle-down analysis (MS/MS) for localization of conjugation site was performed in PRM mode isolating species at 950 m/z for Fc/2-DOTA, with 300 Th isolation window, using 240 000 resolution and averaging 10 µscans. HCD (higher energy collision-induced dissociation) was used as a fragmentation method with a normalized collision energy (NCE) of 10, 12, 15 and 17-8 %. Each NCE analysis was performed in triplicates.

Intact mass measurement data were analyzed with Protein Deconvolution (Thermo Fischer Scientific, Sunnyvale, CA, U.S.A.) using a Respect algorithm with 99% noise rejection confidence and 20 ppm accuracy of average mass identification. Middle-down data were grouped by used NCE values for Fc/2-DOTA proteoform and spectral averaging was performed across the elution peak of this proteoform as well as across NCE replicates using Peak-by-Peak software (Spectroswiss, Lausanne, Switzerland). The resulting averaged fragmentation mass spectra were deconvolved using Deconvolution option of Peak-by-Peak software

(Spectroswiss, Lausanne, Switzerland). Data obtained with 4 different NCE values were combined together to create a fragmentation map with assigned b- and y-fragment ions using ProSight Lite software (Kelleher research group, Northwestern University) with 10 ppm mass accuracy tolerance.

Average degree of conjugation (DoC) calculation from LC-FTMS analysis

The average DoC values were calculated using the intact mass LC-FTMS data with Eq. 1. These results were derived from the relative peak intensities in deconvoluted mass spectra.

$$DoC = \frac{\sum_{k=0}^{k=n} k \times I(DoC_k)}{\sum_{k=0}^{k=n} I(DoC_k)}$$

where I(DoCk) is relative peak intensity of conjugates with k add-on molecules per antibody.

Table S5. Random conjugation experiments with trastuzumab[1]

Compound	Antibody	DoC mAb	Labeled mAb	Selectivity Fc/Fab	DoC Fc	DoC Fab
DOTA-NHS	Tmab	1.34	73%	1.46	0.57	0.4
DTPA-SCN	Tmab	2.16-2.6	88%	1.41	1.13	0.8
FITC	Tmab	3.09	96%	1.05	1.47	1.4

[1]Tmab was incubated with 10 eq. of NHS or isothiocyanate payload and stirred for 16h at RT in 0.2M carbonate buffer pH 9.5

Radiolabeling

Radiolabeling of NODAGA-atezolizumab with Copper-64

Prior radiolabeling, NODAGA-atezolizumab was conditioned in sodium acetate buffer 0.4 M pH 4.6 by ultracentrifugation and stored at 4°C. Copper-64 ([^{64}Cu]copper chloride in 0.1 M HCl solution) was provided by ARRONAX (Saint Herblain, France). NODAGA-atezolizumab was added to the [^{64}Cu]copper in sodium acetate 2.5 M buffer and incubated at 42°C for 30 minutes. Free ([^{64}Cu]copper was then quenched with an excess of EDTA 1 mM. The radiochemical purity of [^{64}Cu]Co-NODAGA-atezolizumab (hereafter referred as [^{64}Cu]Cu-atezolizumab) was controlled by instant thin layer chromatography (iTLC).

ITLC

iTLC analysis were performed using dried iTLC-SG Glass microfiber chromatography paper impregnated with silica gel (Agilent Technologies, Folsom, CA 95630). Citrate buffer 0.1 M pH 5 was used as mobile phase. Radiochromatogram profiles were obtained with a Scan-RAM TLC scanner (LabLogic, Sheffield, United Kingdom). [64Cu]Cu-atezolizumab remained at Rf = 0 while the unbound ([64Cu]cupper migrated with the solvent front.

Radio-SEC

Radio-SEC analysis was performed using an Ultimate 3000 SD System (Thermo Fisher Scientific, Waltham, MA, USA) coupled to a GabiStar detector (Raytest, Straubenhard, Germany). 5 µg of [^{64}Cu]Cu-atezolizumab was loaded and separated with a size exclusion column, XBridge protein BEH 200 Å SEC 3.5 µm, dimension 7.8 × 300 mm (Waters, Baden-Dättwil, Switzerland). Elution was performed using a phosphate buffer saline (PBS) at pH 6.8 (1 mL/min) as mobile phase and was monitored via absorbance at 220/280 nm and γ detection.

In vitro and *in vivo* characterization

Cell line and tumor model

The human breast adenocarcinoma MDA-MB-231 (PD1 high expression) cell line was purchased from American Type Culture Collection (ATCC, Manassas, VA, USA).
The cells were cultured in DMEM (Thermo Fisher Scientific, Waltham, MA, USA) supplemented with 10% fetal bovine serum (FBS, Thermo Fisher Scientific, Waltham, MA, USA) and 1% penicillin/streptomycin (Thermo Fisher Scientific, Waltham, MA, USA). Cells were incubated at 37 °C in a humidified atmosphere containing 5% CO_2. Xenografts of MDA-MB-231 tumors were established by subcutaneous injection of 5×10^6 cells in the right shoulder of 6 – 8 weeks old female BALB/c Nude mice (CAnN.Cg-*Foxn1*^{nu}/Crl, Charles River Laboratories, Wilmington, MA, USA). All experiments involving animals were conducted in compliance with the Swiss legislation for care and use of laboratory animals under the license VD-3781.

Stability in human serum

Immediately after radiolabeling, [^{64}Cu]Cu-atezolizumab was added to 1 mL of human serum and incubated at 37°C under gentle shaking (350 rpm). Sample aliquots were taken after 3, 24, and 48 hours of incubation, and analyzed by iTLC and radio-SEC.

Radio-immunoreactive fraction

The immunoreactive fraction of the radiolabeled atezolizumab was tested by incubating a constant amount of [^{64}Cu]Cu-atezolizumab (15 ng/mL) with increasing numbers (0.25 – 8 × 106) of MDA-MB-231 cells in PBS containing 0.5% Bovine Serum Albumin (PBS/BSA) for 4 hours at 37 °C on a shaking platform. Non-specific binding was assessed by adding an excess of non-radiolabeled atezolizumab (100-fold excess). The cells were centrifuged at 1000 rpm to remove unbound conjugate, and then washed twice with PBS/BSA. The radioactivity of the cell bound conjugate was measured with a gamma counter (Wizard 3", Perkin Elmer, Waltham, Massachusetts). The binding curve was extrapolated to an infinite number of cells by nonlinear regression to calculate the theoretical maximum of cell-bound conjugate (Bmax) using Graphpad Prism 9 (GraphPad Software, San Diego, CA, USA).

[^{64}Cu]Cu-atezolizumab biodistribution study

[^{64}Cu]Cu-atezolizumab (0.25 MBq corresponding to 0.05 µg [^{64}Cu]Cu-atezolizumab completed with 49.95 µg of cold atezolizumab in 100 µl of 0.9% NaCl injectable saline solution) was injected into the lateral tail vein of mice bearing MDA-MB-231 xenografts without anesthesia. Additionally, the specificity of [^{64}Cu]Cu-atezolizumab for PD1 was assessed in a competition experiment whereby cold atezolizumab was coinjected in excess (2 mg).

At different time points (2, 24 and 48 hours post injection), mice bearing MDA-MB-231 tumors were euthanized by CO_2 inhalation and exsanguinated. Blood was collected, organs and tumors were removed, weighed, and the radioactivity was measured with a gamma counter (Wizard 3", Perkin Elmer, Waltham, Massachusetts). The results are expressed as the percentage of injected dose per gram of organs (%ID/g) ± standard deviation (n = 4).

[64Cu]Cu-atezolizumab PET imaging study

PET/CT images were acquired using an Albira Si PET/SPECT/CT (Bruker Biospin Corporation, Woodbridge, CT, USA). 9 MBq of [^{64}Cu]Cu-atezolizumab (corresponding to 50 µg [^{64}Cu]Cu-atezolizumab) was injected into mice bearing MDA-MB-231 xenografts, and PET/CT images were acquired at 2, 24 and 48 hours post injection. Mice were anesthetized for the duration of the imaging experiments by inhalation of 1.5% isoflurane/O_2 and placed on a heated bed (30 – 35 ºC).

For PET imaging, static acquisitions of 10 to 30 minutes (accumulation of 360 – 720 x 10^6 events) were done with an axial FOV of 150 mm and detection of the photopeak at 511 keV ± 30%. For image reconstruction the algorithm used was maximum likelihood expectation maximization (MLME) with 12 iterations and corrected for scatter, random events detection and radionuclide decay. The CT anatomical reference image was obtained with the following parameters: 400 µA intensity and 35 kV voltage, 600 projections. CT images were reconstructed using a filtered back-projection (FBP) algorithm with de-ringing correction. Image preparation and analysis was done using PMOD software (PMOD technologies, version 4.3, Zurich, Switzerland). The volume of interest around the tumors were drawn semi-automatically using the iso-contour tool on the PET image and correlated with the fused CT image. CT and PET voxels are in Hounsfield Units (HU) and % ID/g respectively.

Figures

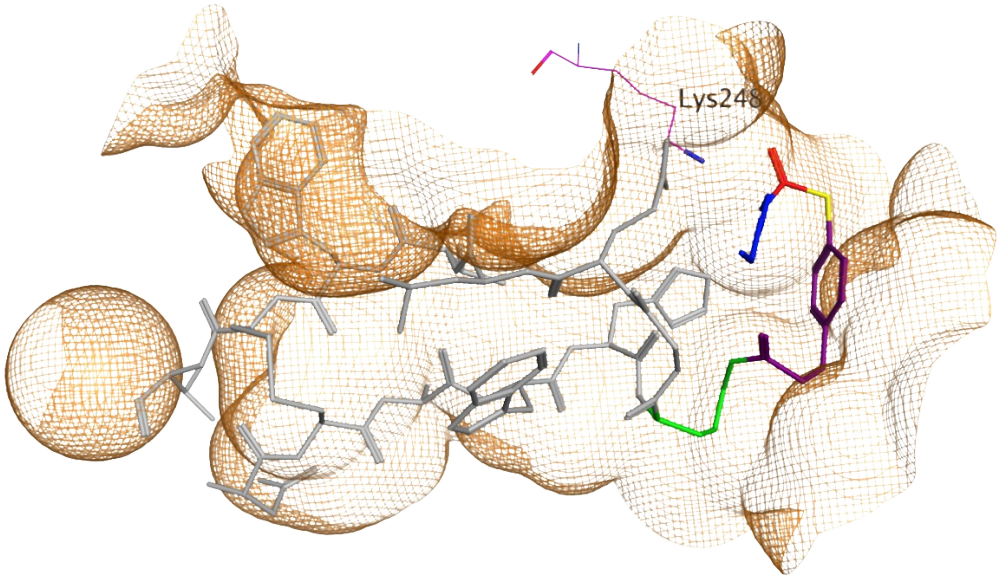

Figure S1. Energy minimization of Fc-III-L6Orn-thioester reactive conjugate.
The two methylenes that provide additional flexibility are color-coded in purple next to the phenyl ring (green: L6Orn; purple: chemical modulator; yellow: thiol; red: carbonyl; blue: linker).

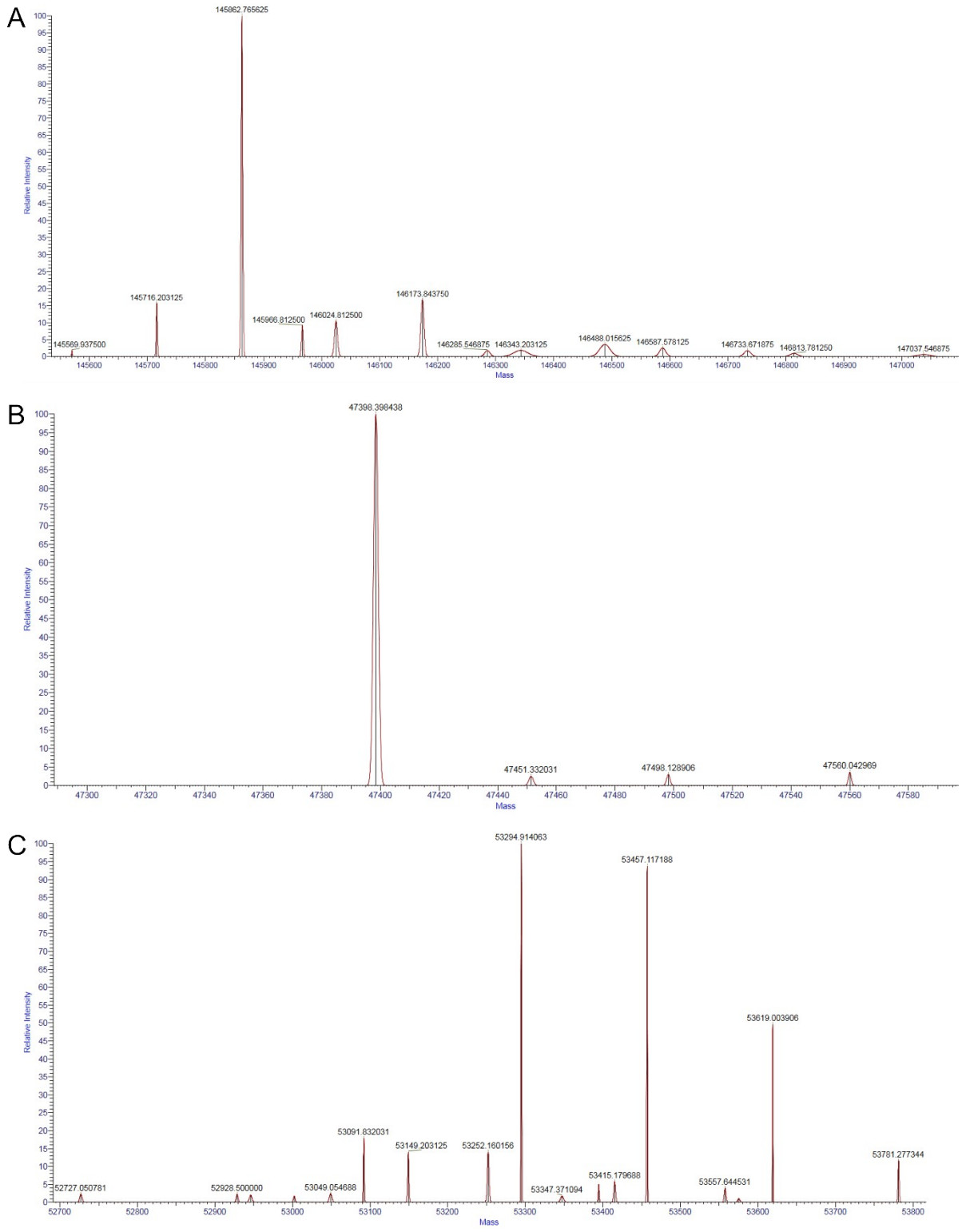

Figure S2. Deconvolved mass spectra of trastuzumab.
Deglycosylated (A); glycosylated trastuzumab cleaved by GingisKHAN enzyme into Fab (B) and Fc (C).

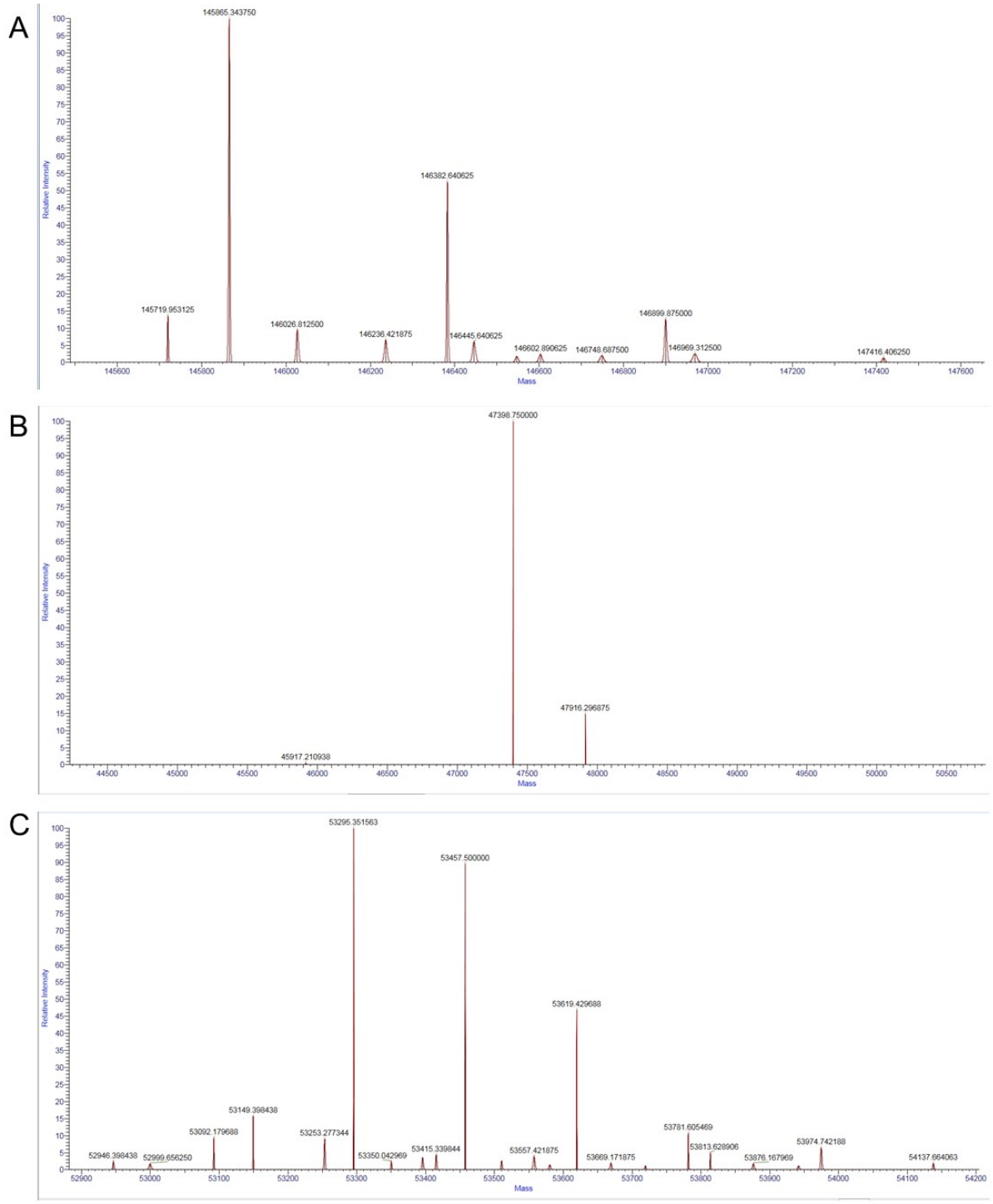

Figure S3. Deconvolved mass spectra of trastuzumab-DOTA (after the reaction of Fc-III-D1K-DOTA with trastuzumab).
Deglycosylated intact antibody conjugate (A); antibody conjugate cleaved into Fab (B) and Fc (C) with GingisKHAN enzyme.

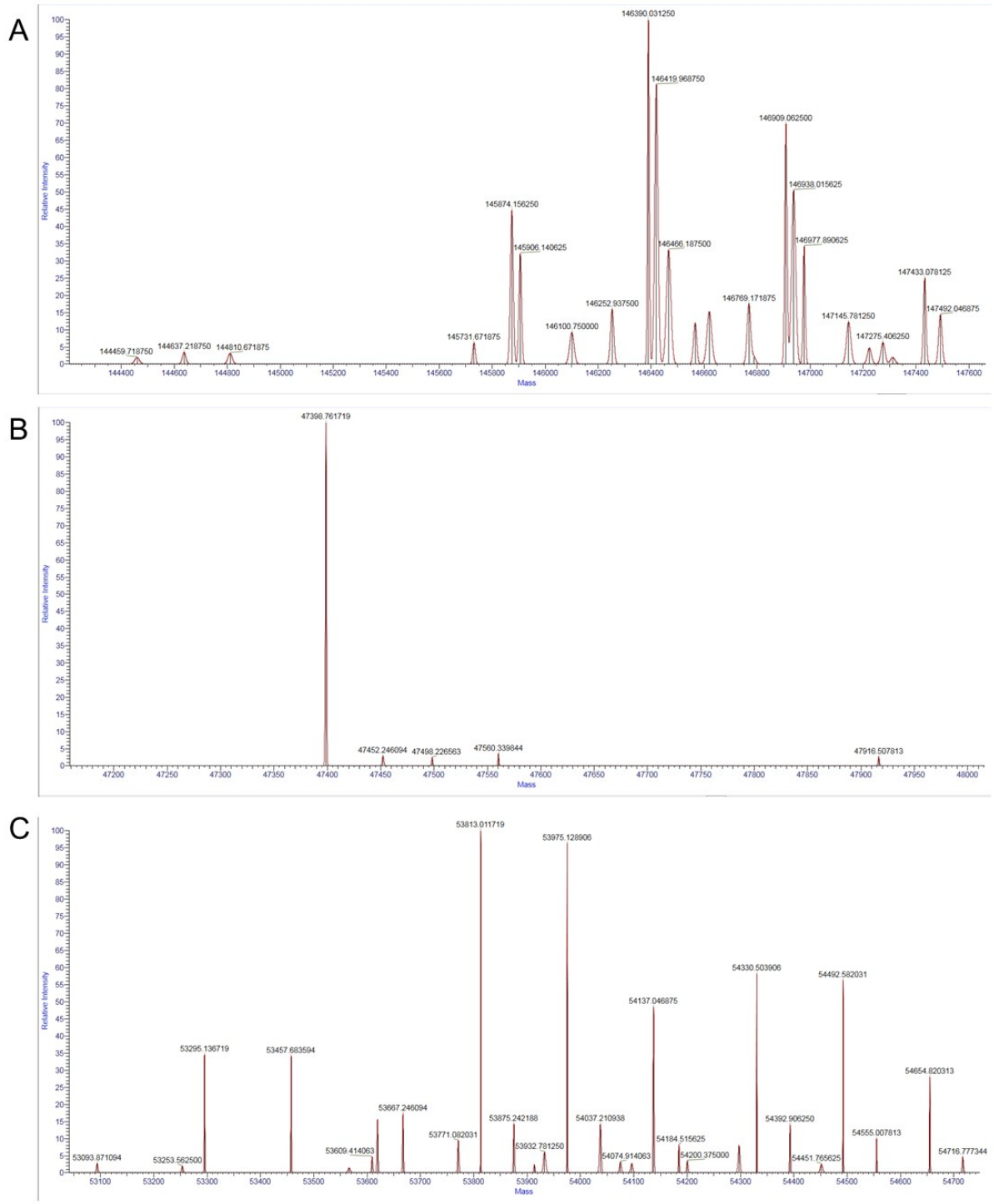

Figure S4. Deconvolved mass spectra of trastuzumab-DOTA (after the reaction of Fc-III-A3K-DOTA with trastuzumab).
Deglycosylated intact antibody conjugate (A); antibody conjugate cleaved into Fab (B) and Fc (C) with GingisKHAN enzyme.

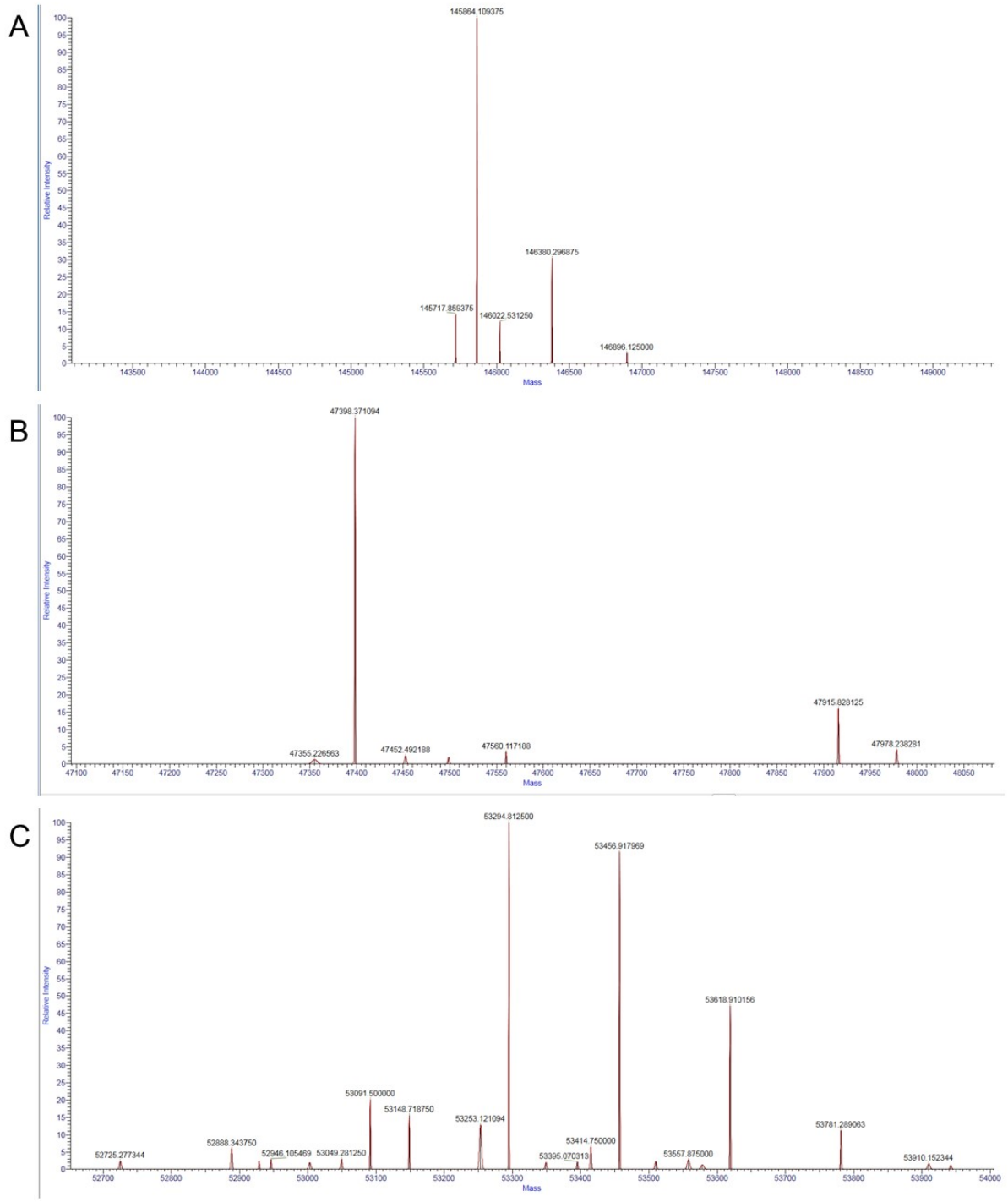

Figure S5. Deconvolved mass spectra of trastuzumab-DOTA (after the reaction of Fc-III-W4K-DOTA with trastuzumab).
Deglycosylated intact antibody conjugate (A); antibody conjugate cleaved into Fab (B) and Fc (C) with GingisKHAN enzyme.

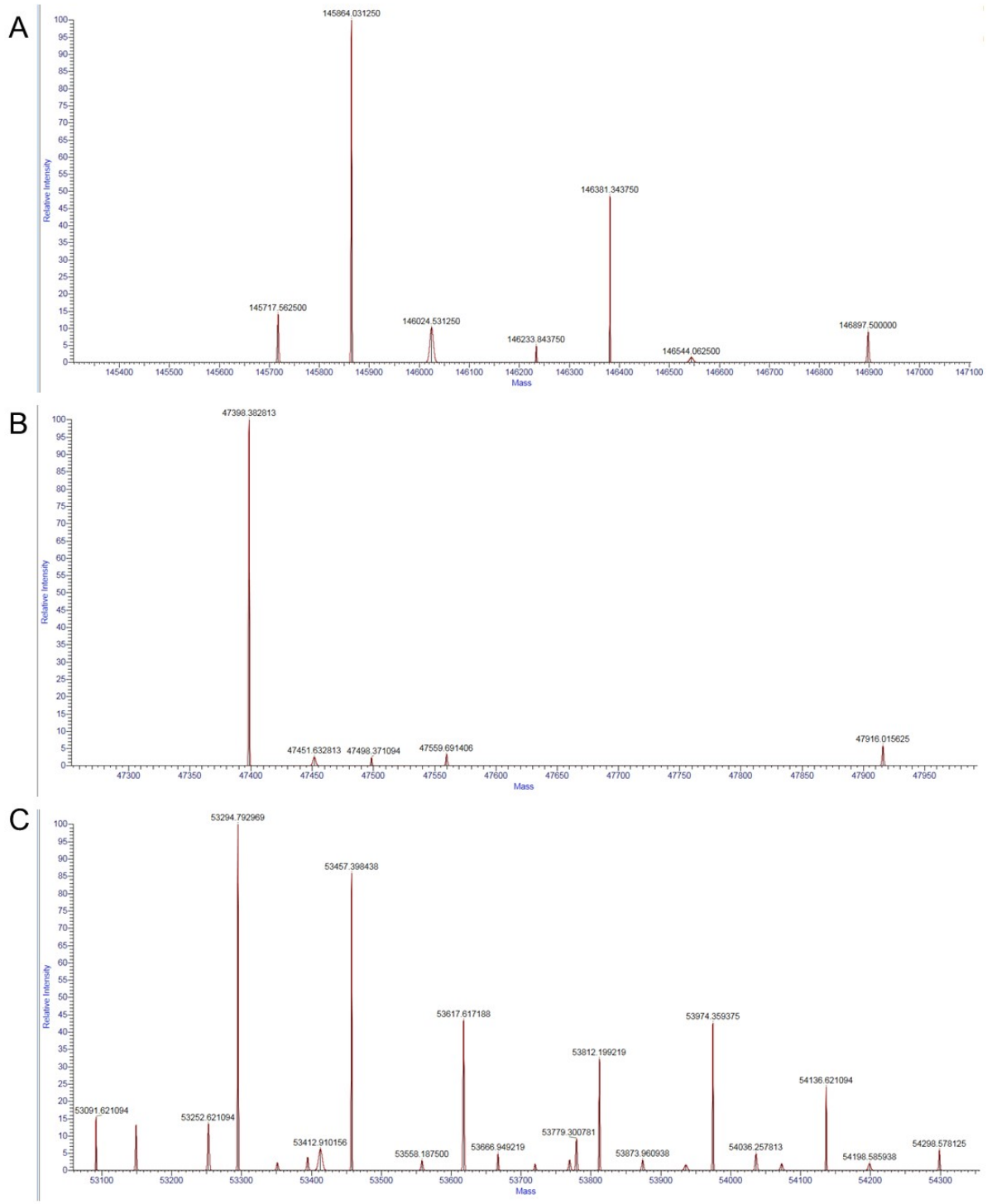

Figure S6. Deconvolved mass spectra of trastuzumab-DOTA (after the reaction of Fc-III-H5K-DOTA with trastuzumab).
Deglycosylated intact antibody conjugate (A); antibody conjugate cleaved into Fab (B) and Fc (C) with GingisKHAN enzyme.

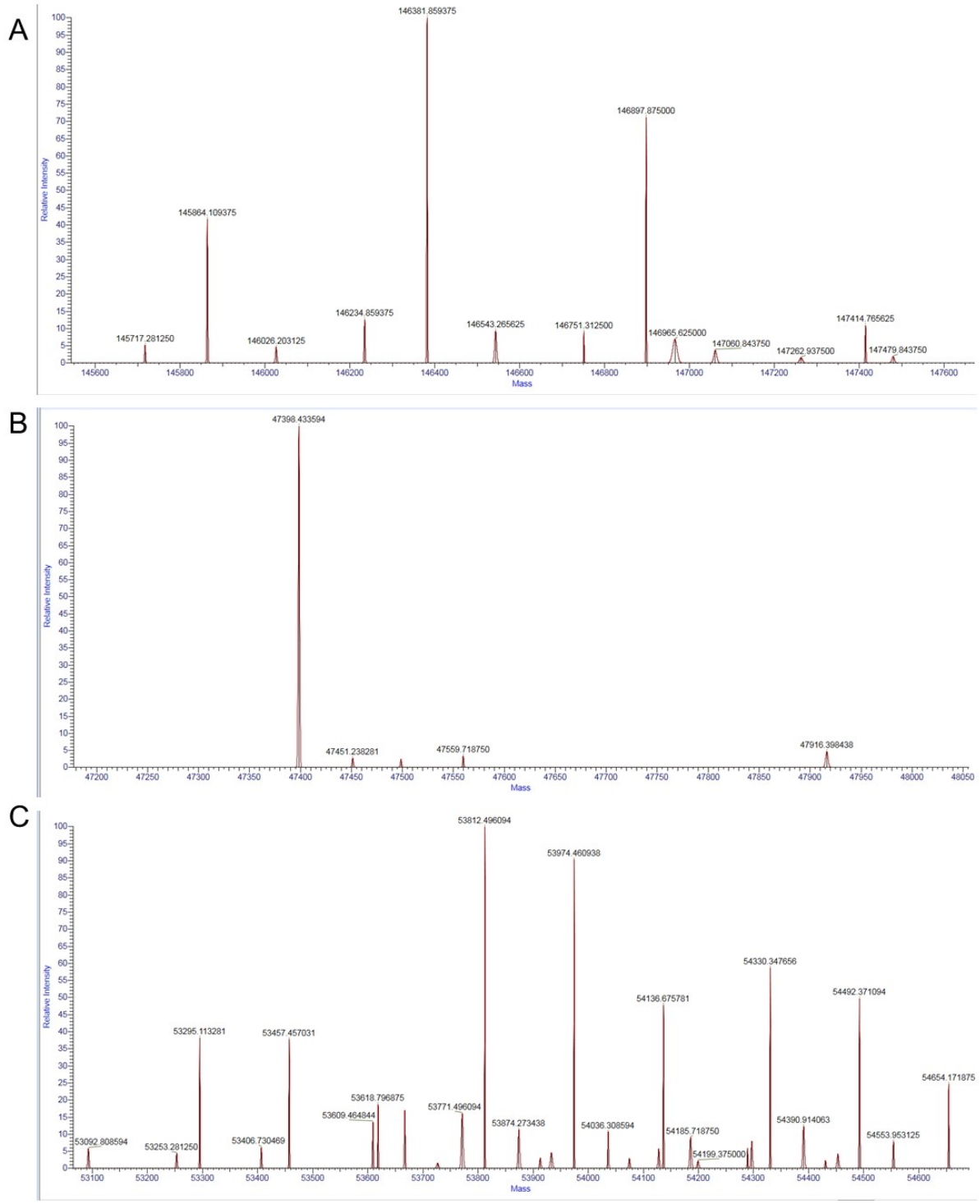

Figure S7. Deconvolved mass spectra of trastuzumab-DOTA (after the reaction of Fc-III-L6K-DOTA with trastuzumab).
Deglycosylated intact antibody conjugate (A); antibody conjugate cleaved into Fab (B) and Fc (C) with GingisKHAN enzyme.

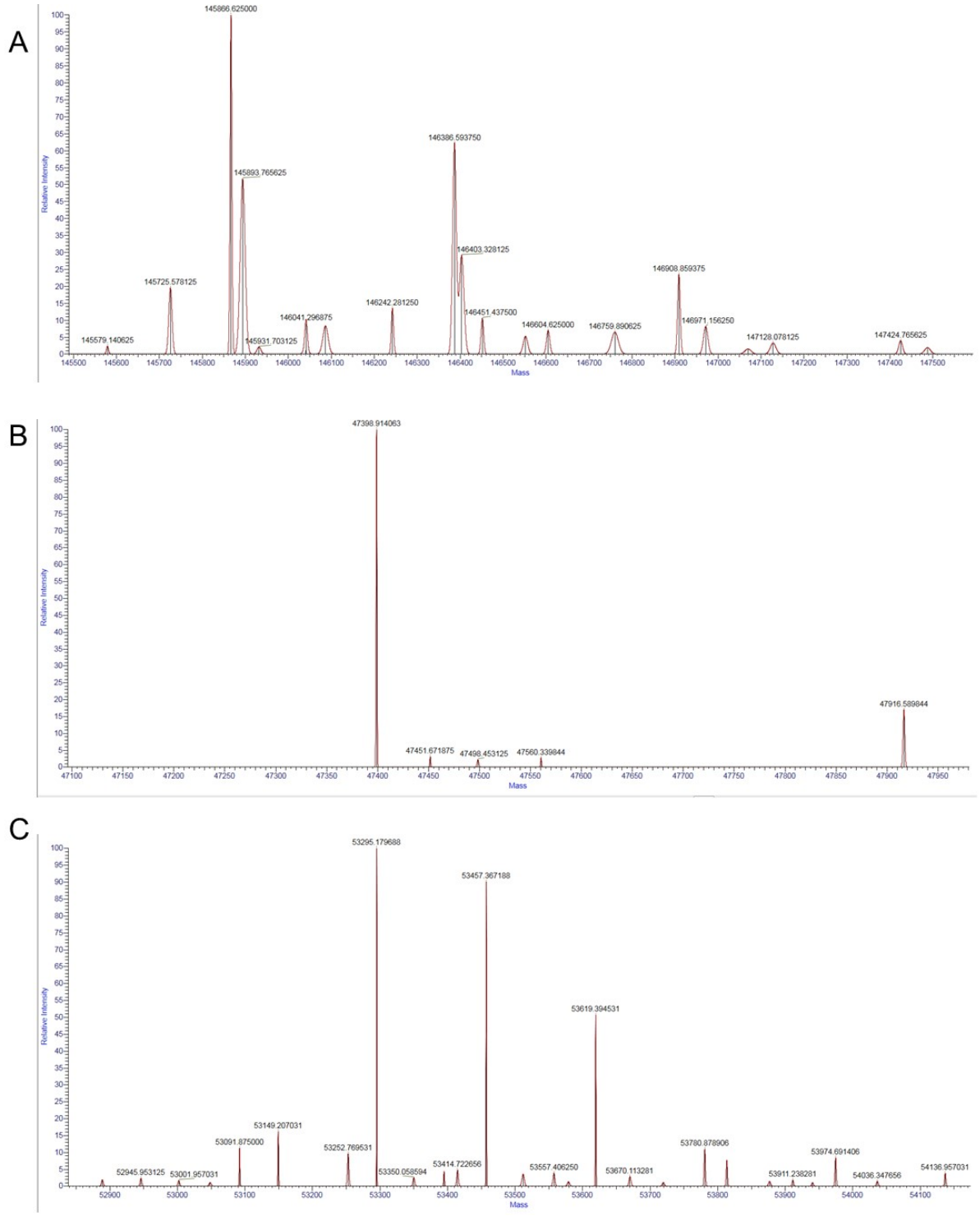

Figure S8. Deconvolved mass spectra of trastuzumab-DOTA (after the reaction of Fc-III-G7K-DOTA with trastuzumab).
Deglycosylated intact antibody conjugate (A); antibody conjugate cleaved into Fab (B) and Fc (C) with GingisKHAN enzyme.

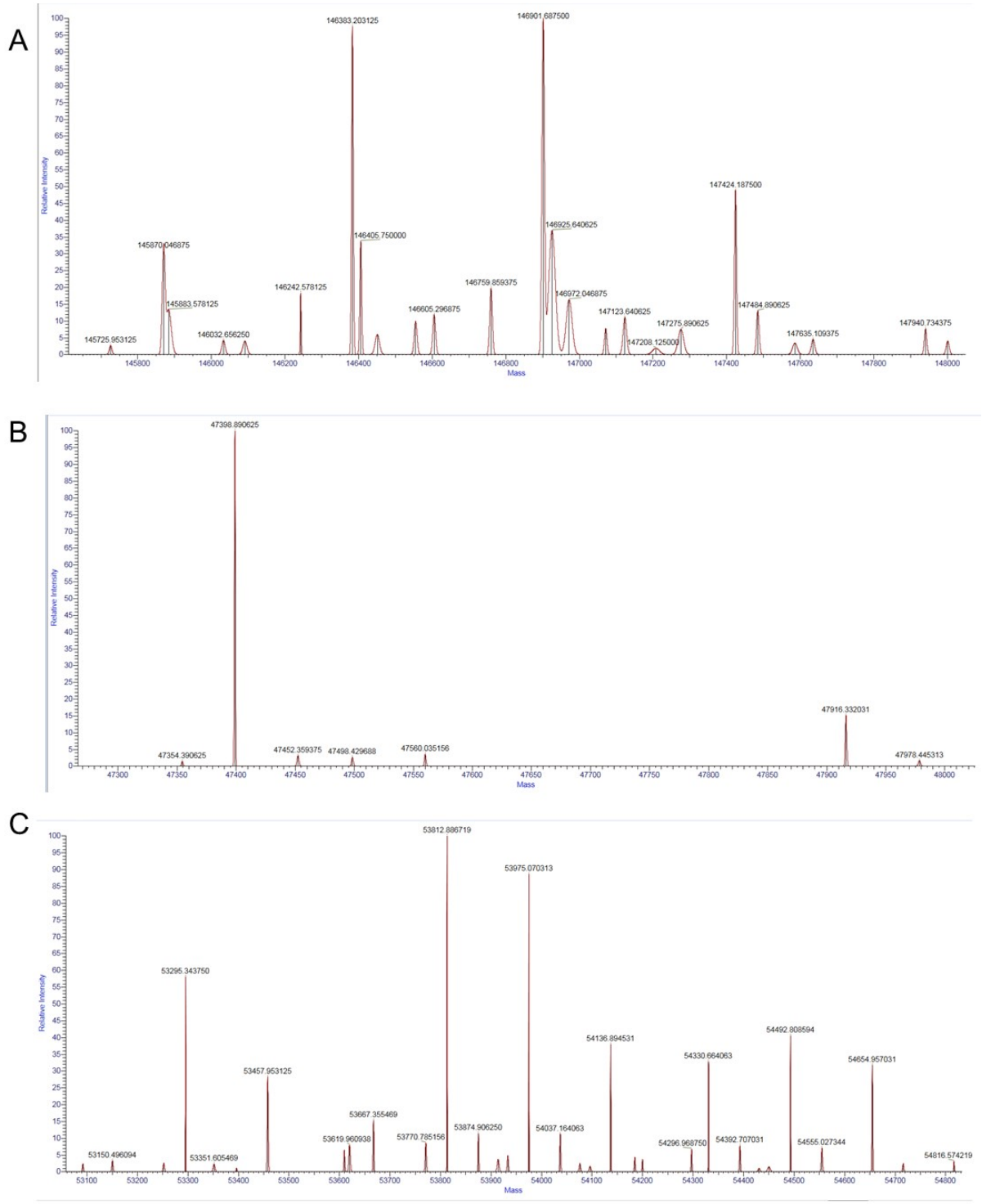

Figure S9. Deconvolved mass spectra of trastuzumab-DOTA (after the reaction of Fc-III-E8K-DOTA with trastuzumab).
Deglycosylated intact antibody conjugate (A); antibody conjugate cleaved into Fab (B) and Fc (C) with GingisKHAN enzyme.

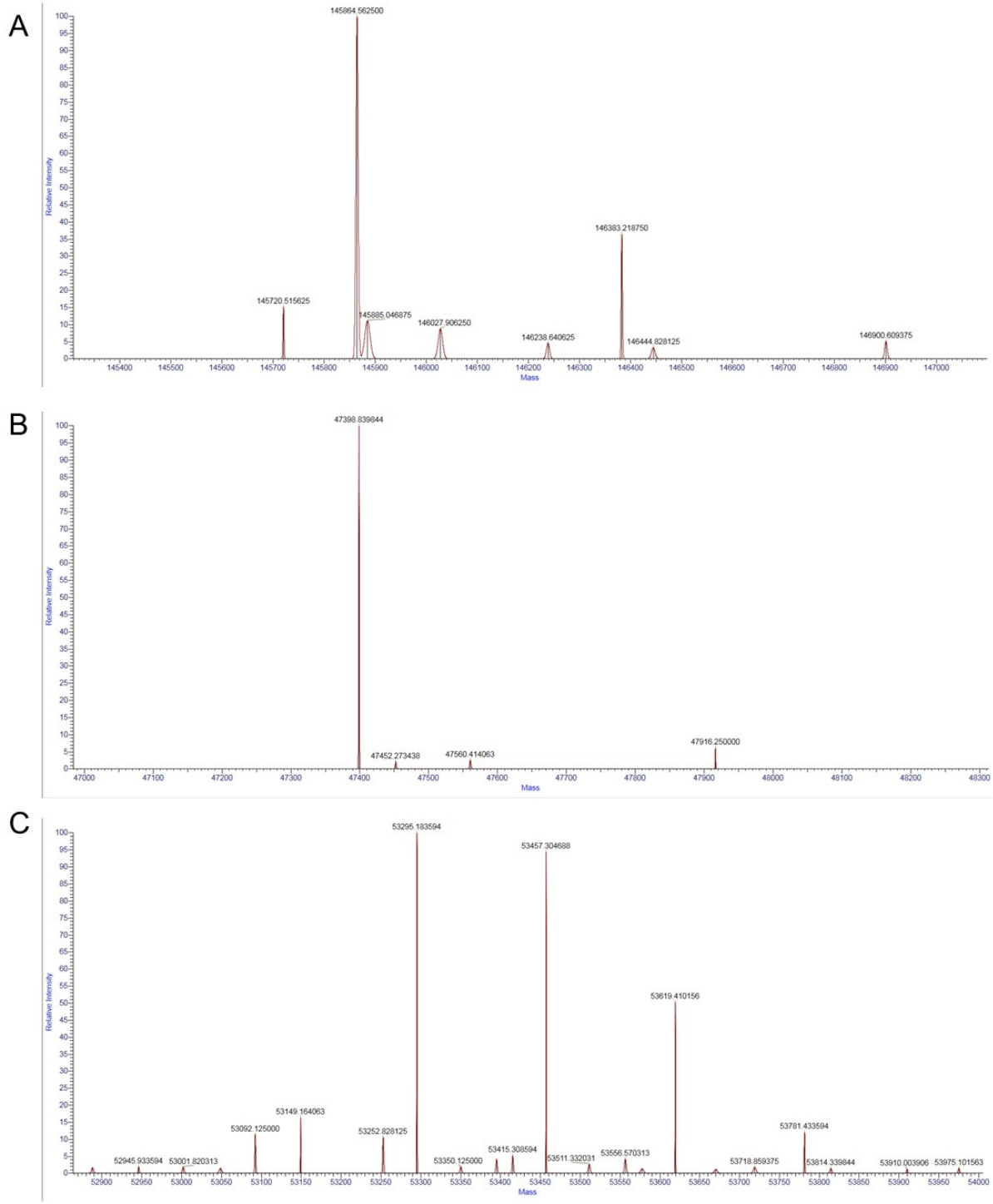

Figure S10. Deconvolved mass spectra of trastuzumab-DOTA (after the reaction of Fc-III-L9K-DOTA with trastuzumab).
Deglycosylated intact antibody conjugate (A); antibody conjugate cleaved into Fab (B) and Fc (C) with GingisKHAN enzyme.

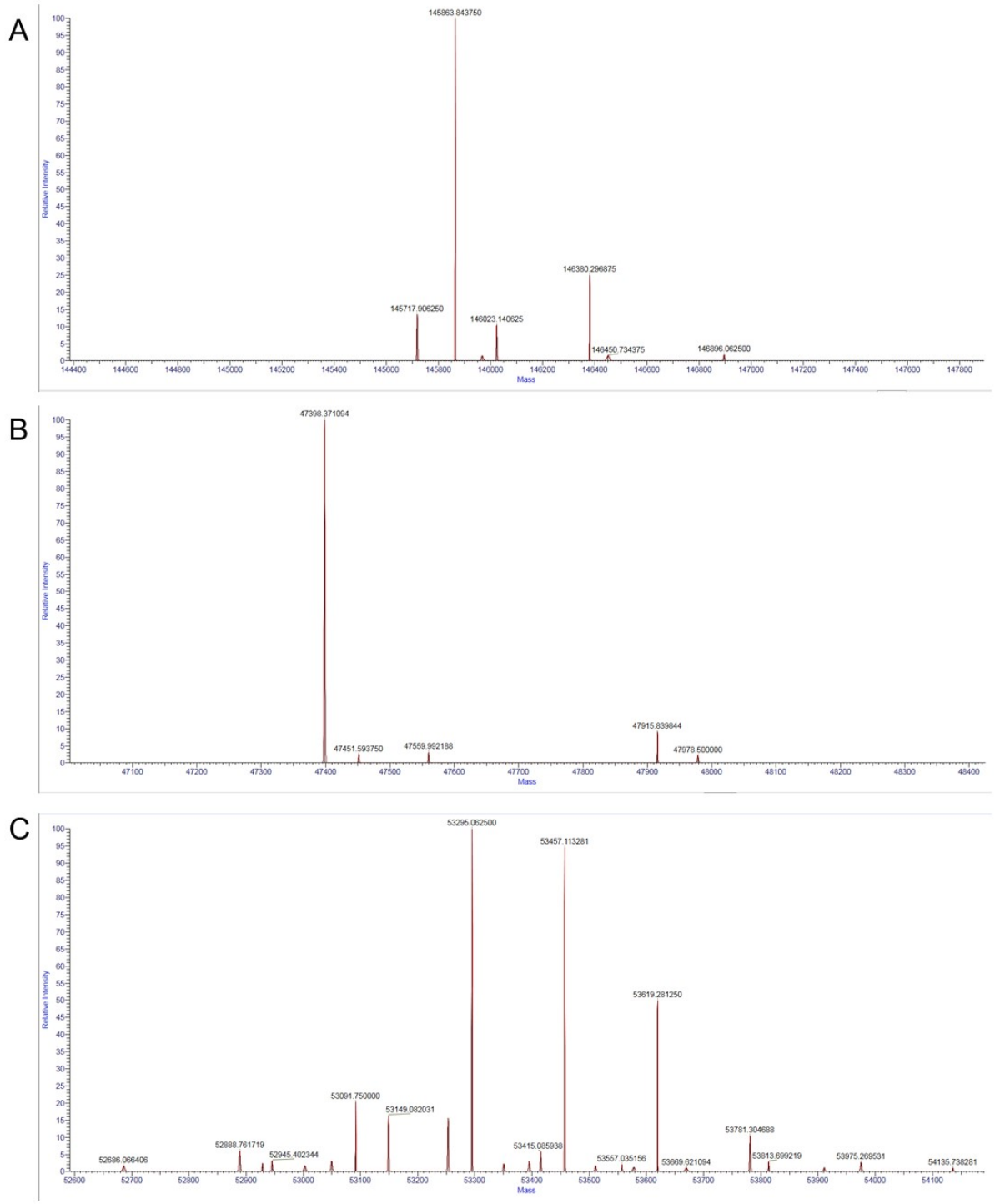

Figure S11. Deconvolved mass spectra of trastuzumab-DOTA (after the reaction of Fc-III-V10K-DOTA with trastuzumab).
Deglycosylated intact antibody conjugate (A); antibody conjugate cleaved into Fab (B) and Fc (C) with GingisKHAN enzyme.

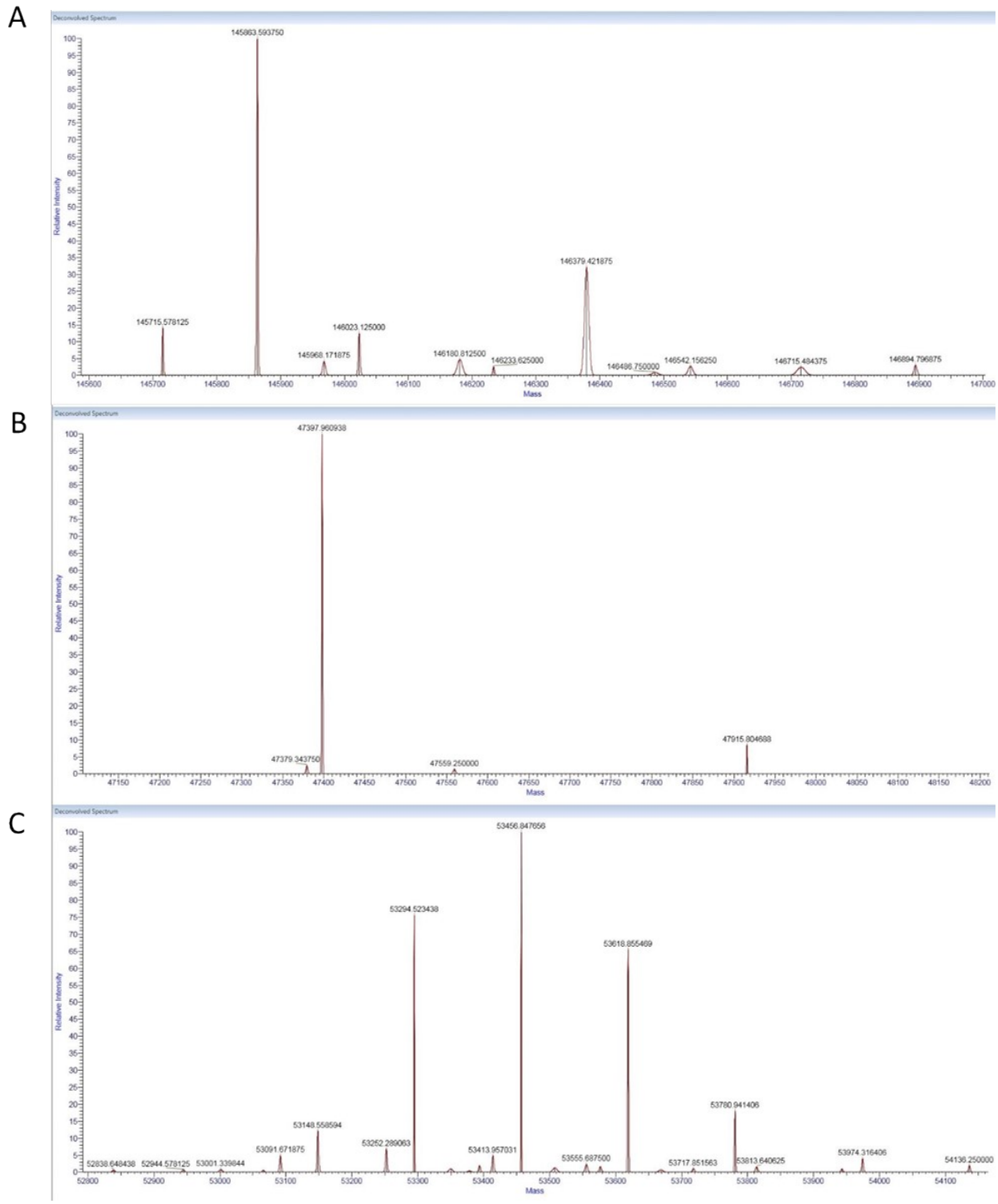

Figure S12. Deconvolved mass spectra of trastuzumab-DOTA (after the reaction of Fc-III-W11K-DOTA with trastuzumab).
Deglycosylated intact antibody conjugate (A); antibody conjugate cleaved into Fab (B) and Fc (C) with GingisKHAN enzyme.

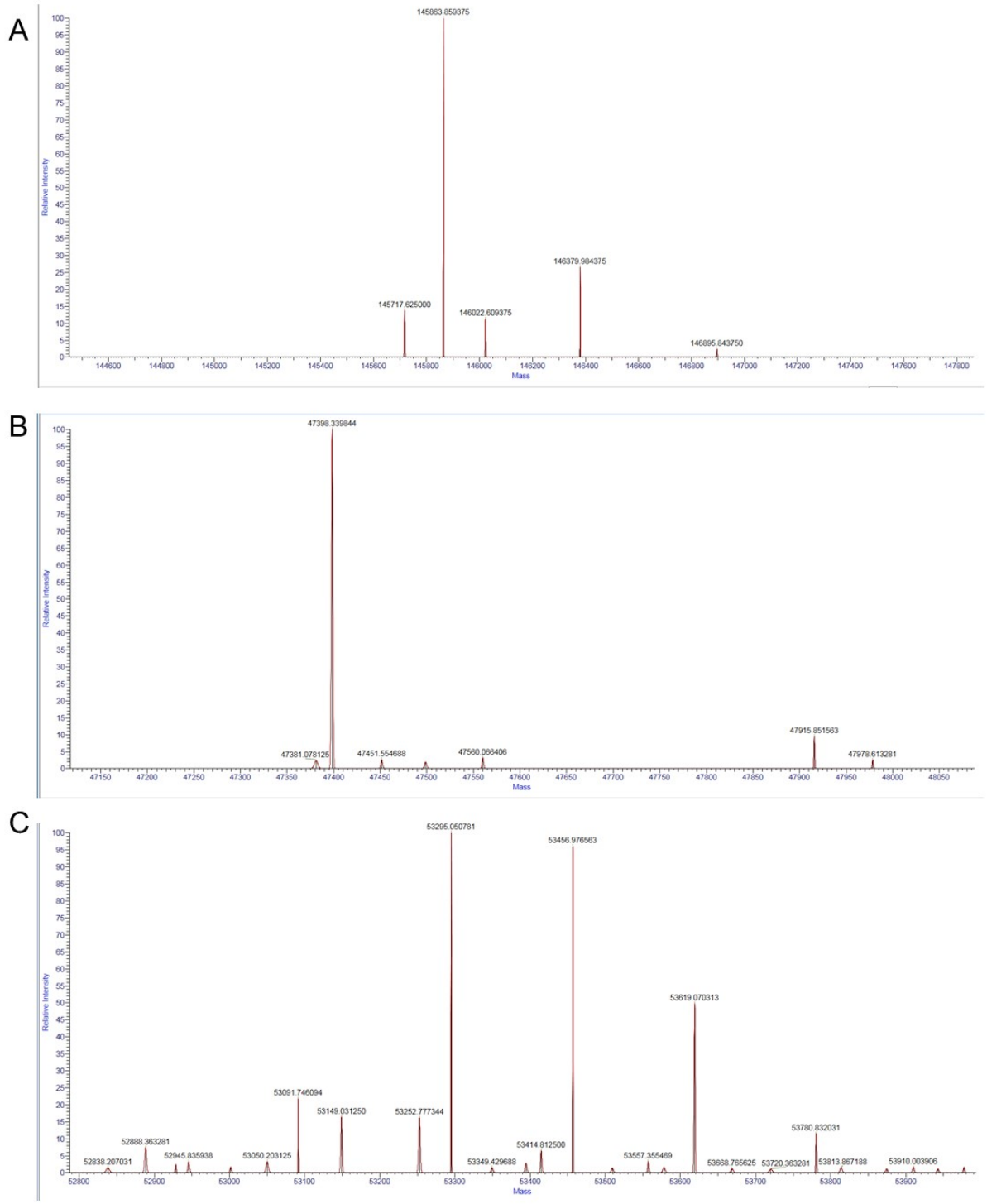

Figure S13. Deconvolved mass spectra of trastuzumab-DOTA (after the reaction of Fc-III-T13K-DOTA with trastuzumab).
Deglycosylated intact antibody conjugate (A); antibody conjugate cleaved into Fab (B) and Fc (C) with GingisKHAN enzyme.

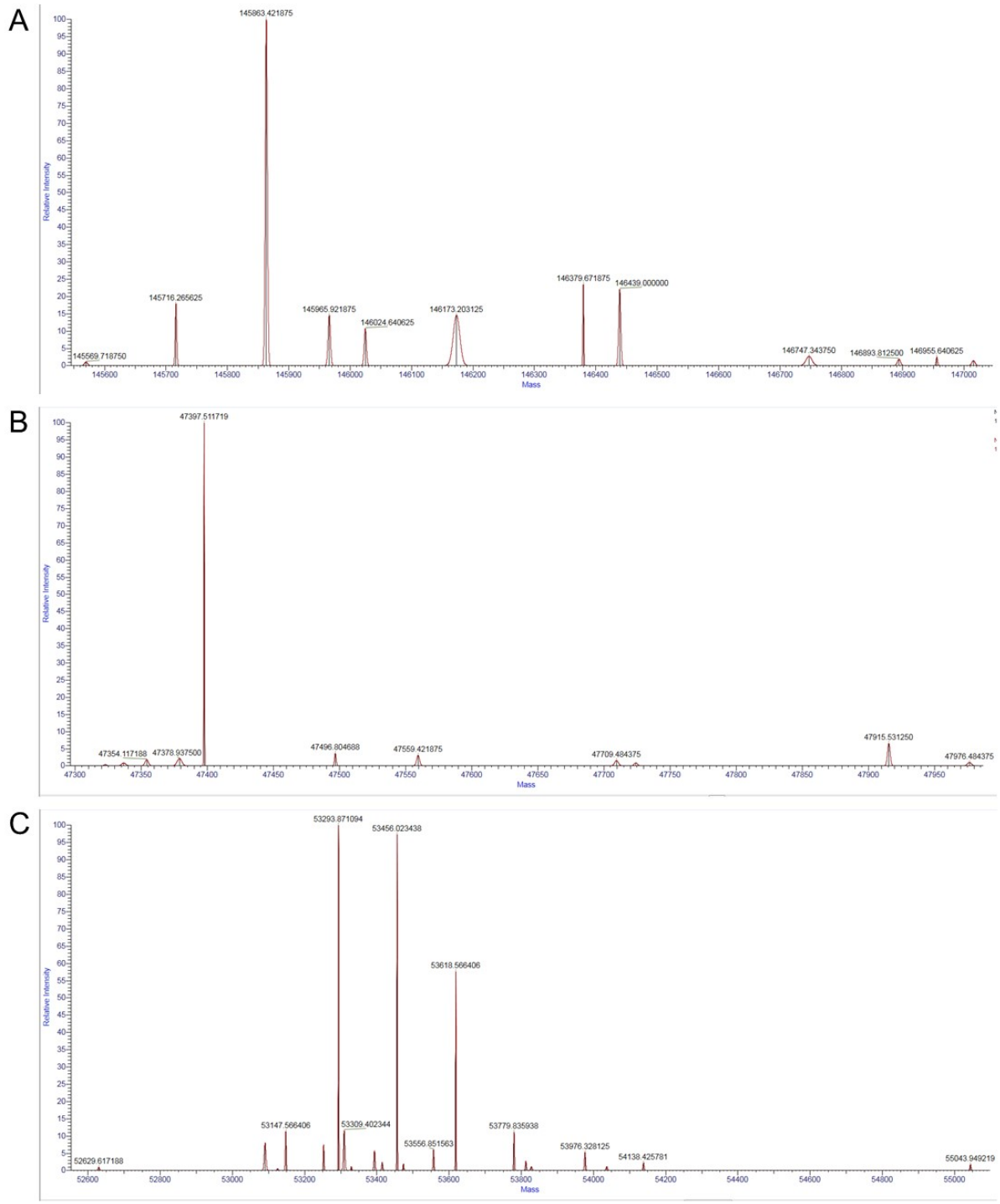

Figure S14. Deconvolved mass spectra of trastuzumab-DOTA (after the reaction of Fc-III-A3Dap-DOTA with trastuzumab).
Deglycosylated intact antibody conjugate (A); antibody conjugate cleaved into Fab (B) and Fc (C) with GingisKHAN enzyme.

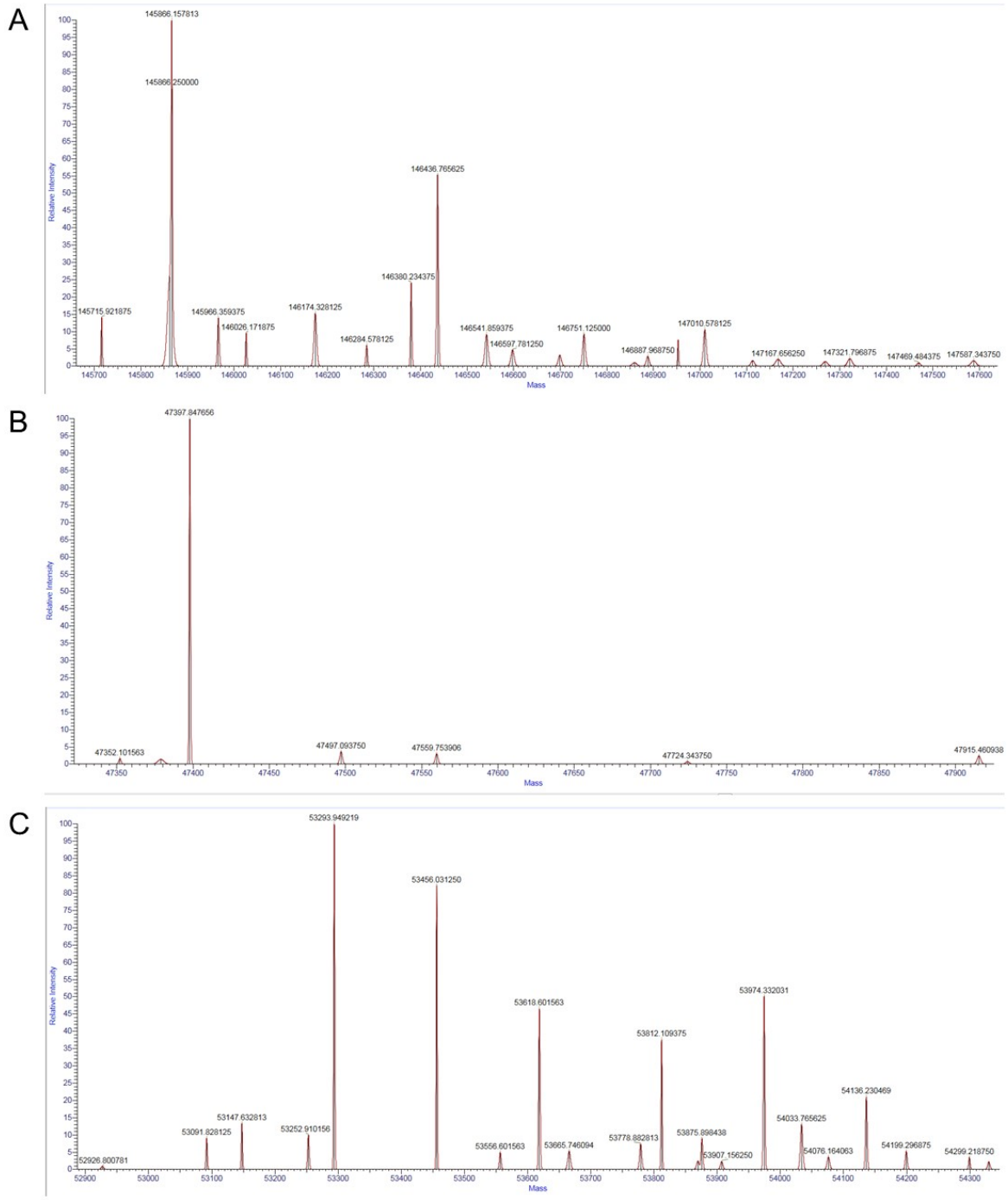

Figure S15. Deconvolved mass spectra of trastuzumab-DOTA (after the reaction of Fc-III-A3Orn-DOTA with trastuzumab). Deglycosylated intact antibody conjugate (A); antibody conjugate cleaved into Fab (B) and Fc (C) with GingisKHAN enzyme.

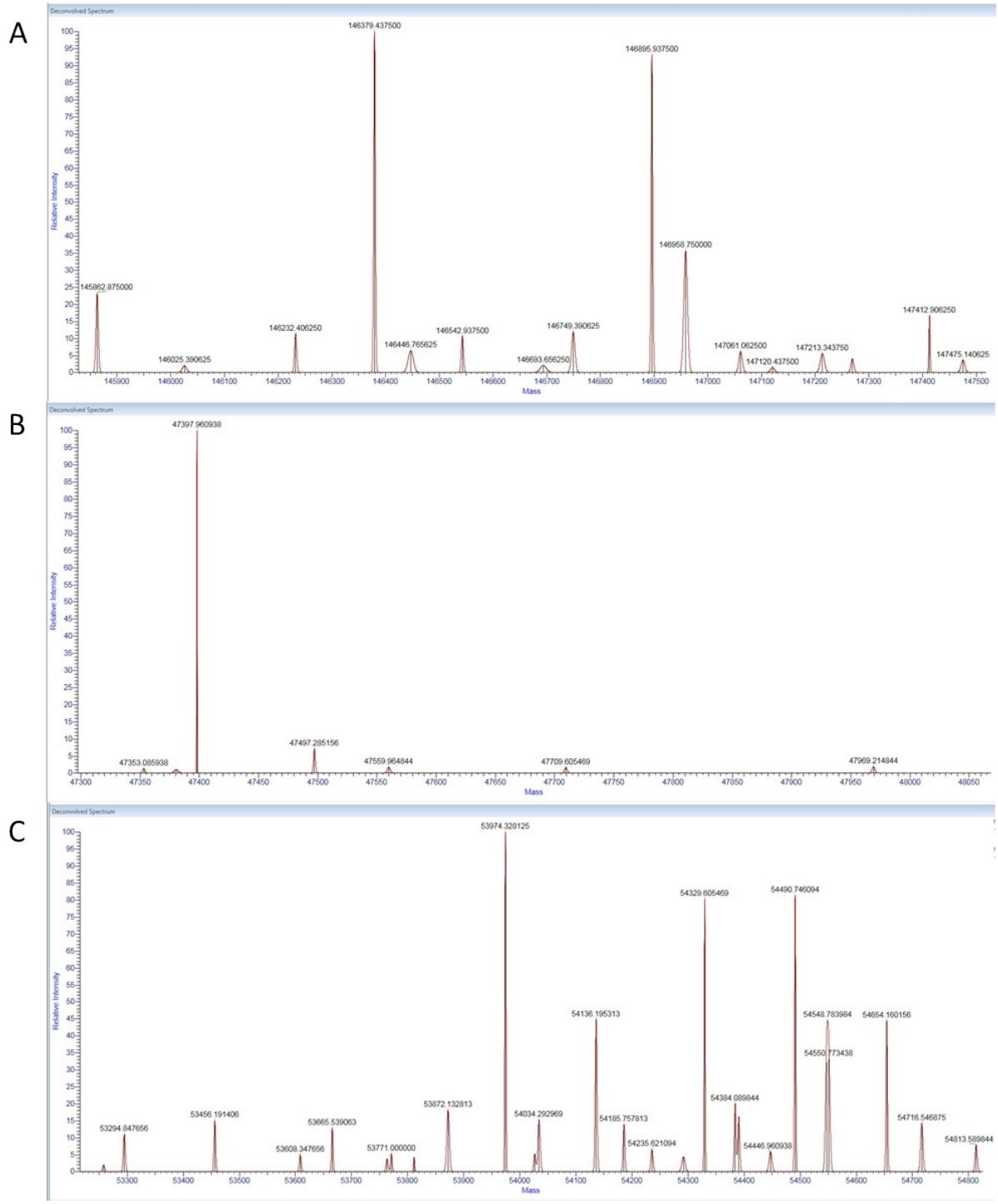

Figure S16. Deconvolved mass spectra of trastuzumab-DOTA (after the reaction of Fc-III-A3hK-DOTA with trastuzumab).
Deglycosylated intact antibody conjugate (A); antibody conjugate cleaved into Fab (B) and Fc (C) with GingisKHAN enzyme.

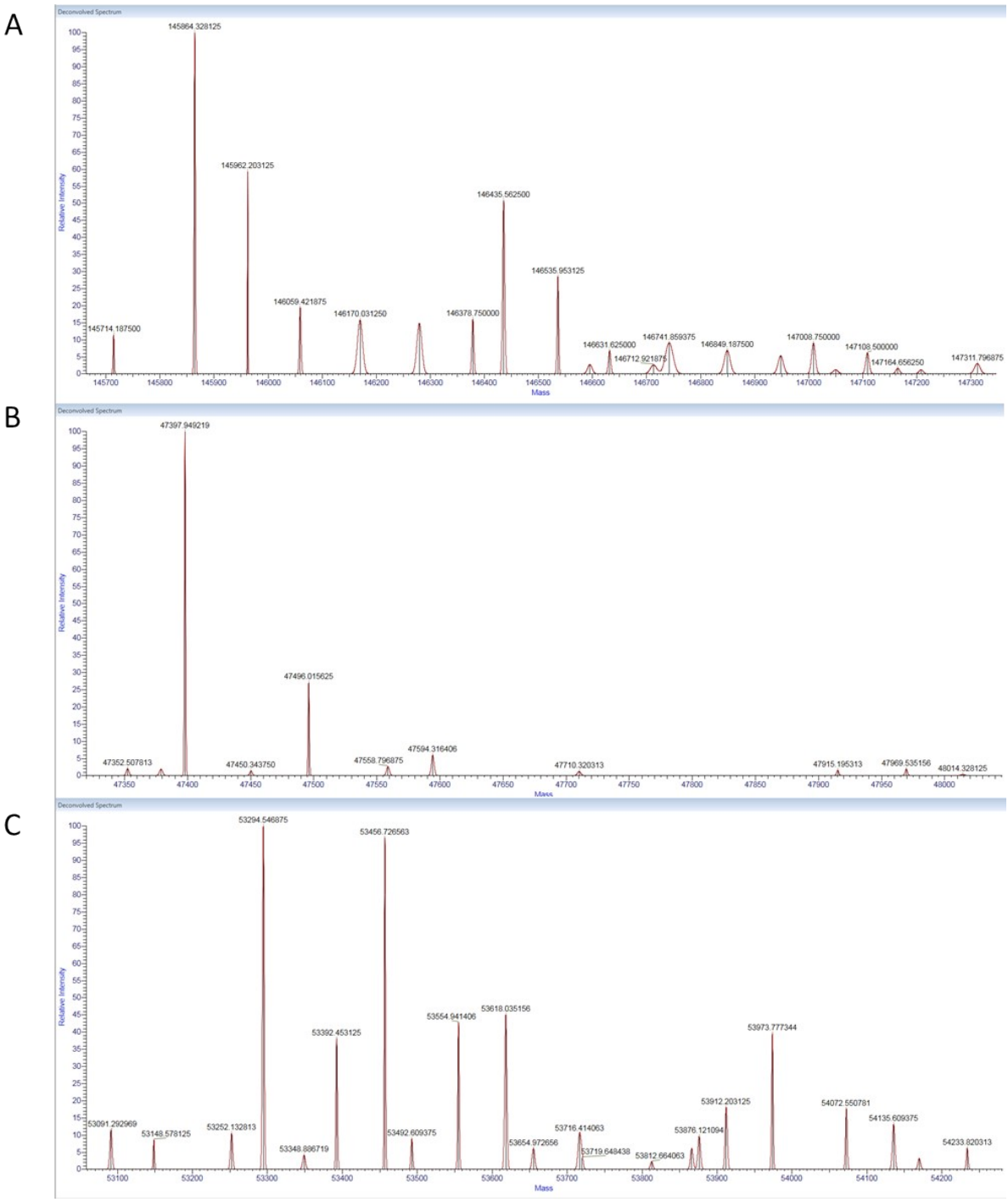

Figure S17. Deconvolved mass spectra of trastuzumab-DOTA (after the reaction of Fc-III-A3Dap-PEG1-DOTA with trastuzumab).
Deglycosylated intact antibody conjugate (A); antibody conjugate cleaved into Fab (B) and Fc (C) with GingisKHAN enzyme.

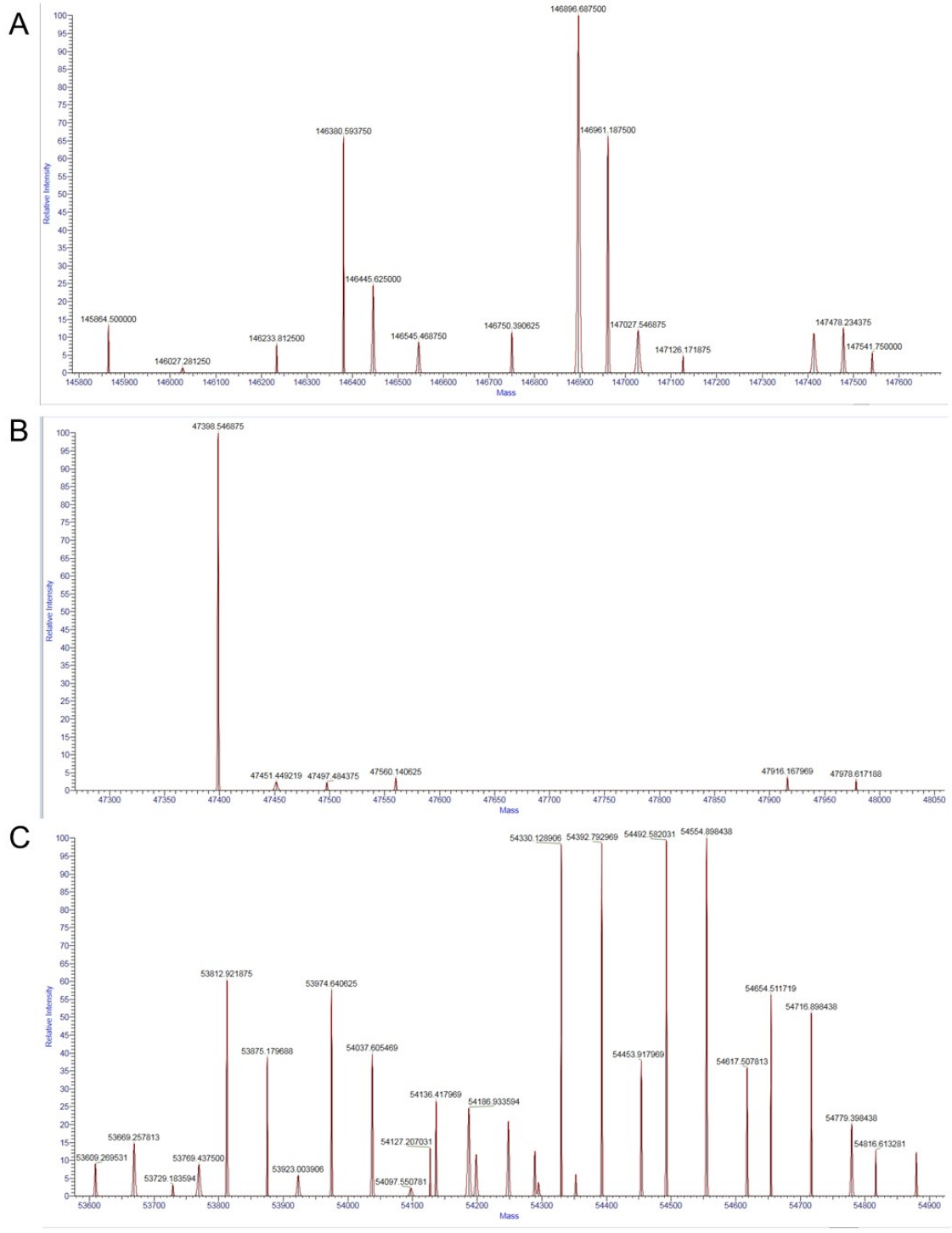

Figure S18. Deconvolved mass spectra of trastuzumab-DOTA (after the reaction of Fc-III-L6Dap-DOTA with trastuzumab).
Deglycosylated intact antibody conjugate (A); antibody conjugate cleaved into Fab (B) and Fc (C) with GingisKHAN enzyme.

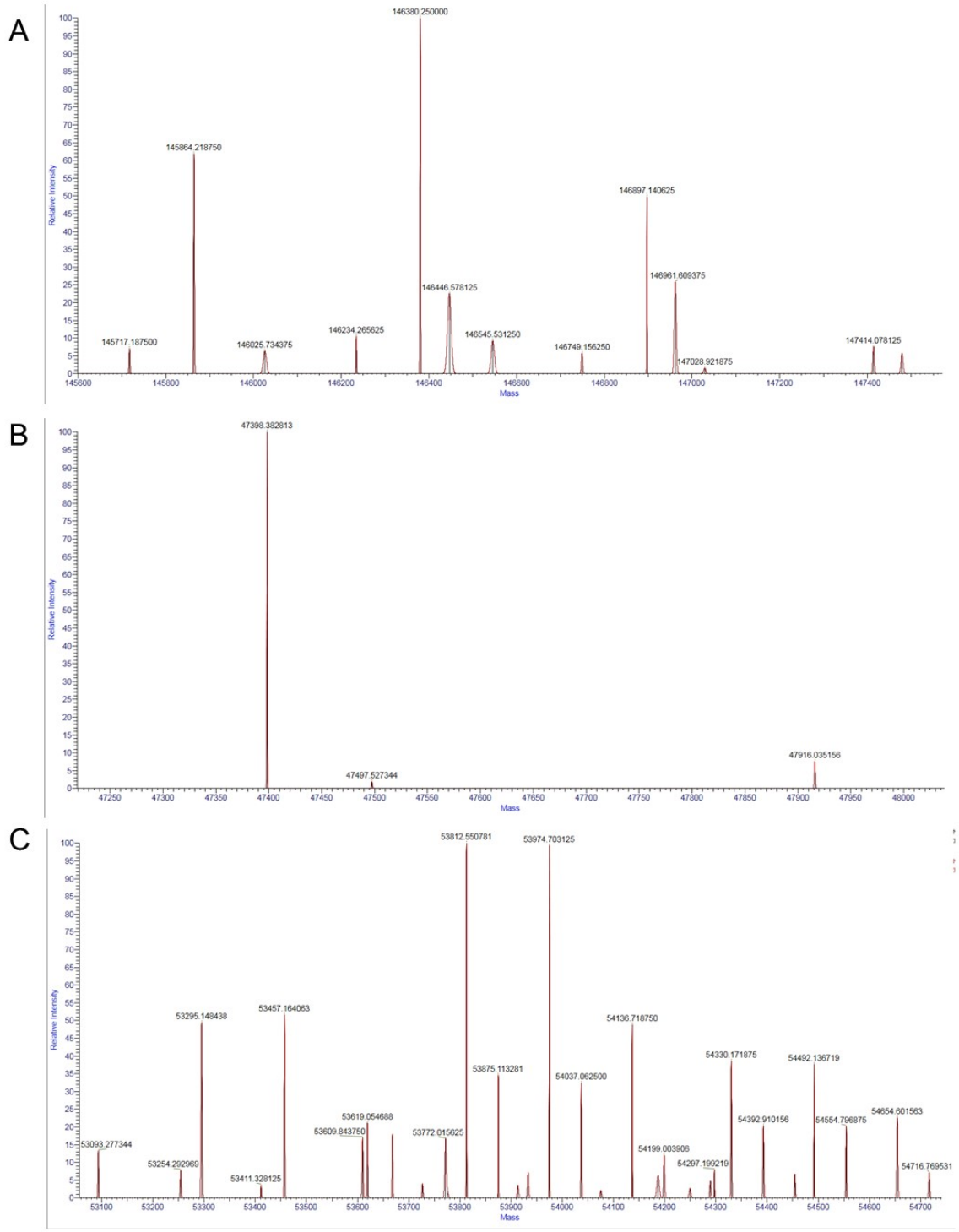

Figure S19. Deconvolved mass spectra of trastuzumab-DOTA (after the reaction of Fc-III-L6Dab-DOTA with trastuzumab).
Deglycosylated intact antibody conjugate (A); antibody conjugate cleaved into Fab (B) and Fc (C) with GingisKHAN enzyme.

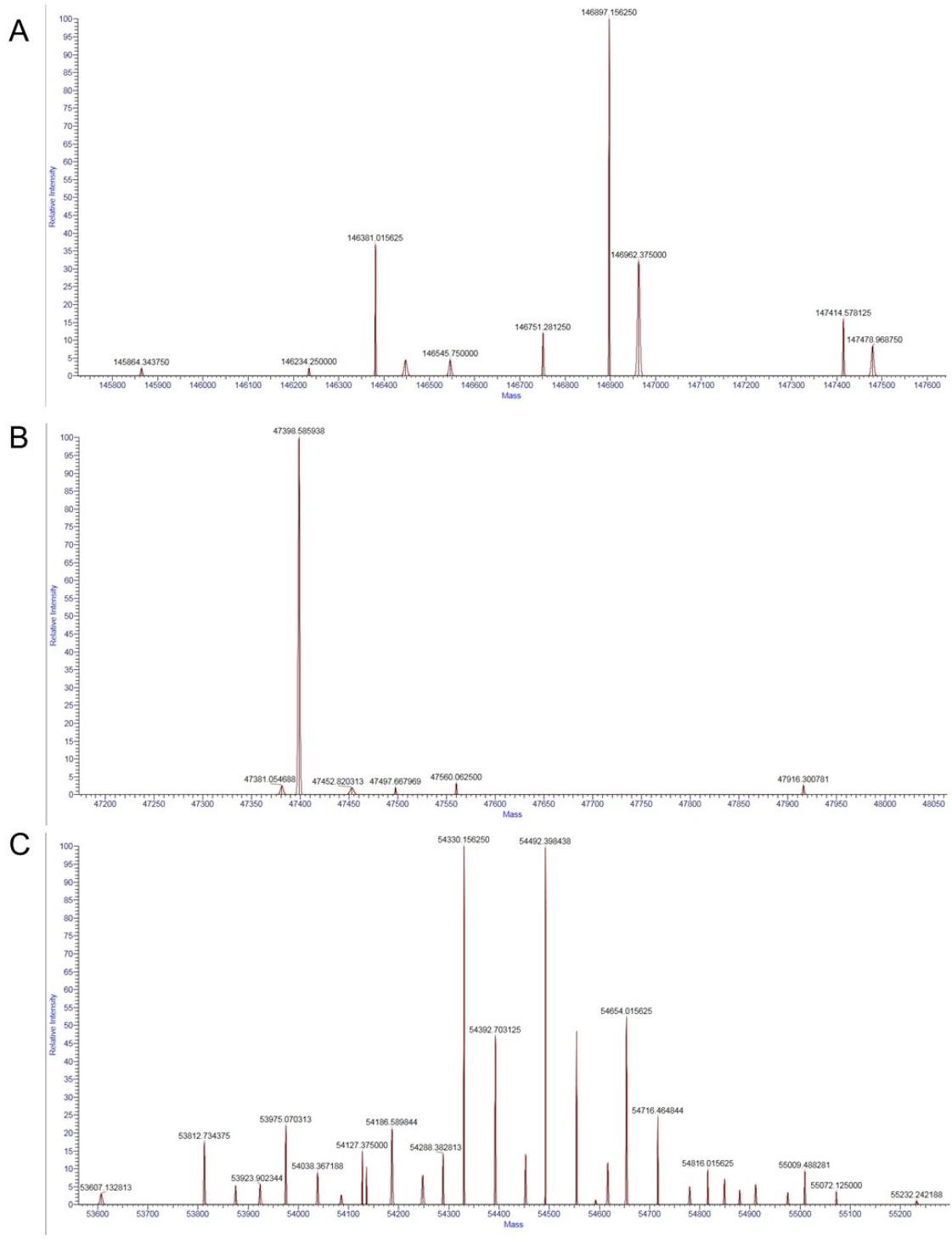

Figure S20. Deconvolved mass spectra of trastuzumab-DOTA (after the reaction of Fc-III-L6Orn-DOTA with trastuzumab).
Deglycosylated intact antibody conjugate (A); antibody conjugate cleaved into Fab (B) and Fc (C) with GingisKHAN enzyme.

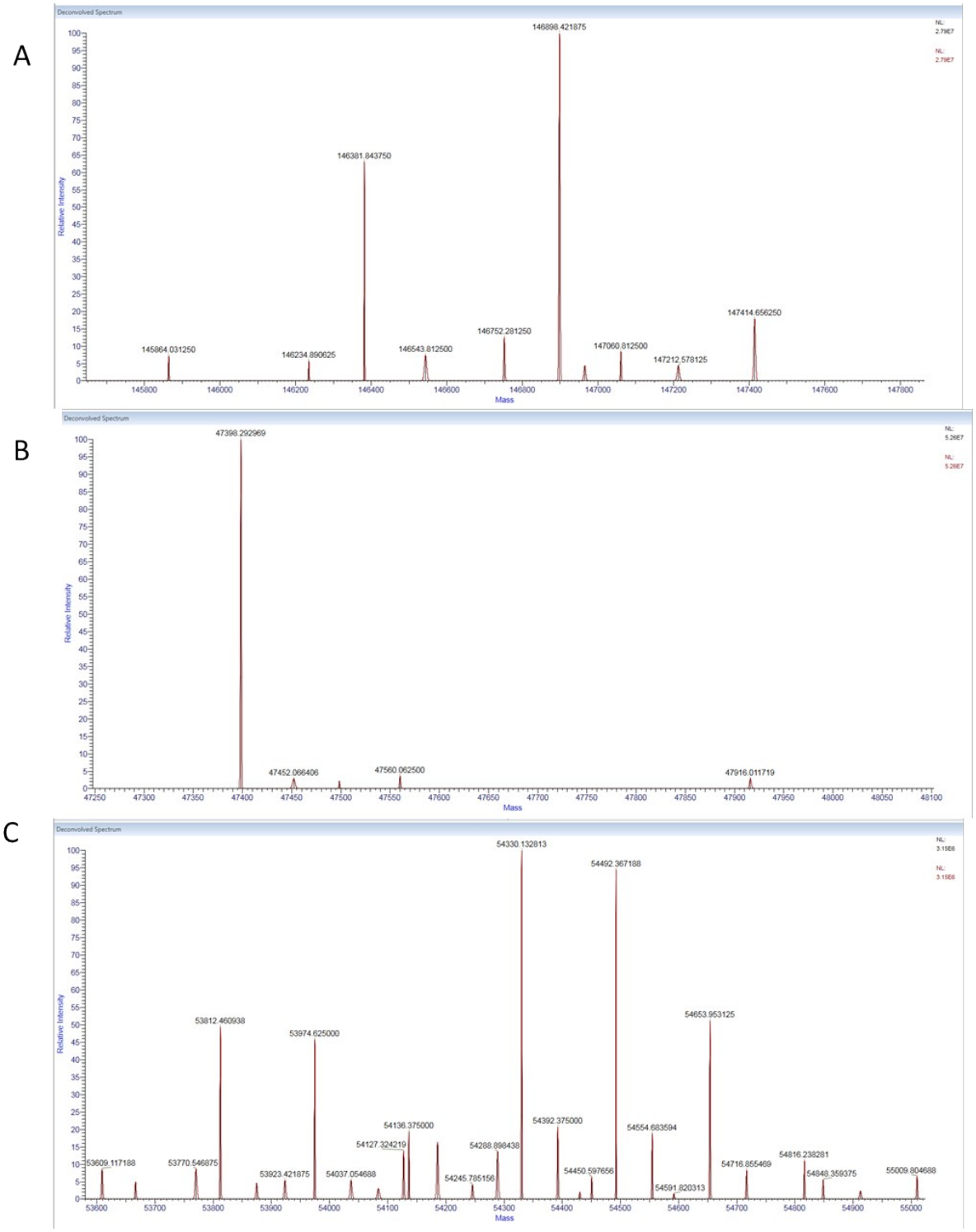

Figure S21. Deconvolved mass spectra of trastuzumab-DOTA (after the reaction of Fc-III-L6K-PEG1-DOTA with trastuzumab).
Deglycosylated intact antibody conjugate (A); antibody conjugate cleaved into Fab (B) and Fc (C) with GingisKHAN enzyme.

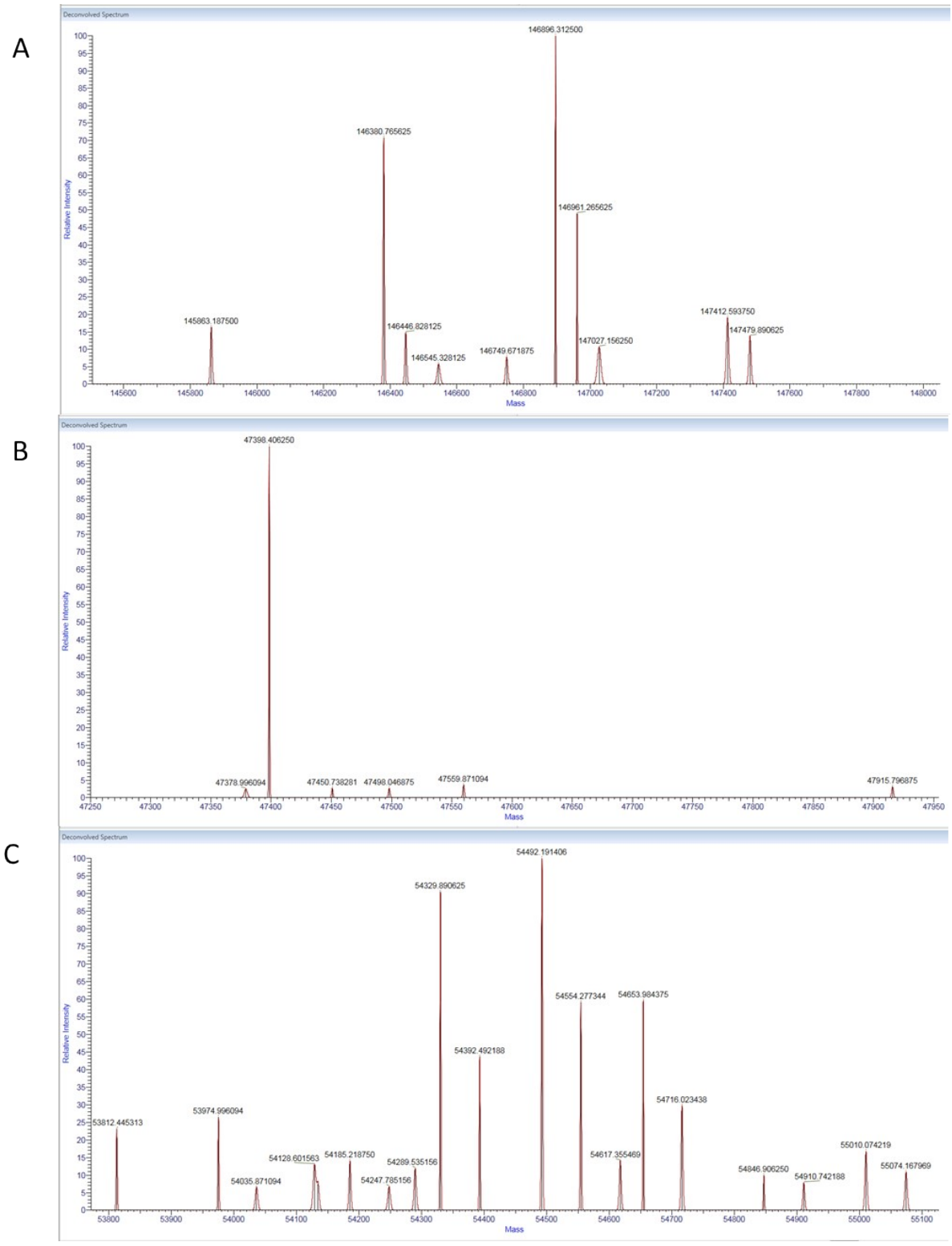

Figure S22. Deconvolved mass spectra of trastuzumab-DOTA (after the reaction of Fc-III-L6K-PEG2-DOTA with trastuzumab).
Deglycosylated intact antibody conjugate (A); antibody conjugate cleaved into Fab (B) and Fc (C) with GingisKHAN enzyme.

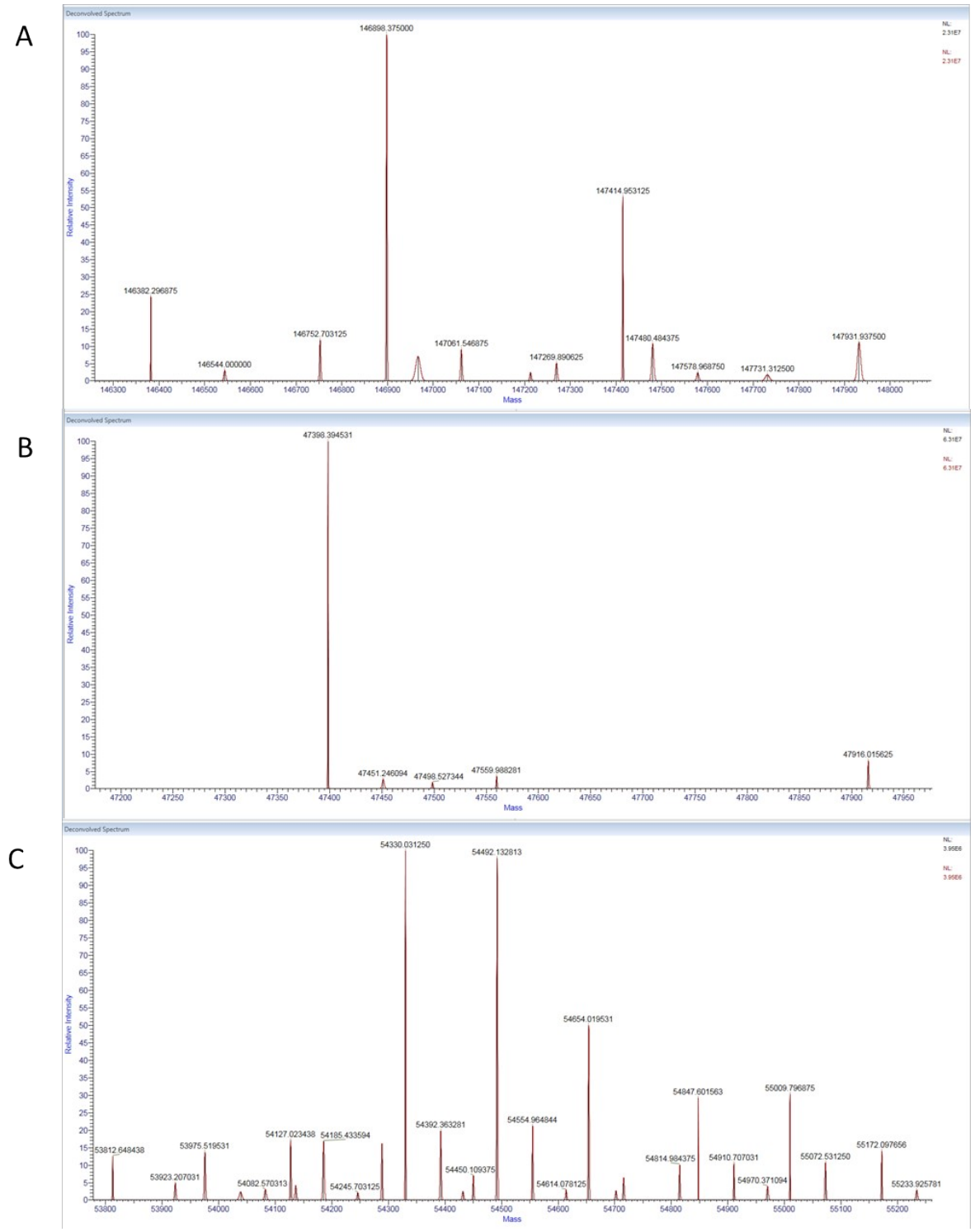

Figure S23. Deconvolved mass spectra of trastuzumab-DOTA (after the reaction of Fc-III-L6K-PEG3-DOTA with trastuzumab).
Deglycosylated intact antibody conjugate (A); antibody conjugate cleaved into Fab (B) and Fc (C) with GingisKHAN enzyme.

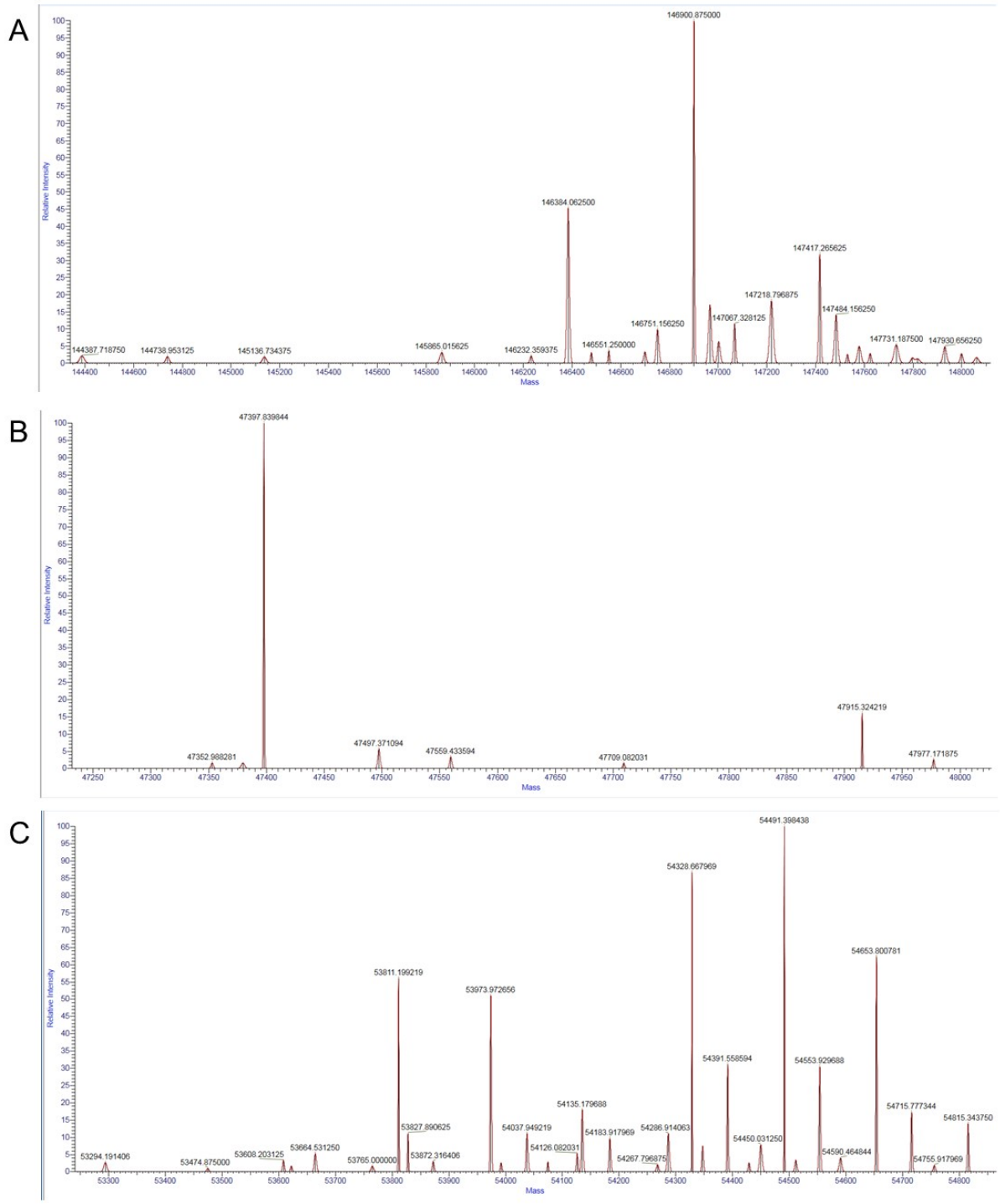

Figure S24. Deconvolved mass spectra of trastuzumab-DOTA (after the reaction of Fc-III-E8Dap-DOTA with trastuzumab).
Deglycosylated intact antibody conjugate (A); antibody conjugate cleaved into Fab (B) and Fc (C) with GingisKHAN enzyme.

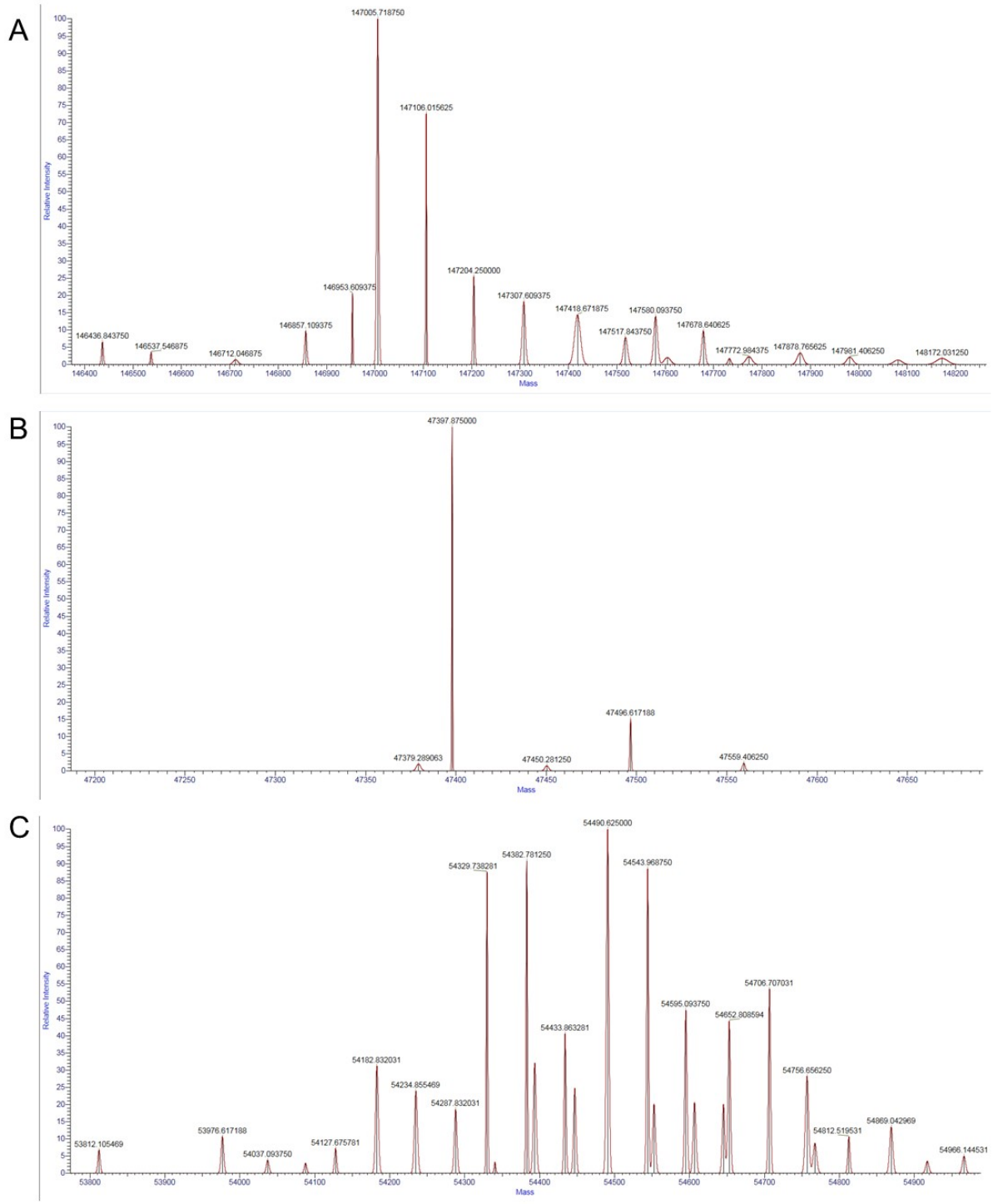

Figure S25. Deconvolved mass spectra of trastuzumab-DOTA (after the reaction of Fc-III-E8Orn-DOTA with trastuzumab).
Deglycosylated intact antibody conjugate (A); antibody conjugate cleaved into Fab (B) and Fc (C) with GingisKHAN enzyme.

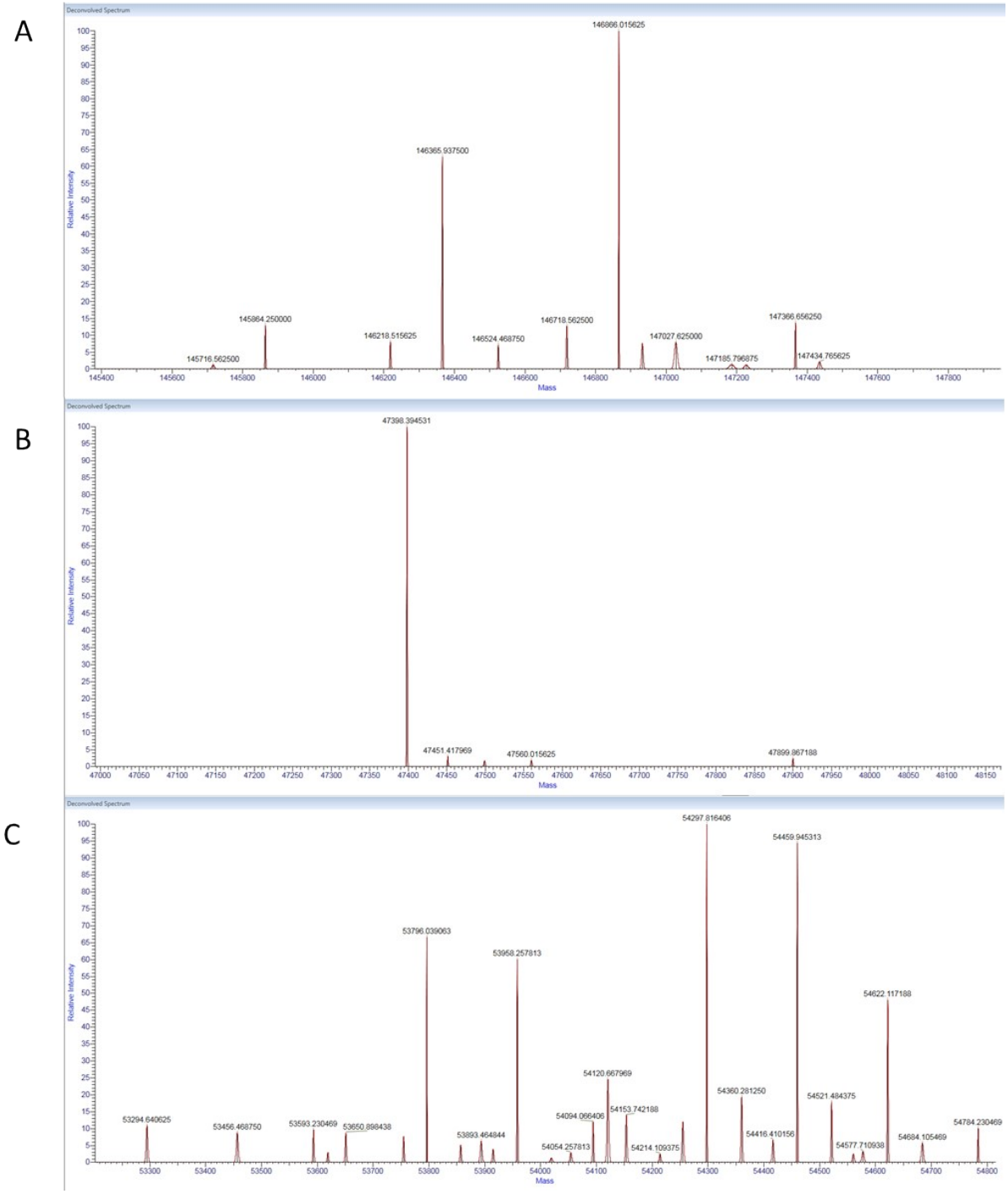

Figure S26. Deconvolved intact mass spectra of trastuzumab-DOTA (after the reaction of Fc-III-L6Dap-thioester-DOTA with trastuzumab).
Deglycosylated intact antibody conjugate (A); antibody conjugate cleaved by GinghisKHAN enzyme into Fab (B) and Fc (C).

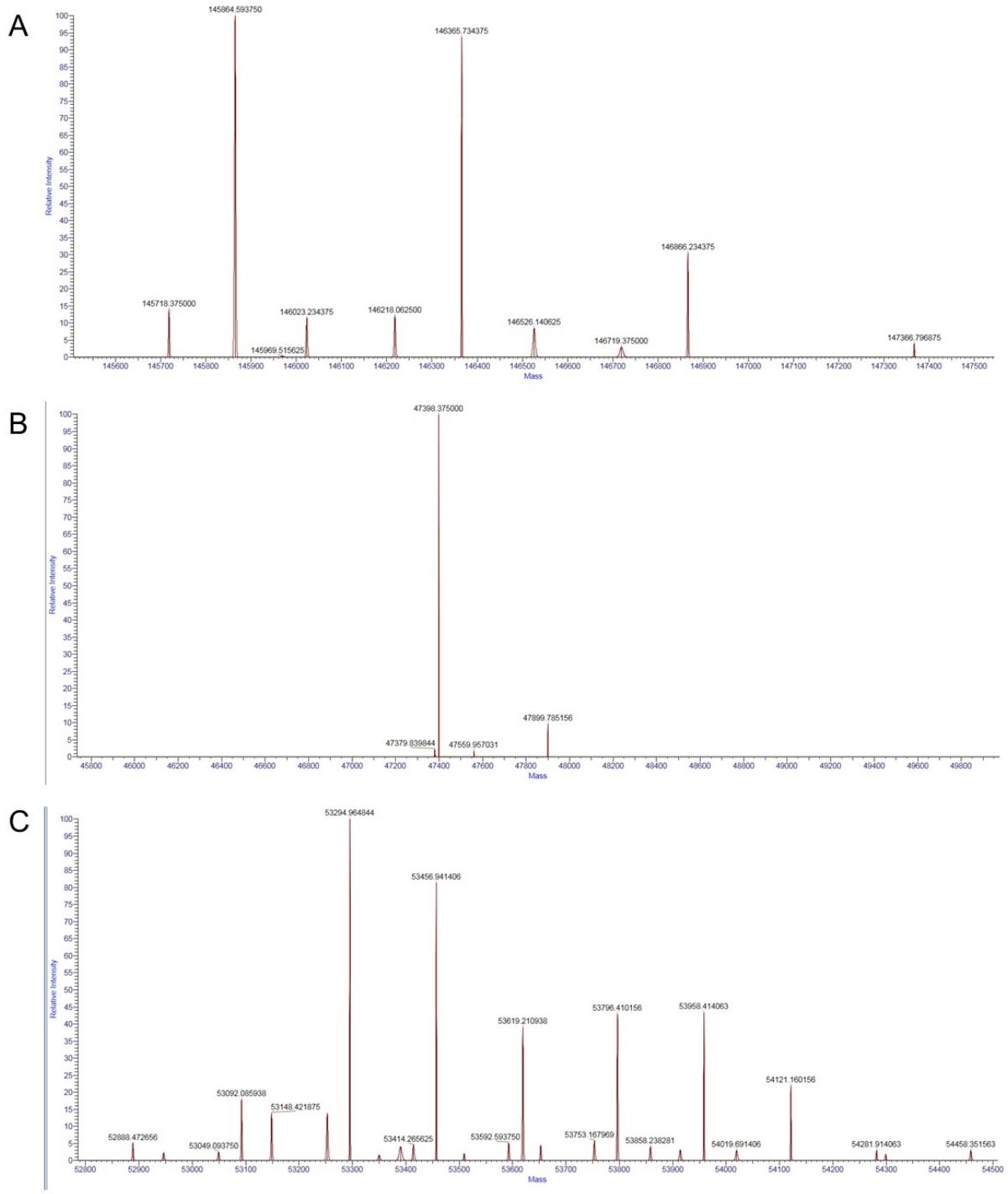

Figure S27. Deconvolved mass spectra of trastuzumab-DOTA (after the reaction of Fc-III-L6Dab-thioester-DOTA with trastuzumab).
Deglycosylated intact antibody conjugate (A); antibody conjugate cleaved into Fab (B) and Fc (C) with GingisKHAN enzyme.

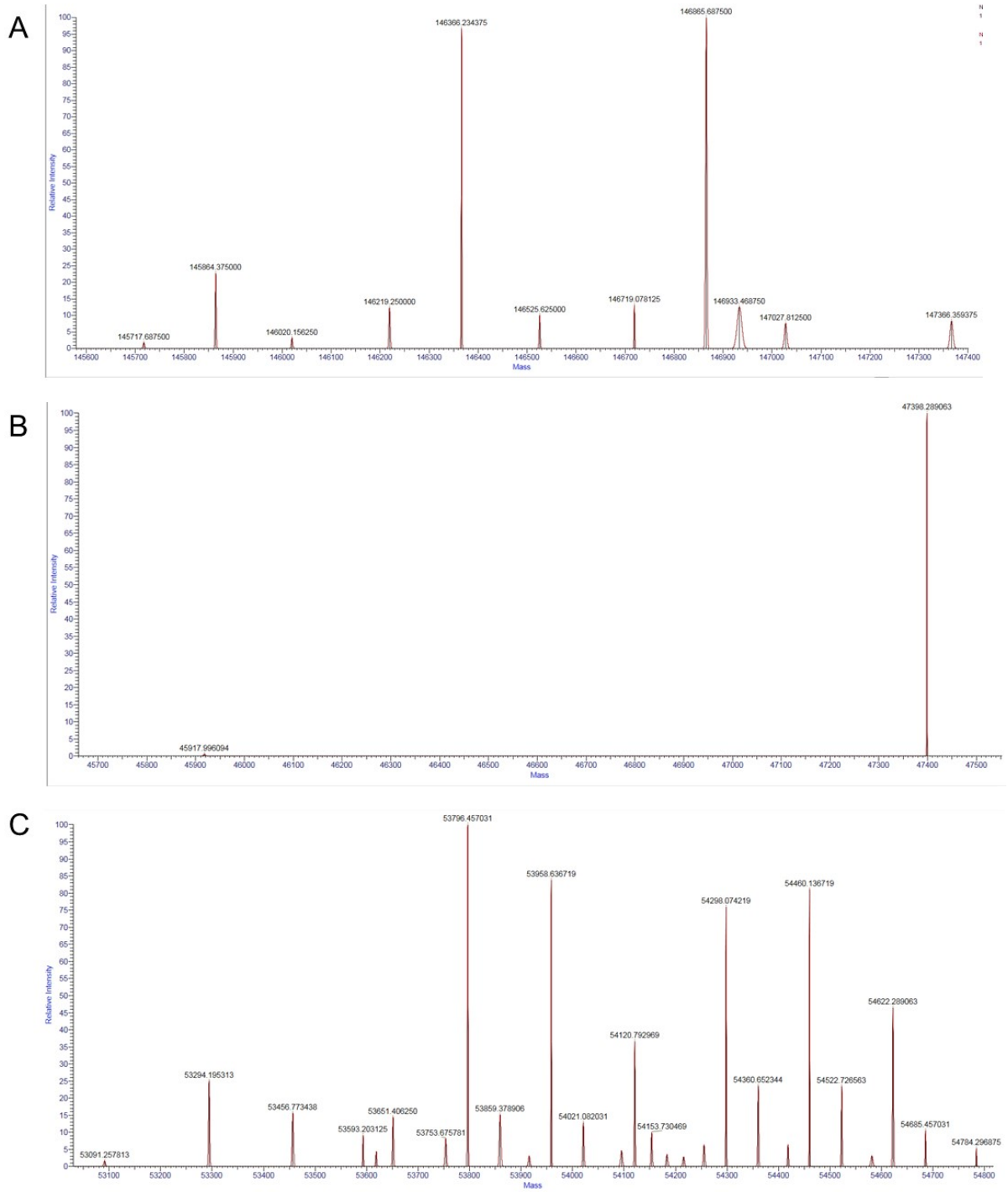

Figure S28. Deconvolved mass spectra of trastuzumab-DOTA (after the reaction of Fc-III-L6Orn-thioester-DOTA with trastuzumab).
Deglycosylated intact antibody conjugate (A); antibody conjugate cleaved into Fab (B) and Fc (C) with GingisKHAN enzyme.

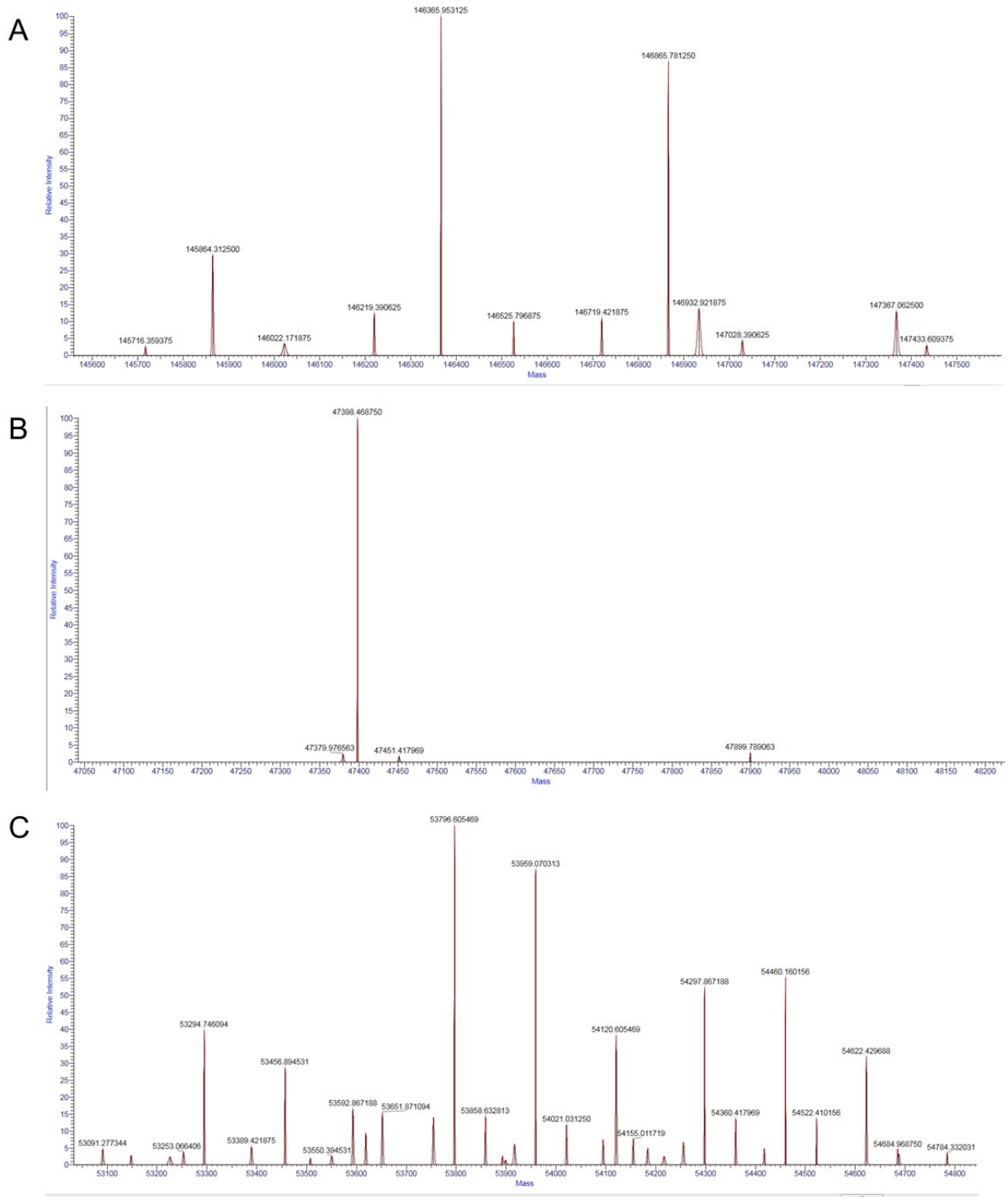

Figure S29. Deconvolved mass spectra of trastuzumab-DOTA (after the reaction of Fc-III-L6K-thioester-DOTA with trastuzumab).
Deglycosylated intact antibody conjugate (A); antibody conjugate cleaved into Fab (B) and Fc (C) with GingisKHAN enzyme.

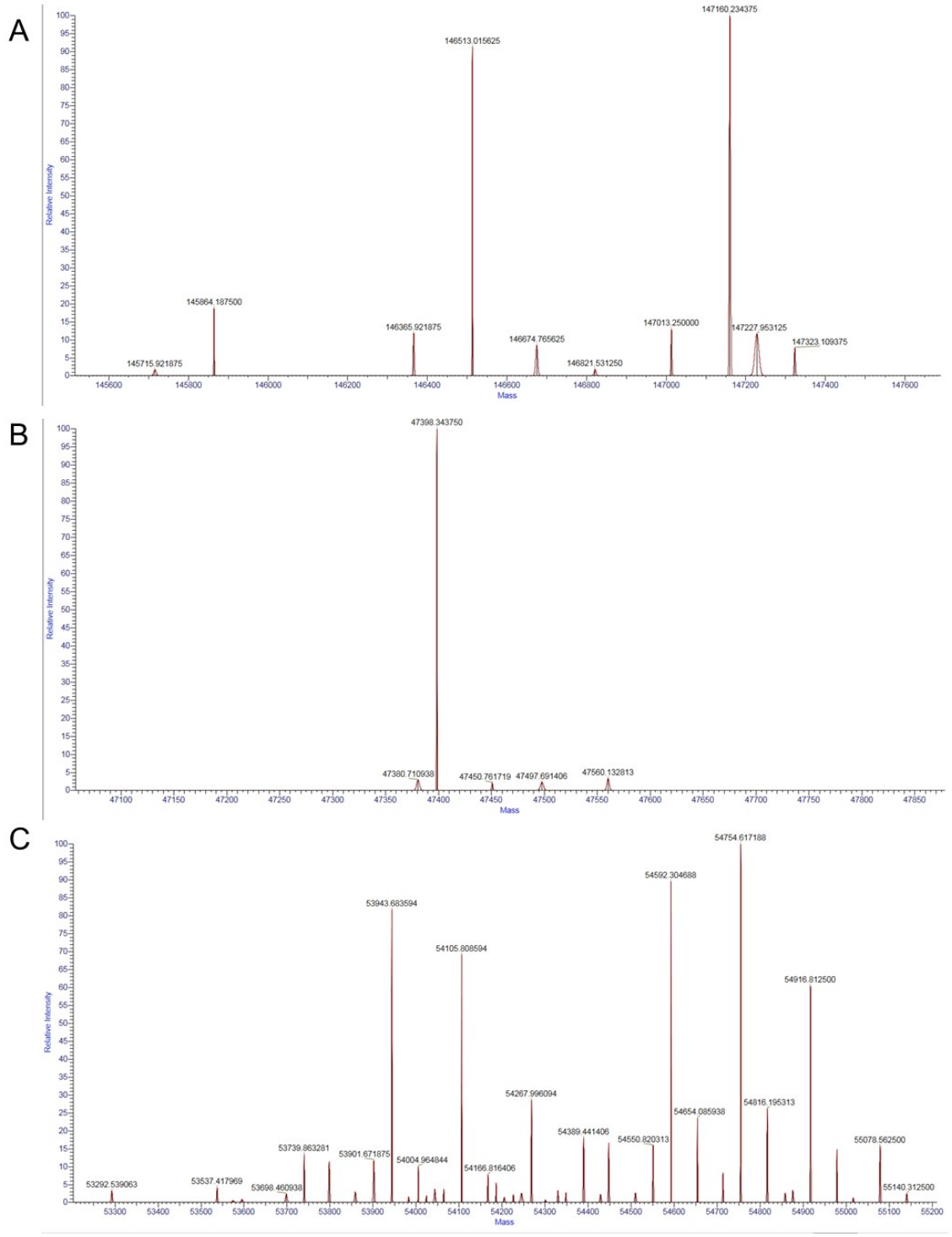

Figure S30. Deconvolved mass spectra of trastuzumab-DOTA (after the reaction of Fc-III-L6Y-DOTA with trastuzumab).
Deglycosylated intact antibody conjugate (A); antibody conjugate cleaved into Fab (B) and Fc (C) with GingisKHAN enzyme.

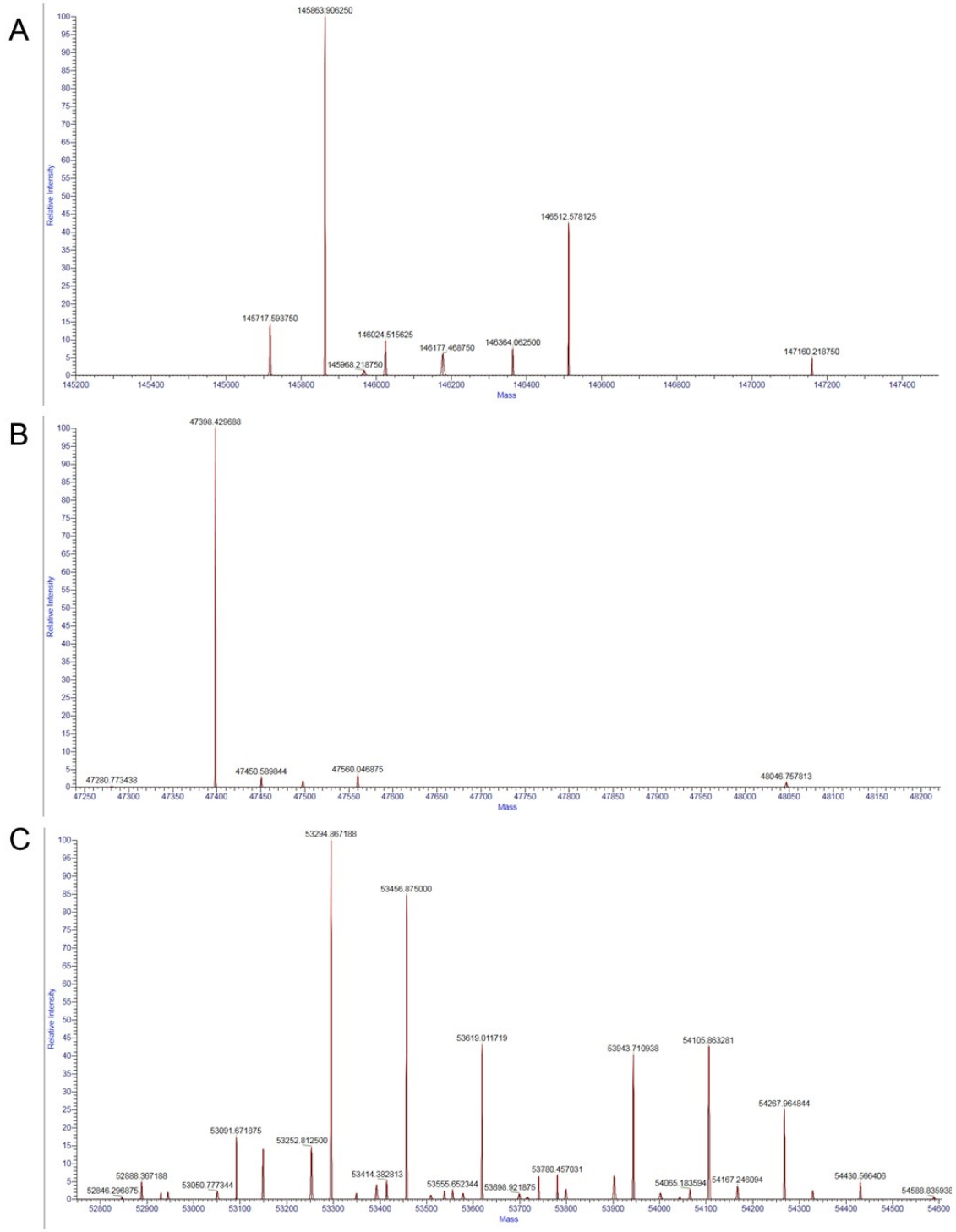

Figure S31. Deconvolved mass spectra of trastuzumab-DOTA (after the reaction of Fc-III-L6hY-DOTA with trastuzumab).
Deglycosylated intact antibody conjugate (A); antibody conjugate cleaved into Fab (B) and Fc (C) with GingisKHAN enzyme.

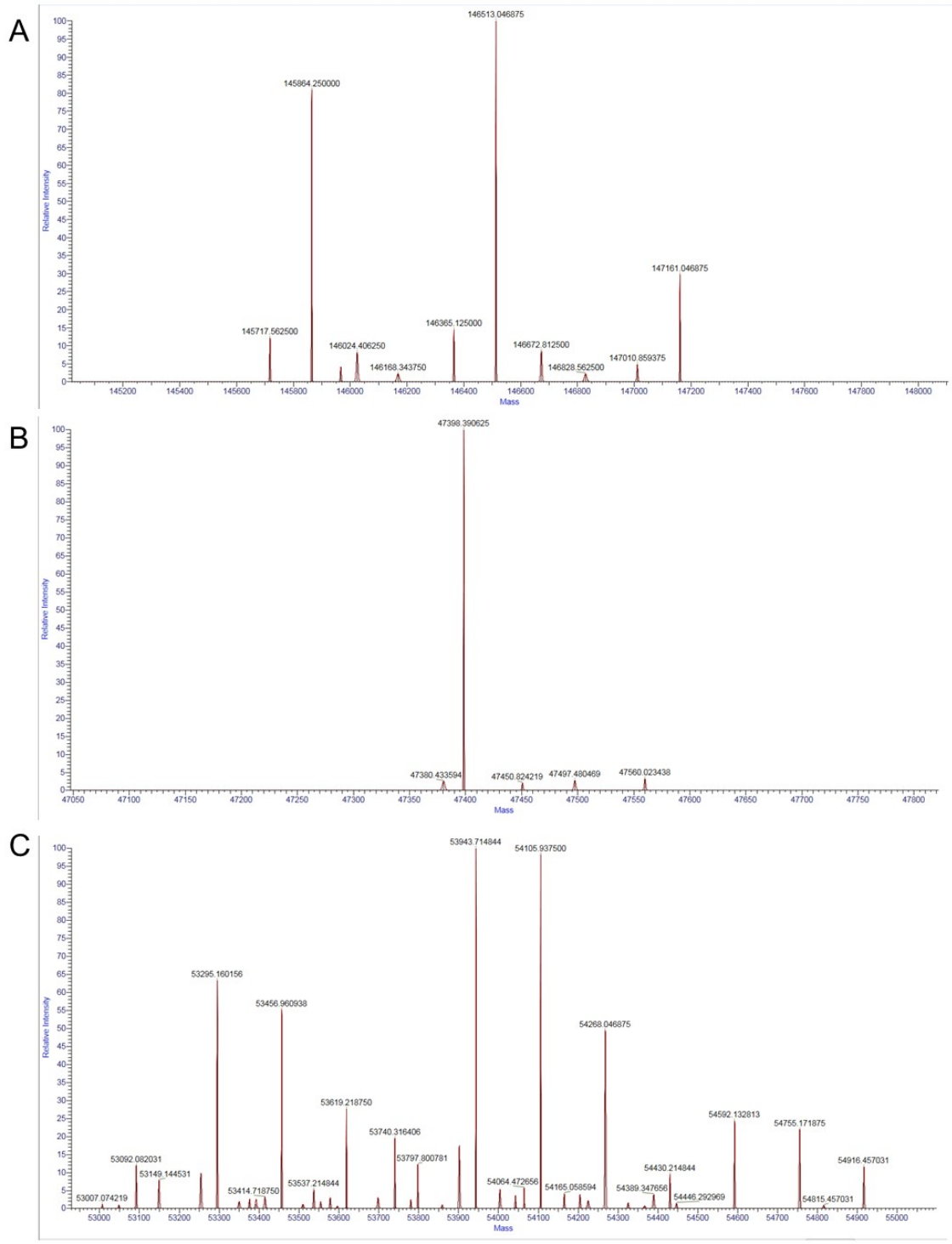

Figure S32. Deconvolved mass spectra of trastuzumab-DOTA (after the reaction of Fc-III-E8hY-DOTA with trastuzumab).
Deglycosylated intact antibody conjugate (A); antibody conjugate cleaved into Fab (B) and Fc (C) with GingisKHAN enzyme.

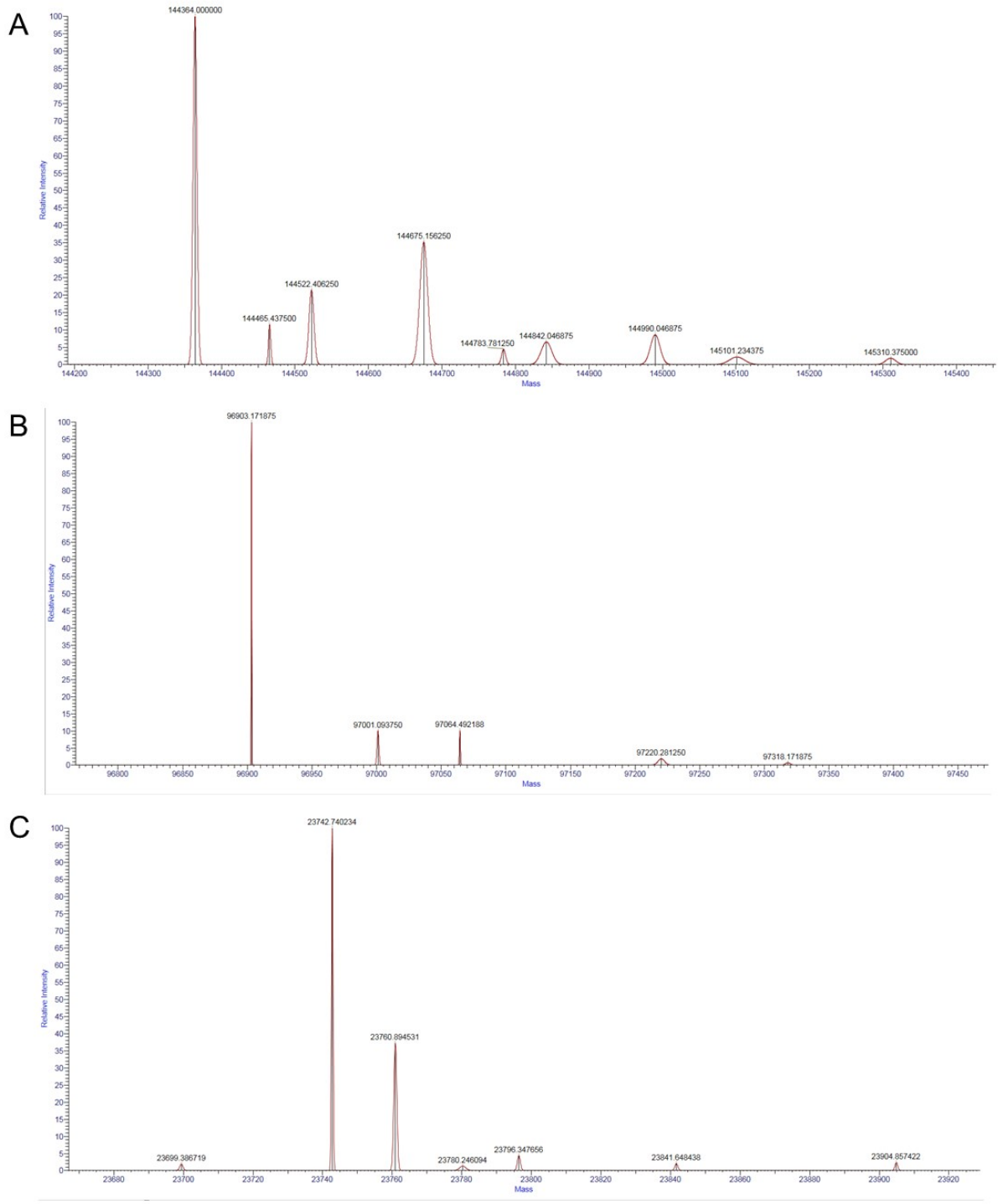

Figure S33. Deconvolved mass spectra of atezolizumab antibody.
Deglycosylated intact antibody (A); antibody cleaved by FabRICATOR enzyme into $F(ab')_2$ (B) and Fc/2 (C).

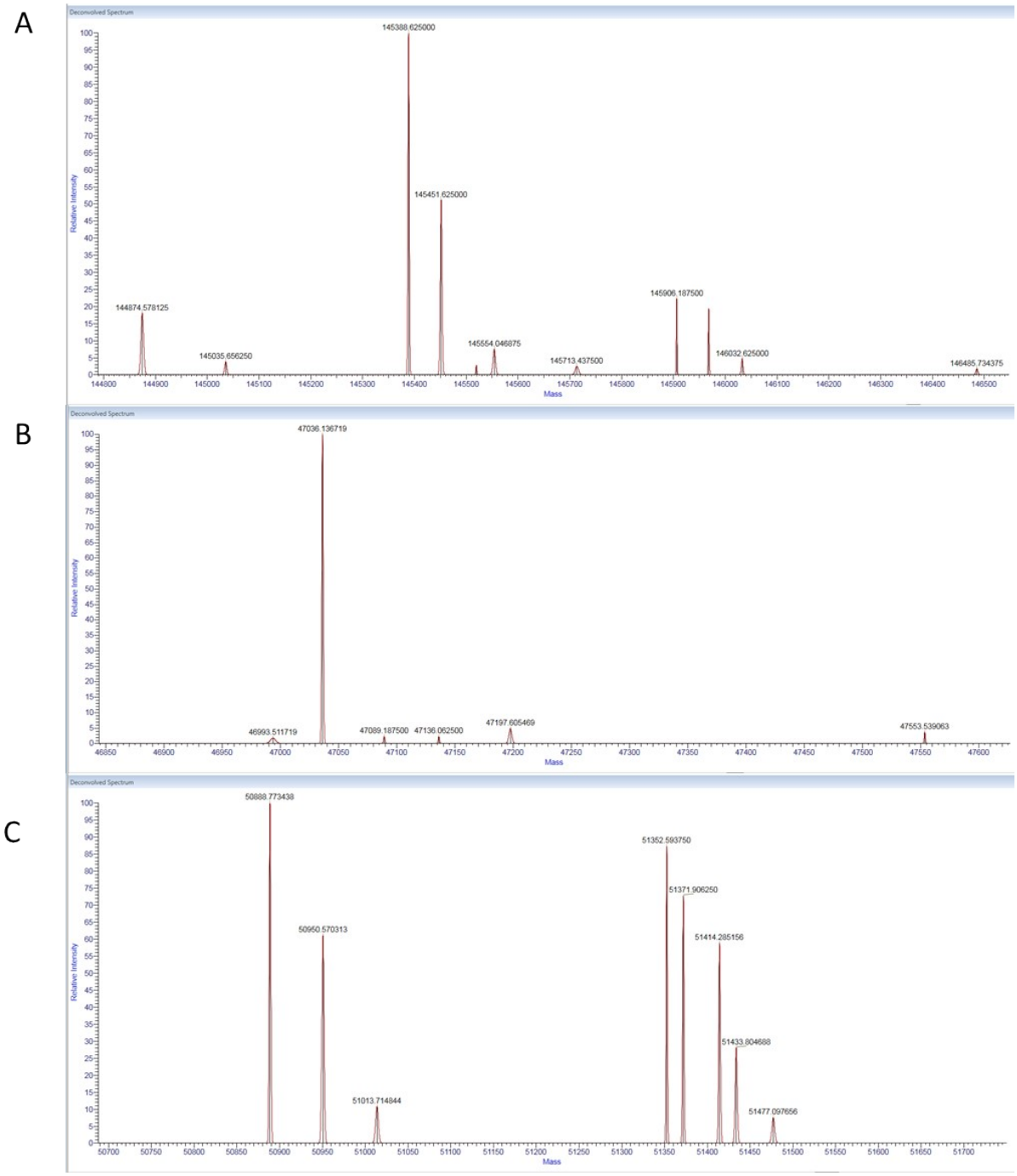

Figure S34. Deconvolved mass spectra of atezolizumab-DOTA (after the reaction of Fc-III-L6Orn-DOTA with atezolizumab).
Deglycosylated intact antibody conjugate (A); antibody conjugate cleaved by GinghisKHAN enzyme into Fab (B) and Fc (C).

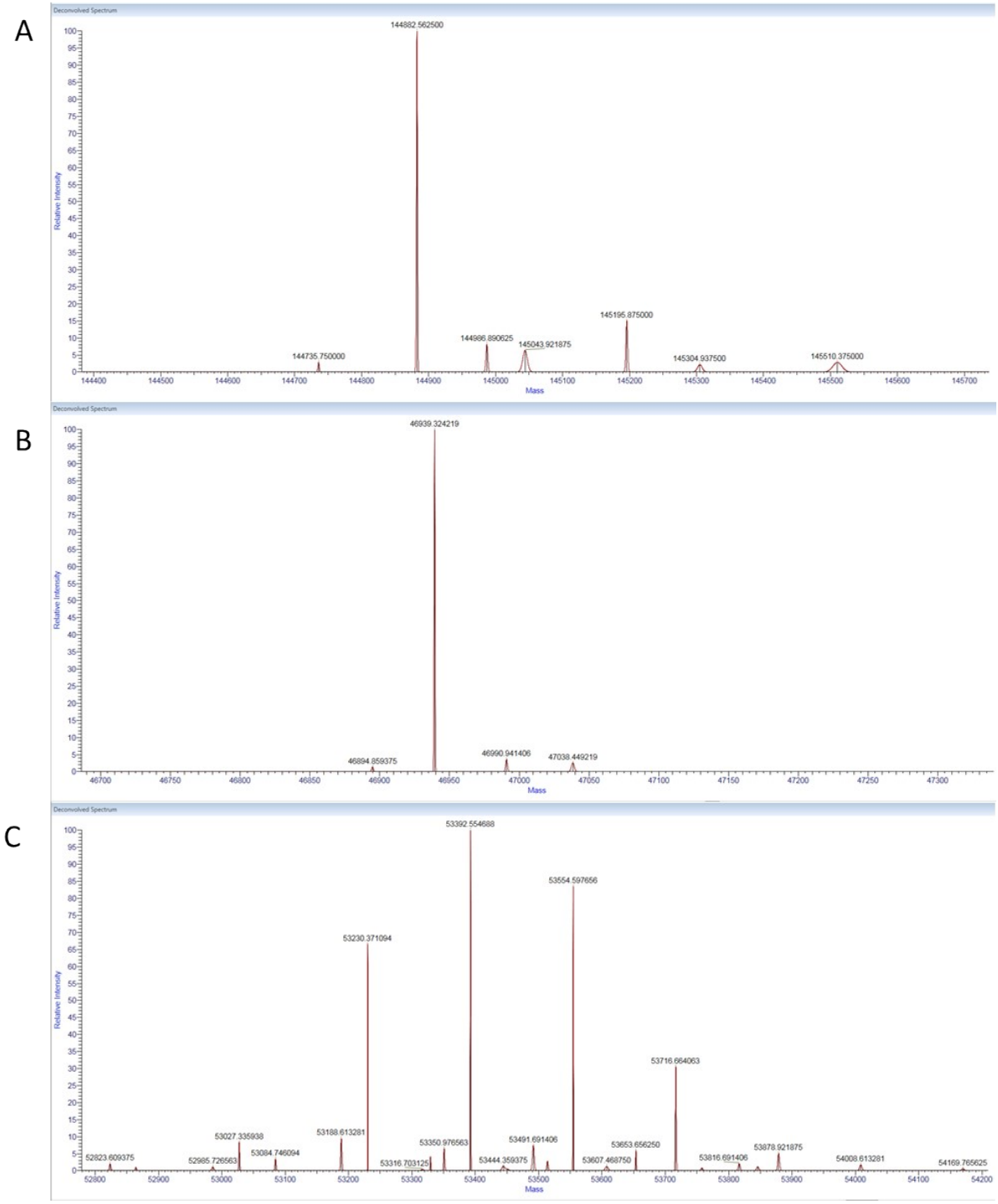

Figure S35. Deconvolved mass spectra of rituximab antibody.
Deglycosylated intact antibody (A); antibody cleaved by GinghisKHAN enzyme into Fab (B) and Fc (C).

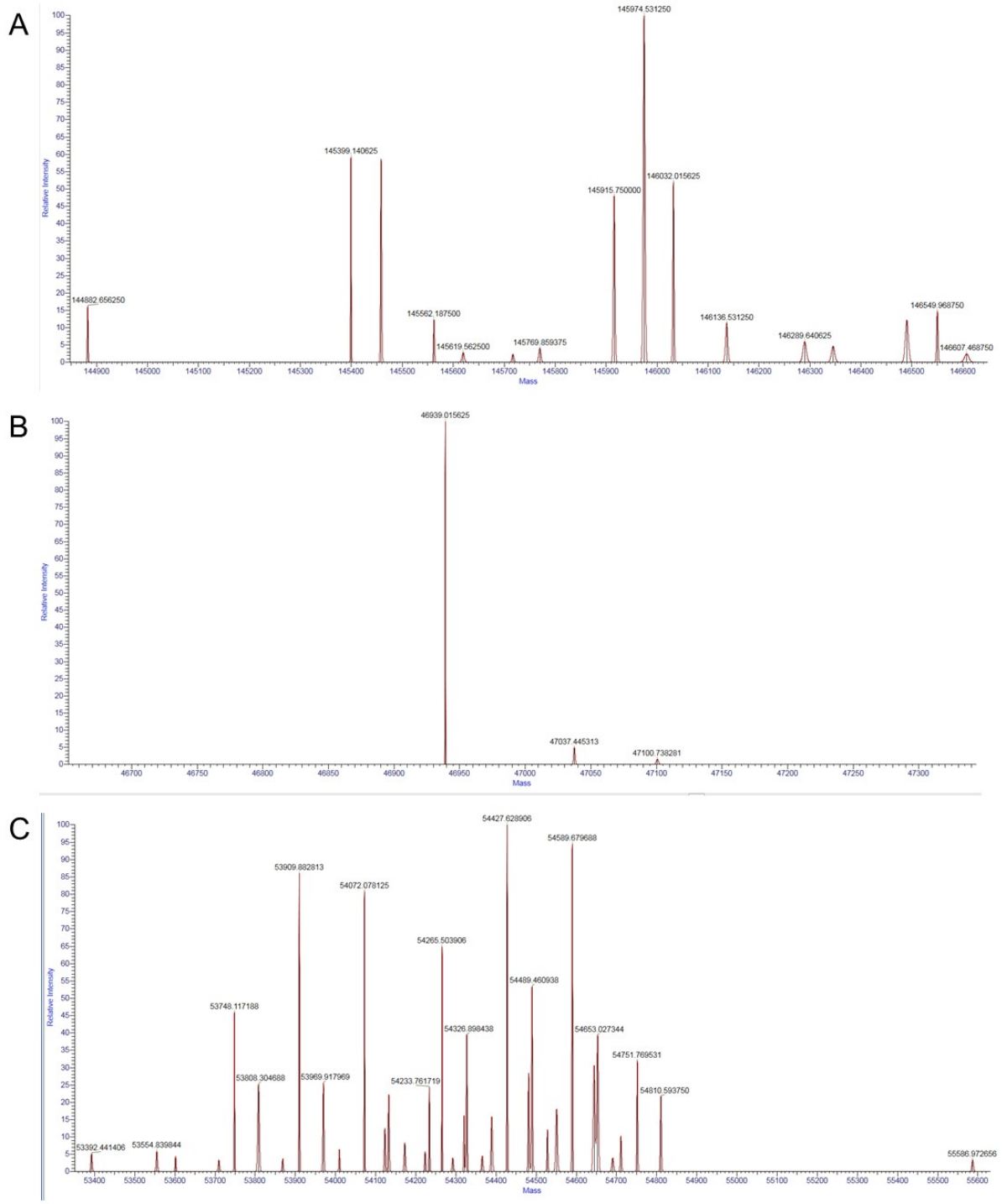

Figure S36. Deconvolved mass spectra of rituximab-DOTA (after the reaction of Fc-III-L6Orn-DOTA with rituximab).

Deglycosylated intact antibody conjugate (A); antibody conjugate cleaved by GinghisKHAN enzyme into Fab (B) and Fc (C).

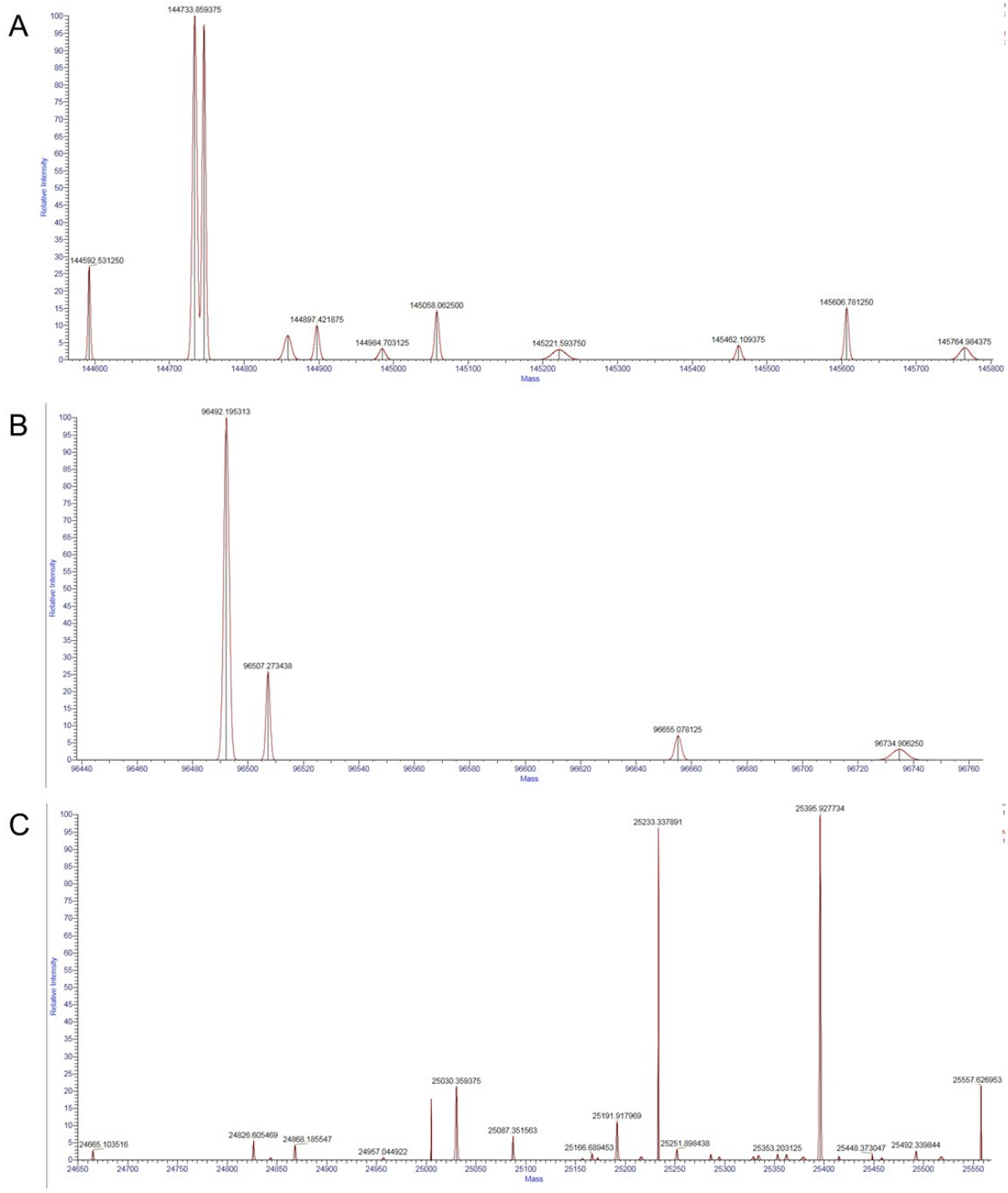

Figure S37. Deconvolved intact mass spectra of panitumumab antibody.
Deglycosylated antibody (A); antibody cleaved by FabRICATOR enzyme into $F(ab')_2$ (B) and Fc/2 (C).

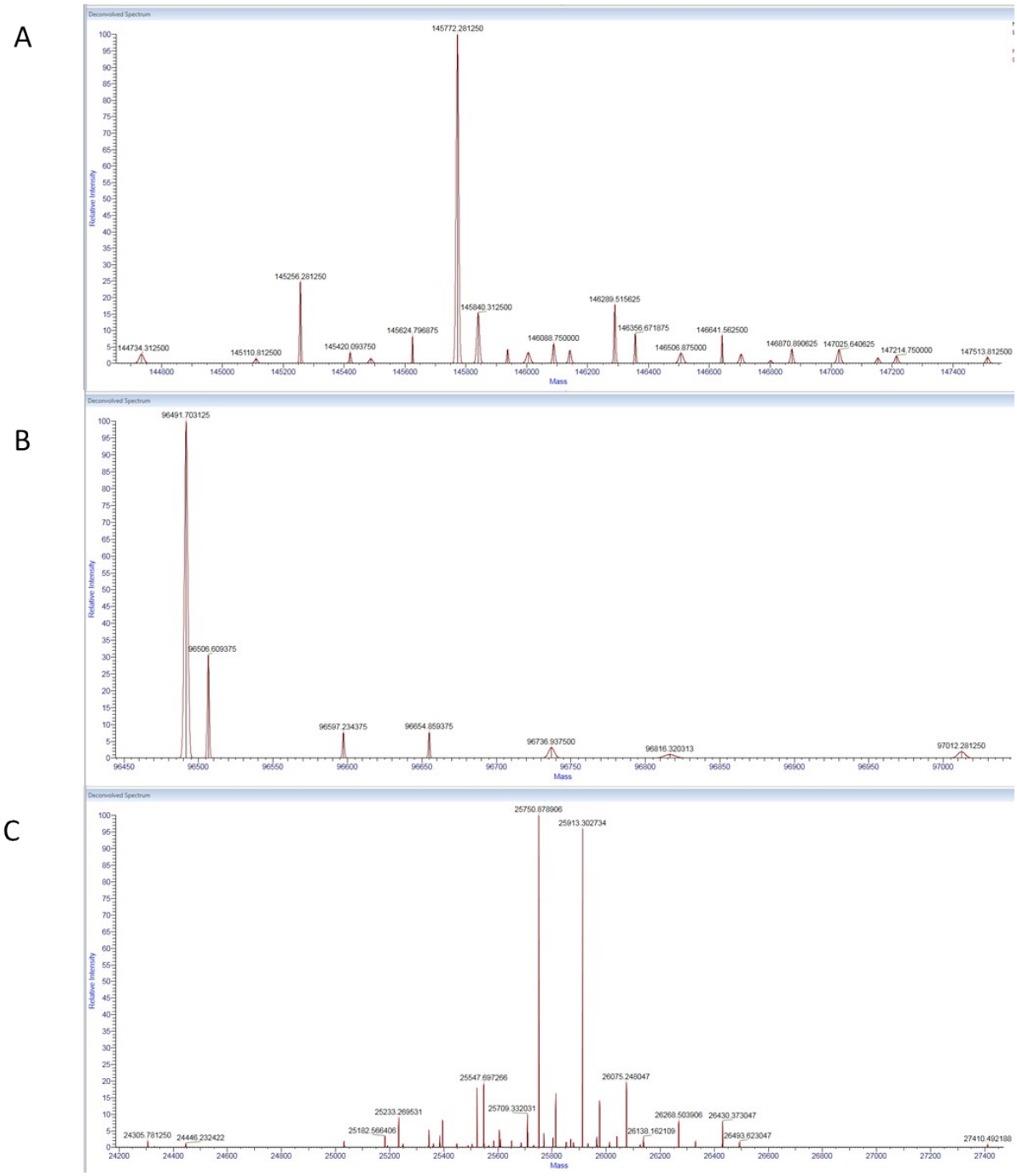

Figure S38. Deconvolved mass spectra of panitumumab-DOTA (after the reaction of Fc-III-L6Orn-DOTA with panitumumab).
Deglycosylated intact antibody conjugate (A); antibody conjugate cleaved by FabRICATOR enzyme into Fab (B) and Fc (C).

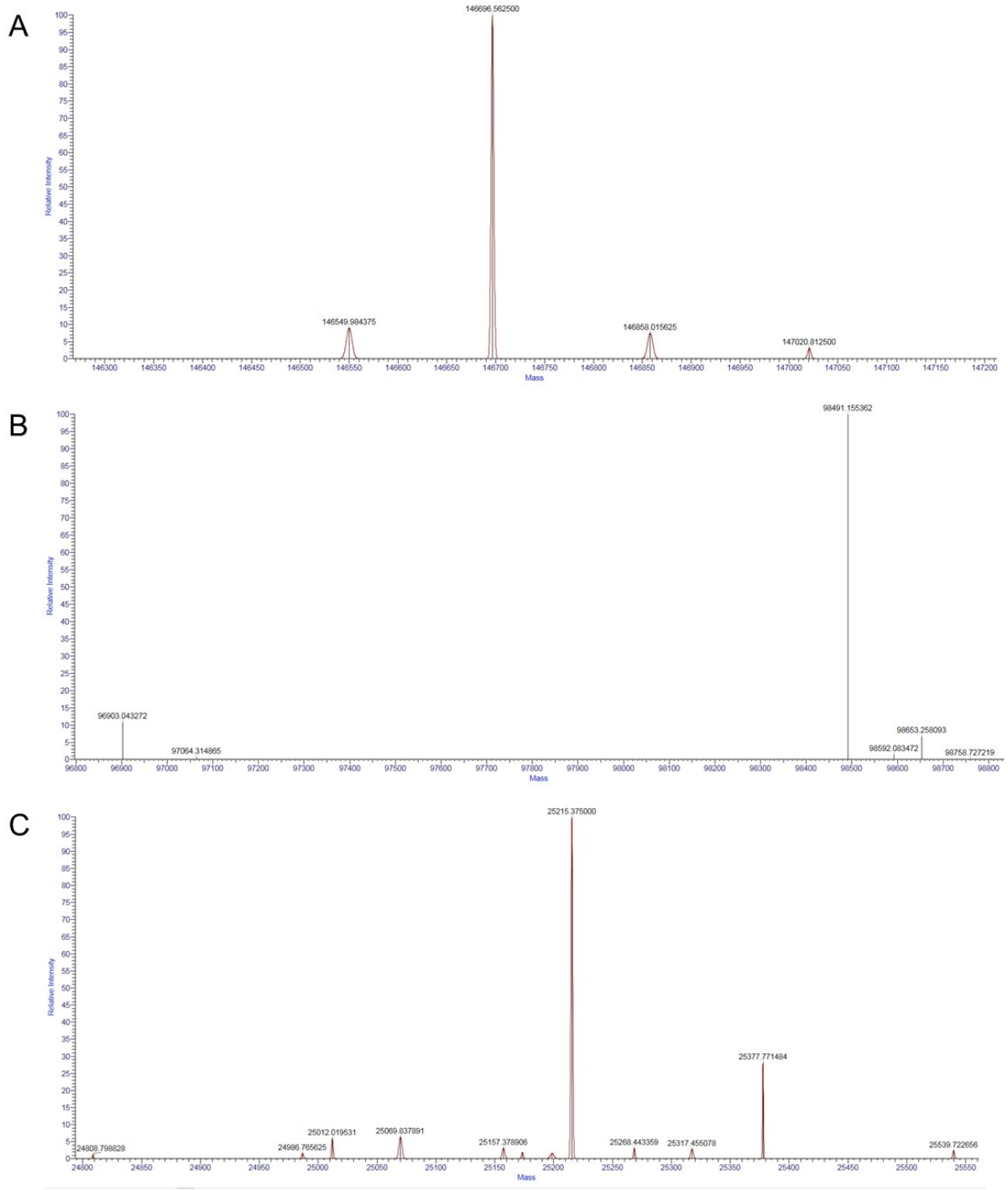

Figure S39. Deconvolved mass spectra of pembrolizumab antibody.
Deglycosylated intact antibody (A); antibody cleaved by FabRICATOR enzyme into $F(ab')_2$ (B) and Fc/2 (C).

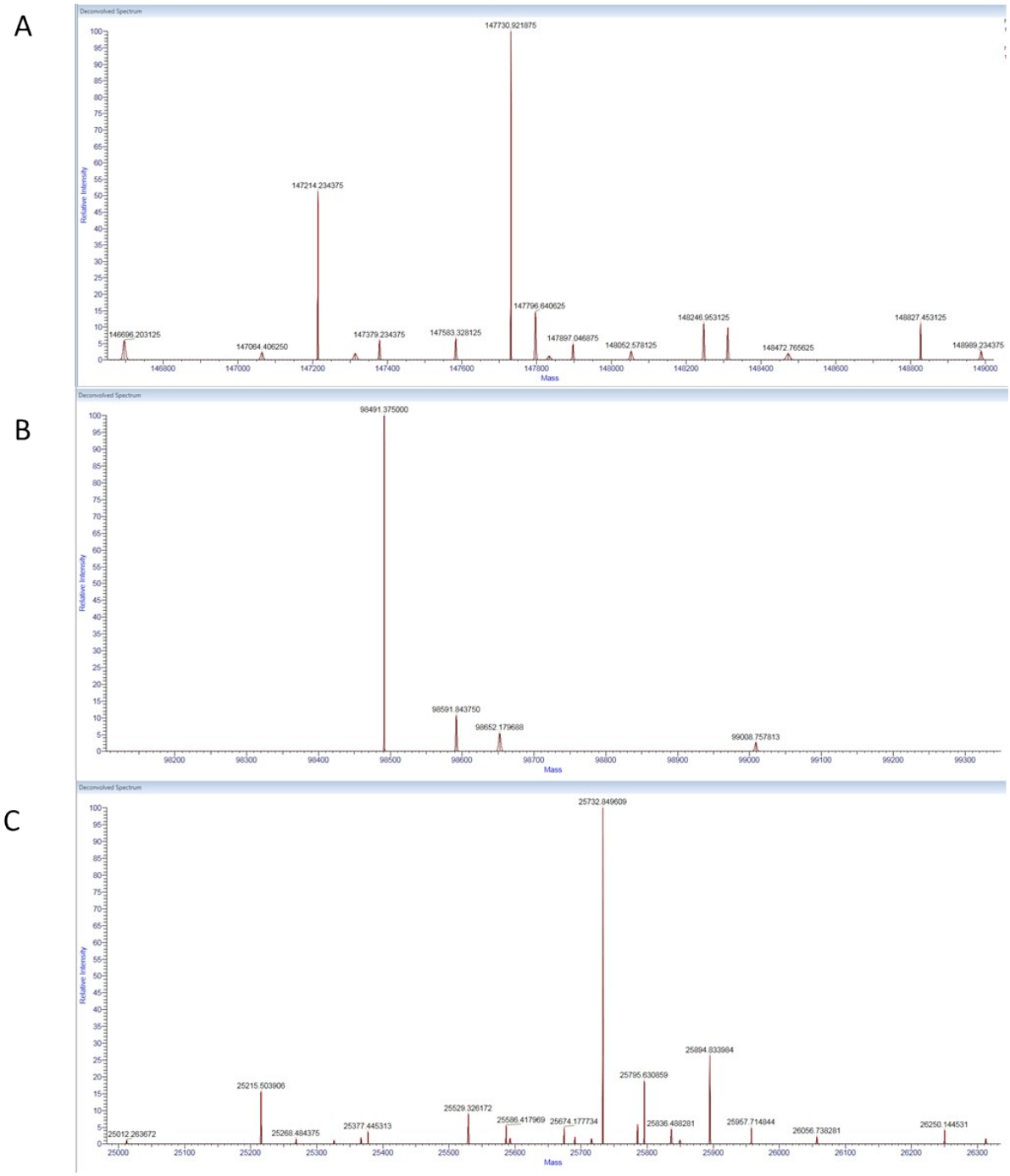

Figure S40. Deconvolved mass spectra of pembrolizumab-DOTA (after the reaction of Fc-III-L6Orn-DOTA with pembrolizumab).
Deglycosylated intact antibody conjugate (A); antibody conjugate cleaved by FabRICATOR enzyme into Fab (B) and Fc (C).

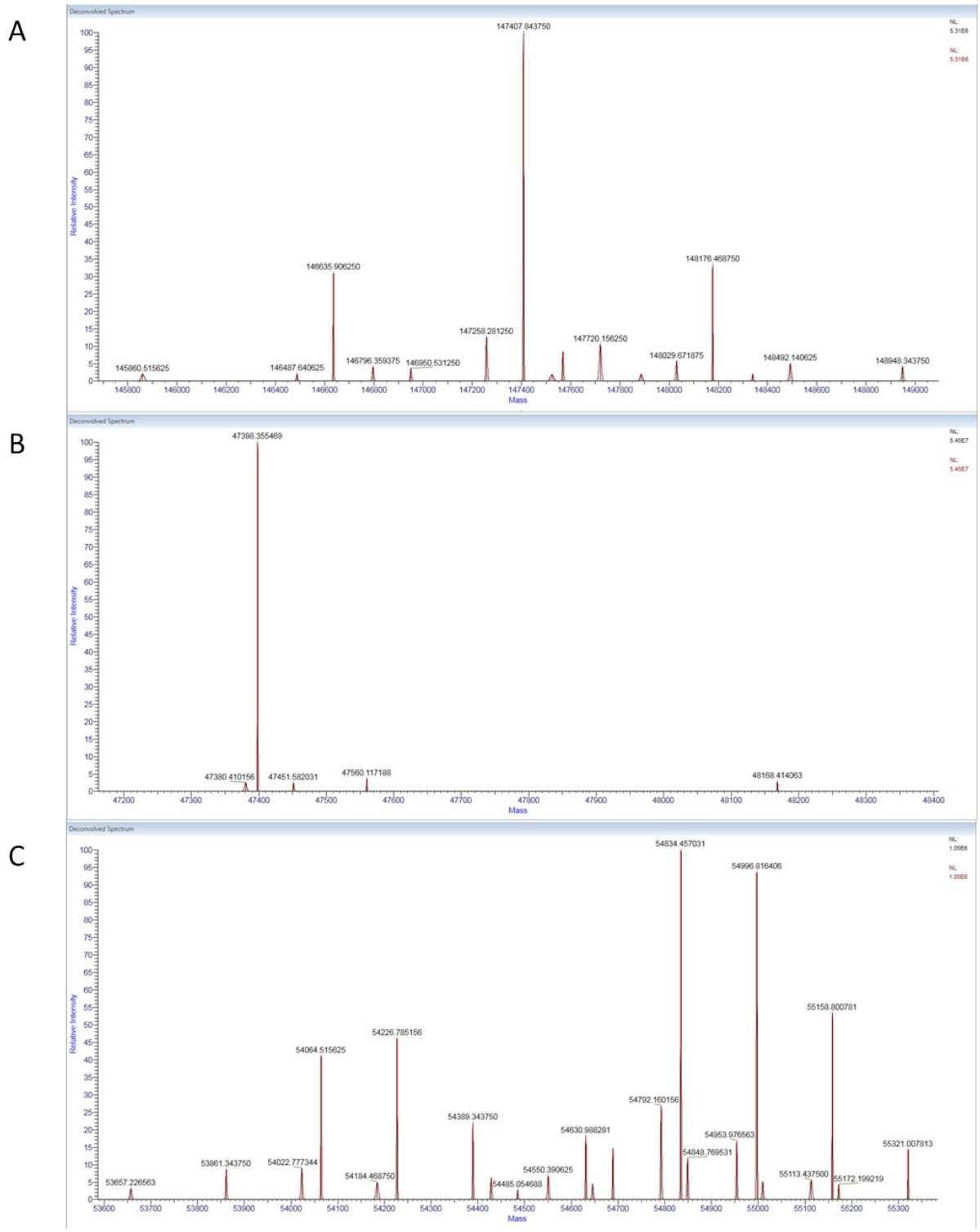

Figure S41. Deconvolved mass spectra of trastuzumab-DTPA (after the reaction of Fc-III-L6Orn-DTPA with trastuzumab).
Deglycosylated intact antibody conjugate (A); antibody conjugate cleaved into Fab (B) and Fc (C) with GinghisKHAN enzyme.

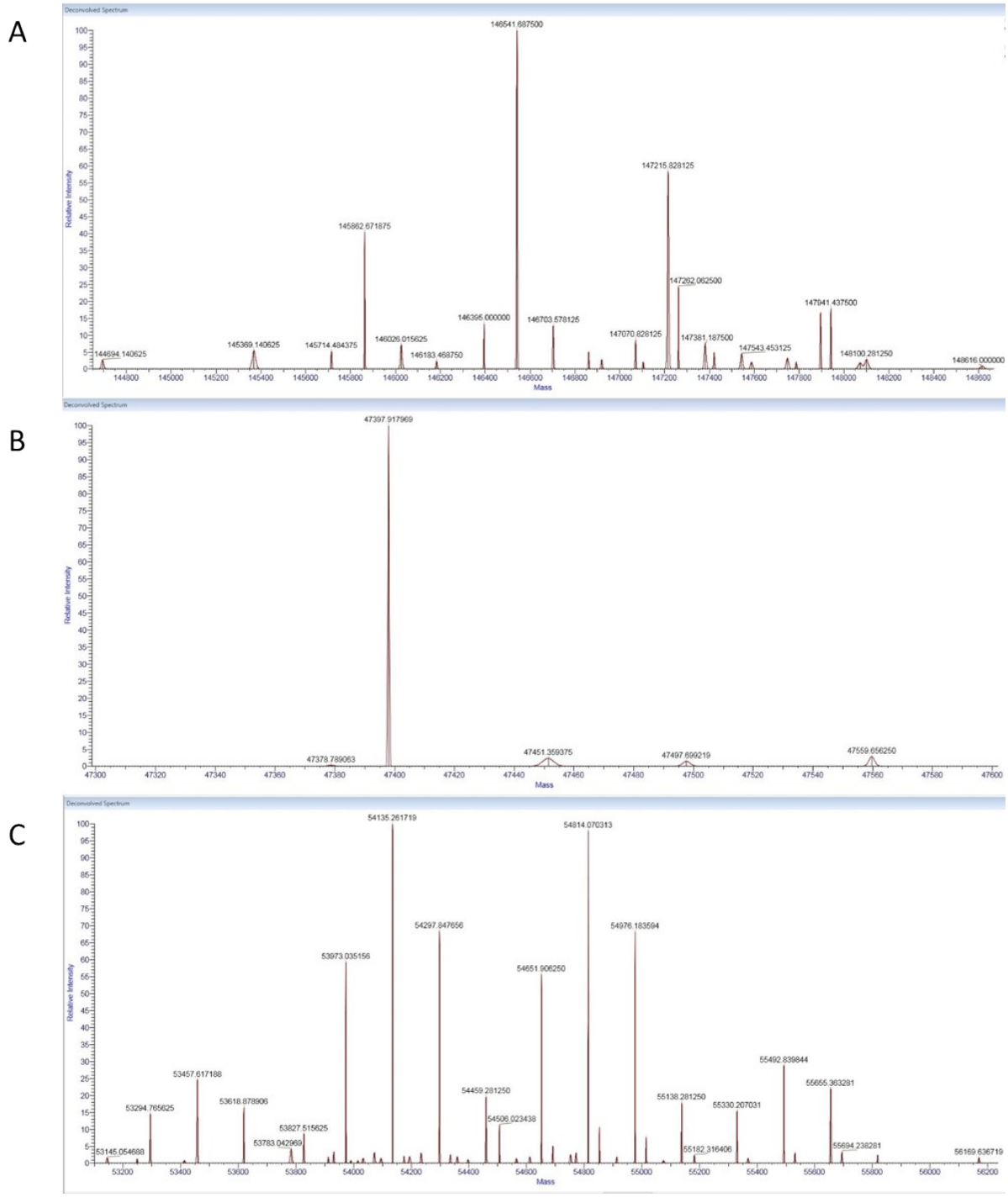

Figure S42. Deconvolved mass spectra of trastuzumab-Bn-TCMC (after the reaction of Fc-III-L6Orn-Bn-TCMC with trastuzumab).
Deglycosylated intact antibody conjugate (A); antibody conjugate cleaved into Fab (B) and Fc (C) with GinghisKHAN enzyme.

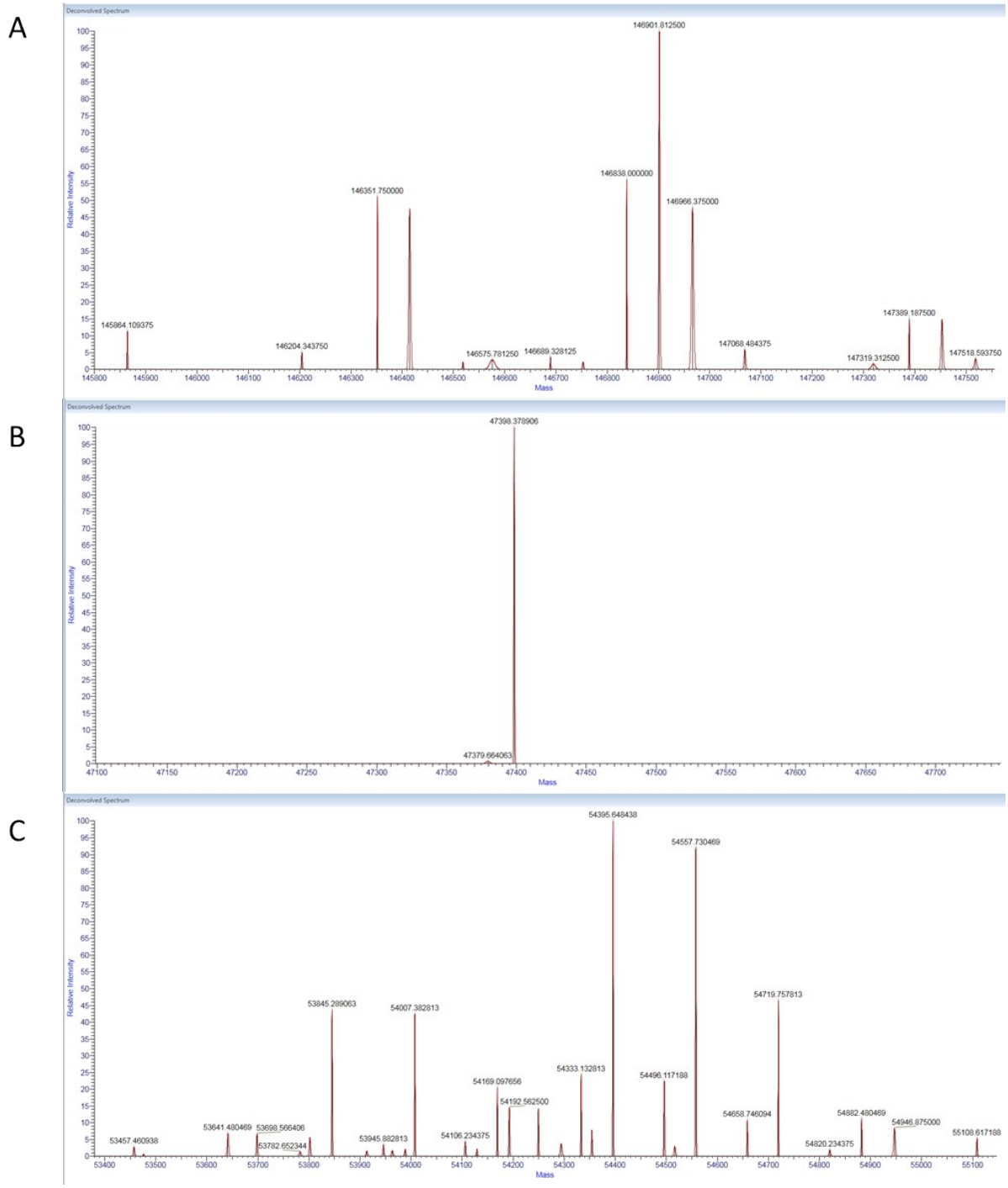

Figure S43. Deconvolved mass spectra of trastuzumab-NODAGA (after the reaction of Fc-III-L6Orn-NODAGA with trastuzumab).
Deglycosylated intact antibody conjugate (A); antibody conjugate cleaved into Fab (B) and Fc (C) with GingisKHAN enzyme.

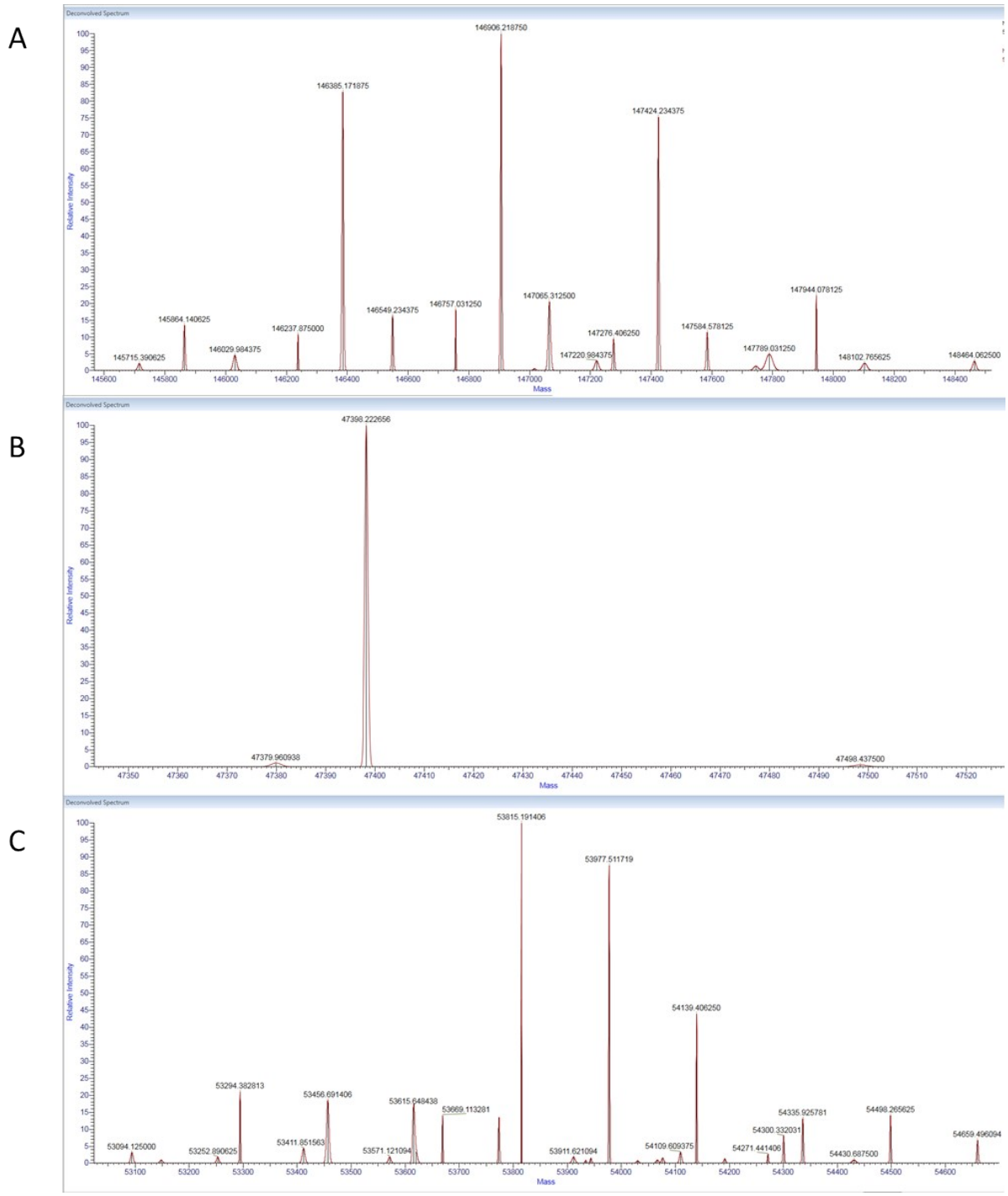

Figure S44. Deconvolved mass spectra of trastuzumab-FITC (after the reaction of Fc-III-L6Orn-FITC with trastuzumab).
Deglycosylated intact antibody conjugate (A); antibody conjugate cleaved into Fab (B) and Fc (C) with GingisKHAN enzyme.

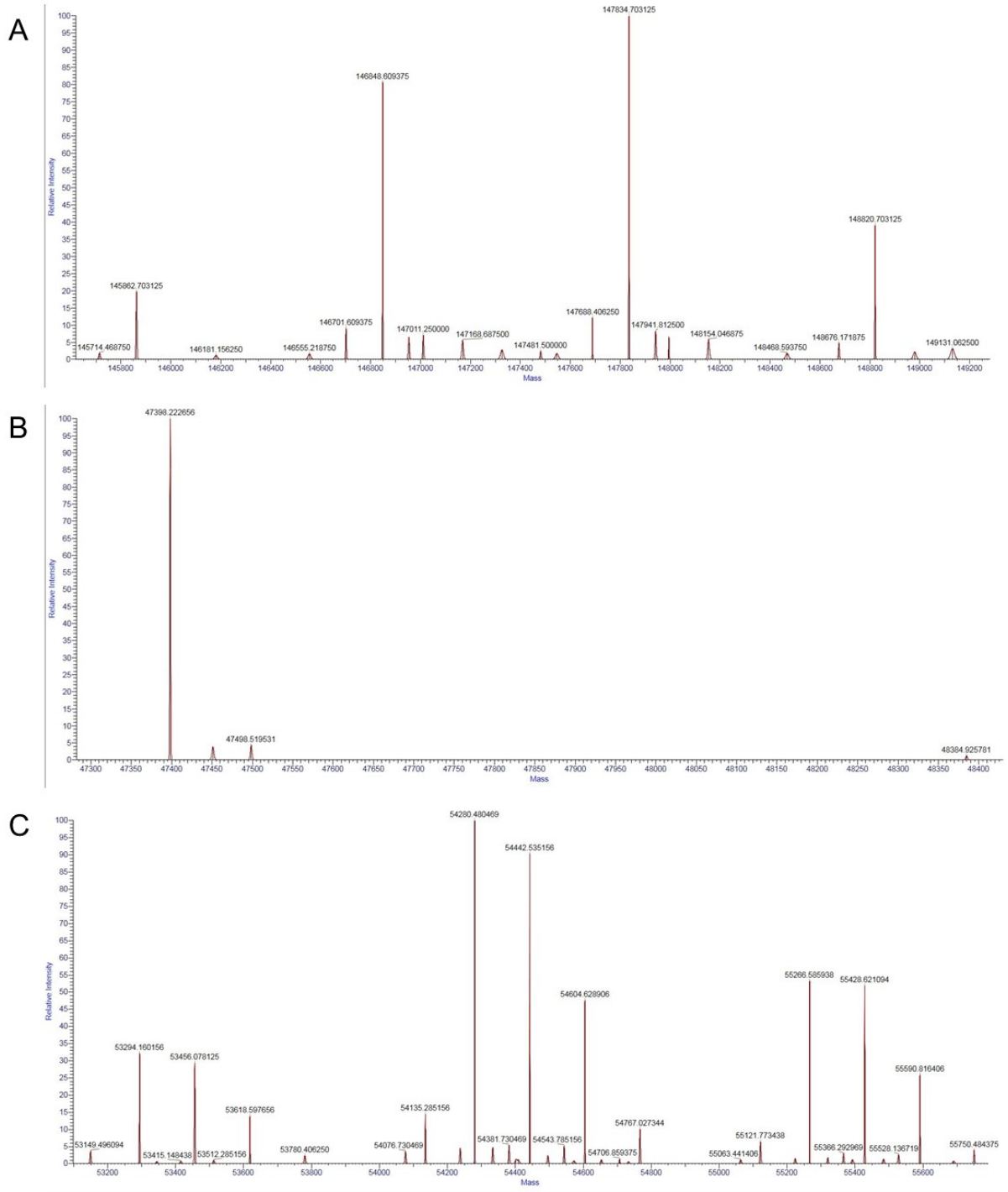

Figure S45. Deconvolved mass spectra of trastuzumab-AF647 (after the reaction of Fc-III-L6Orn-AF647 with trastuzumab).
Deglycosylated intact antibody conjugate (A); antibody conjugate cleaved into Fab (B) and Fc (C) with GingisKHAN enzyme.

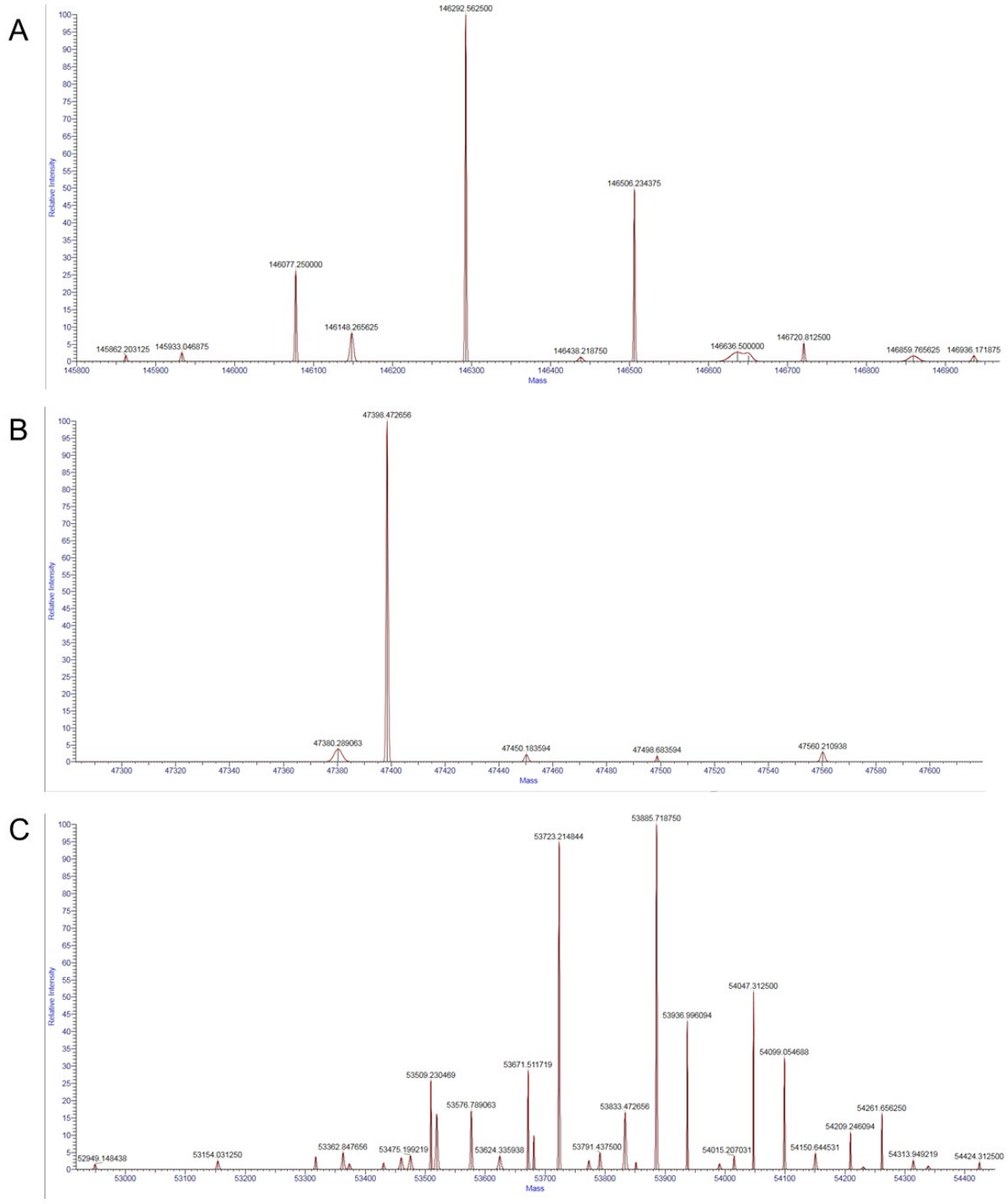

Figure S46. Deconvolved mass spectra of trastuzumab-N_3 (after the reaction of Fc-III-L6Orn-N_3 with trastuzumab).
Deglycosylated antibody conjugate (A); antibody conjugate cleaved into Fab (B) and Fc (C) with GingisKHAN enzyme.

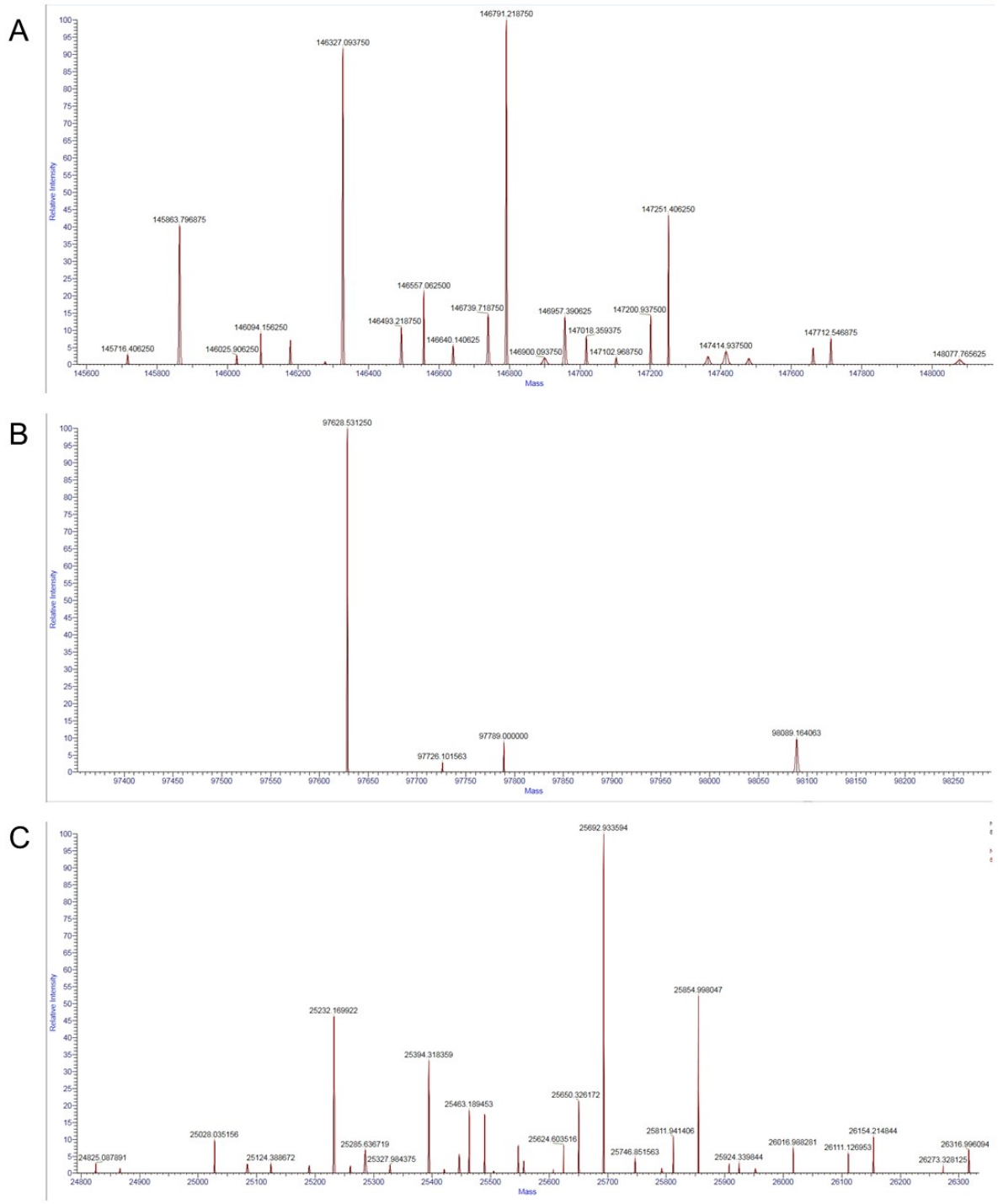

Figure S47. Deconvolved mass spectra of trastuzumab-DBCO (after the reaction of Fc-III-L6Orn-DBCO with trastuzumab).
Deglycosylated antibody conjugate (A); antibody conjugate cleaved into Fab (B) and Fc (C) with GingisKHAN enzyme.

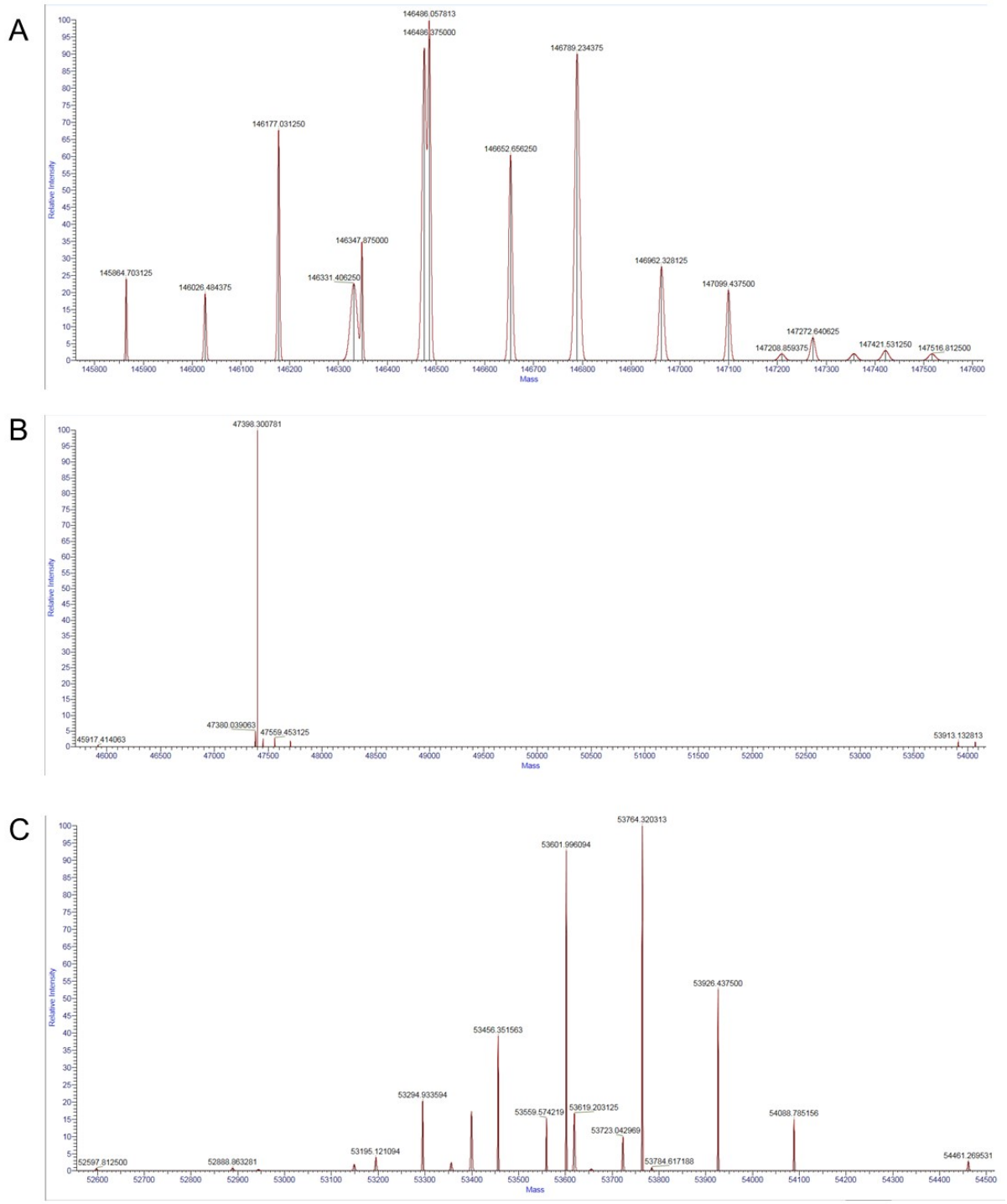

Figure S48. Deconvolved intact mass spectra of trastuzumab-BCN (after the reaction of Fc-III-L6Orn-BCN with trastuzumab).
Deglycosylated intact antibody conjugate (A); antibody conjugate cleaved into Fab (B) and Fc (C) with GingisKHAN enzyme.

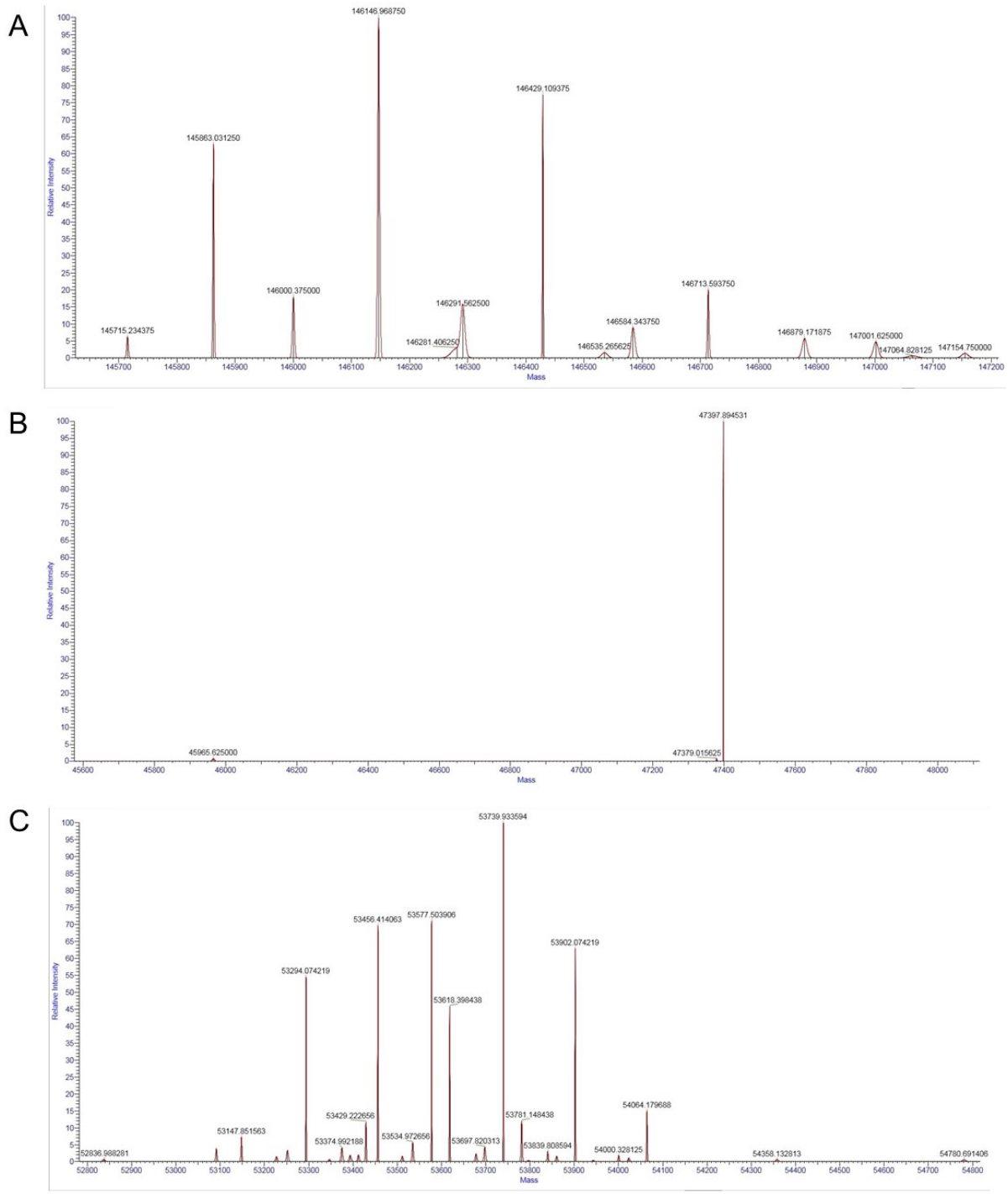

Figure S49. Deconvolved mass spectra of trastuzumab-TCO (after the reaction of Fc-III-L6Orn-TCO with trastuzumab).
Deglycosylated intact antibody conjugate (A); antibody conjugate cleaved into Fab (B) and Fc (C) with GingisKHAN enzyme.

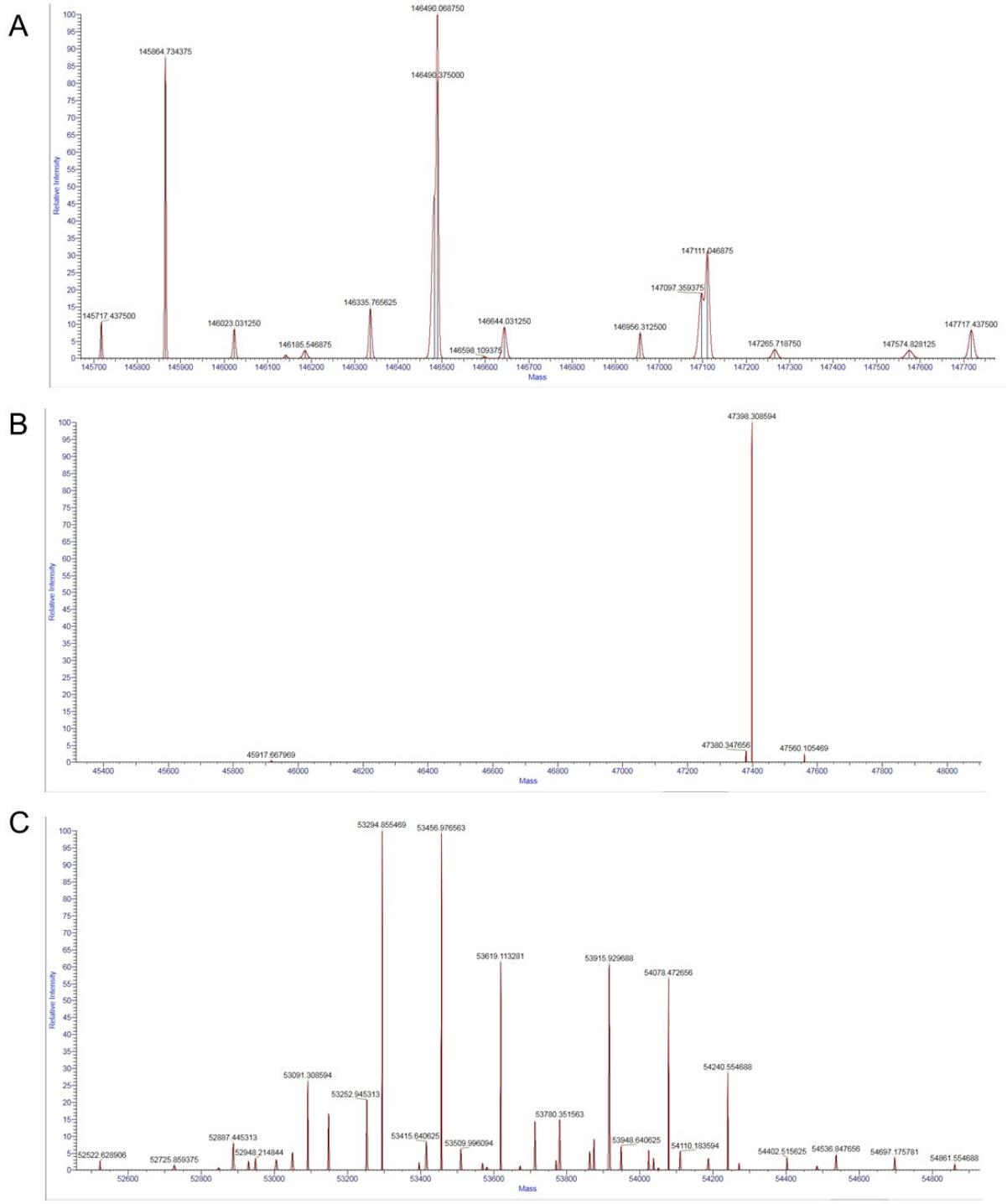

Figure S50. Deconvolved intact mass spectra of trastuzumab-Tz (after the reaction of Fc-III-L6Orn-Tz with trastuzumab).
Deglycosylated intact antibody conjugate (A); antibody conjugate cleaved into Fab (B) and Fc (C) with GingisKHAN enzyme.

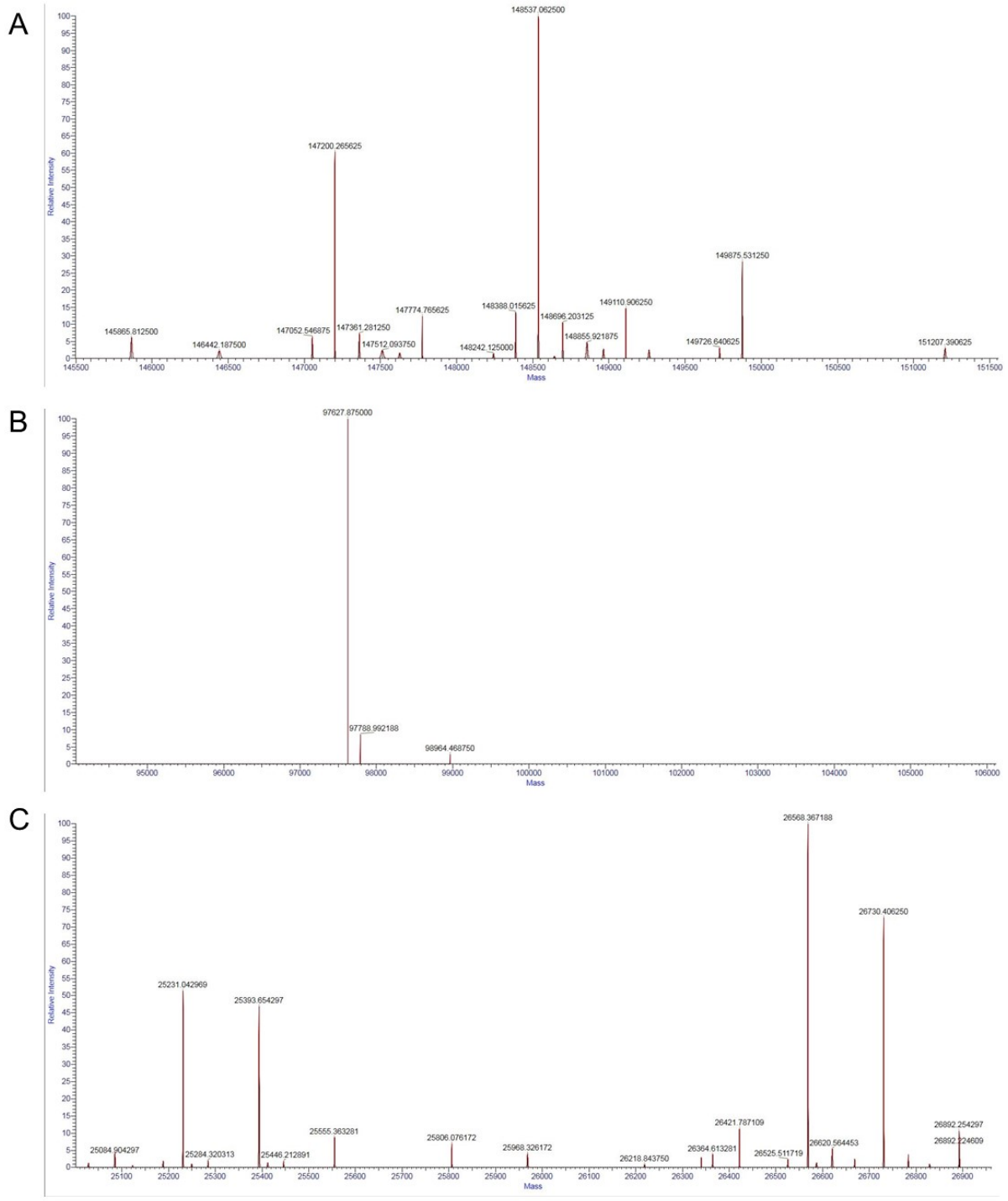

Figure S51. Deconvolved mass spectra of trastuzumab-DOTA (after the reaction of Fc-III-L6Orn-VC-PAB-MMAE with trastuzumab).
Deglycosylated intact antibody conjugate (A); antibody conjugate cleaved into Fab (B) and Fc (C) with FabRICATOR enzyme.

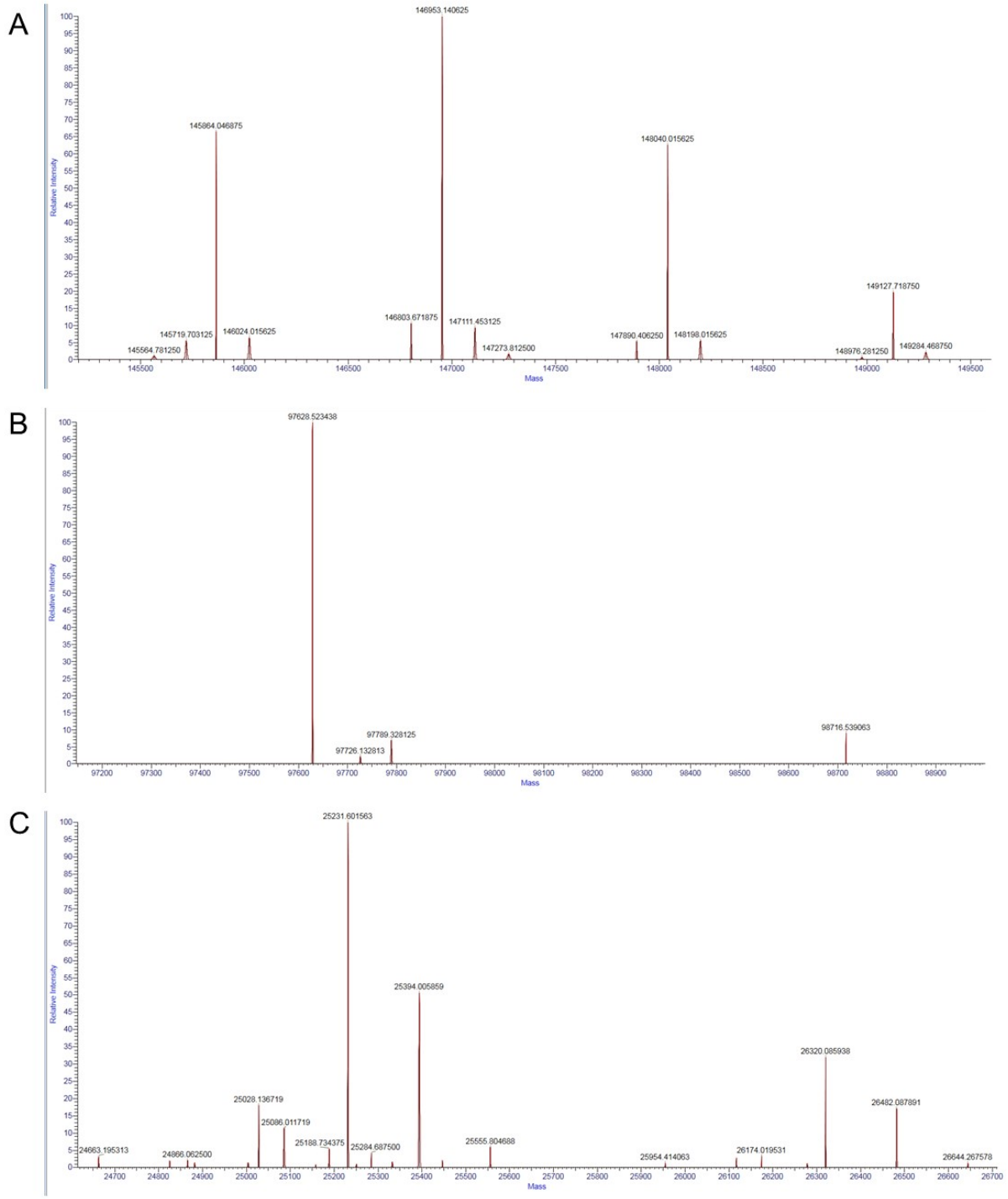

Figure S52. Deconvolved mass spectra of trastuzumab-DOTA (after the reaction of Fc-III-L6Orn-DM1 with trastuzumab).
Deglycosylated intact antibody conjugate (A); antibody conjugate cleaved into Fab (B) and Fc (C) with FabRICATOR enzyme.

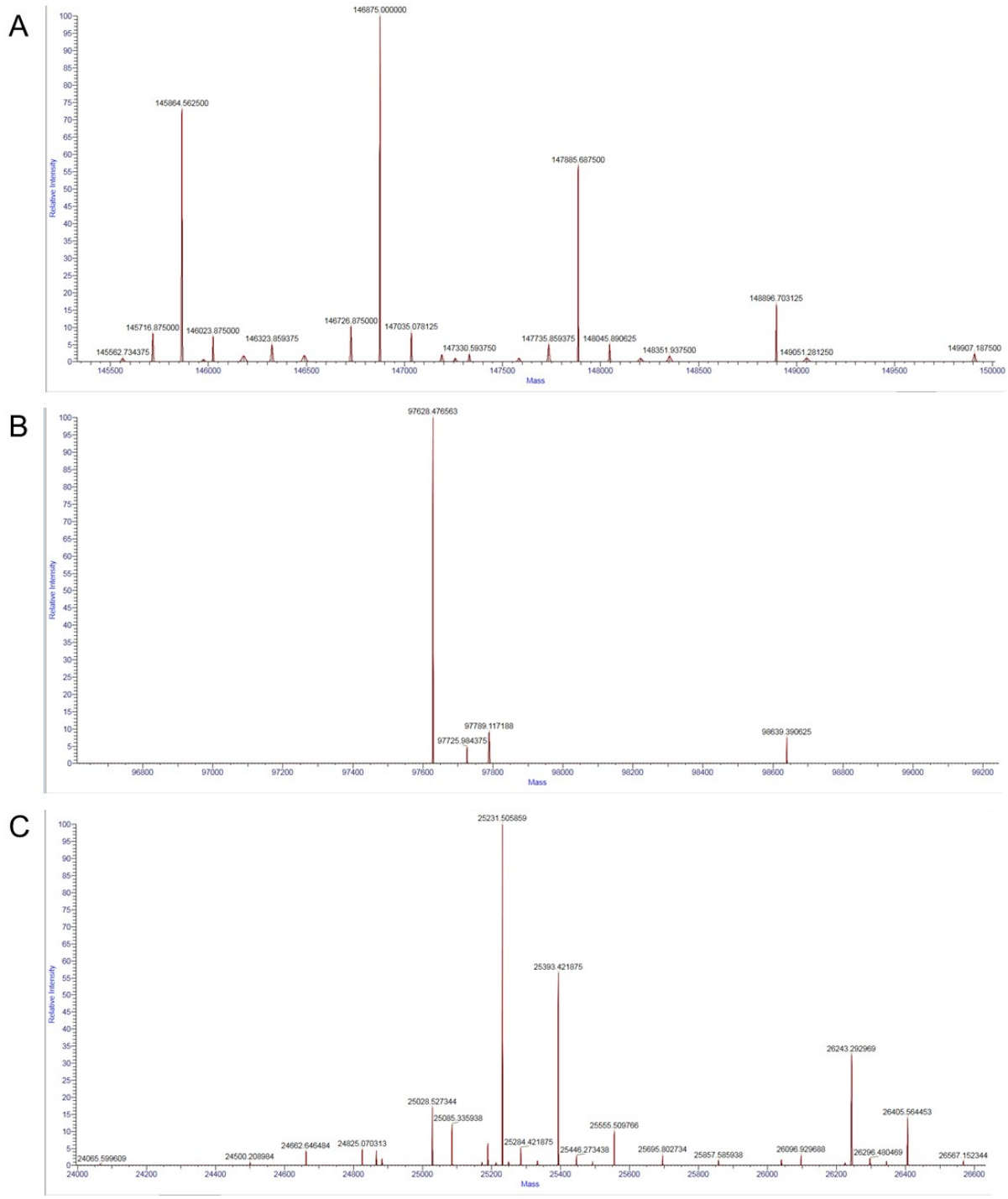

Figure S53. Deconvolved intact mass spectra of trastuzumab-DOTA (after the reaction of Fc-III-L6Orn-DM4 with trastuzumab).
Deglycosylated intact antibody conjugate (A); antibody conjugate cleaved into Fab (B) and Fc (C) with FabRICATOR enzyme.

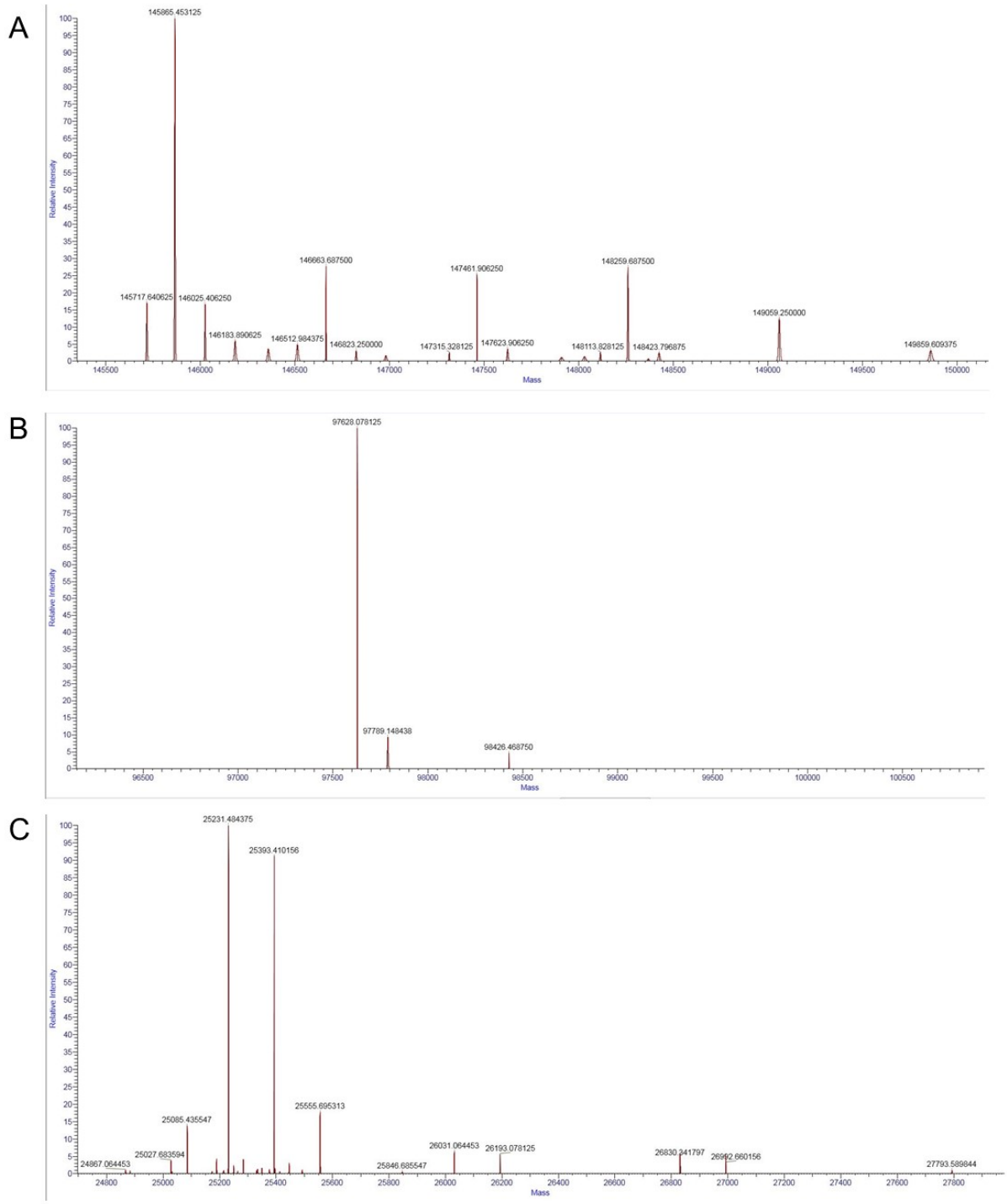

Figure S54. Deconvolved intact mass spectra of trastuzumab-DOTA (after the reaction of Fc-III-L6Orn-PNU with trastuzumab).
Deglycosylated intact antibody conjugate (A); antibody conjugate cleaved into Fab (B) and Fc (C) with FabRICATOR enzyme.

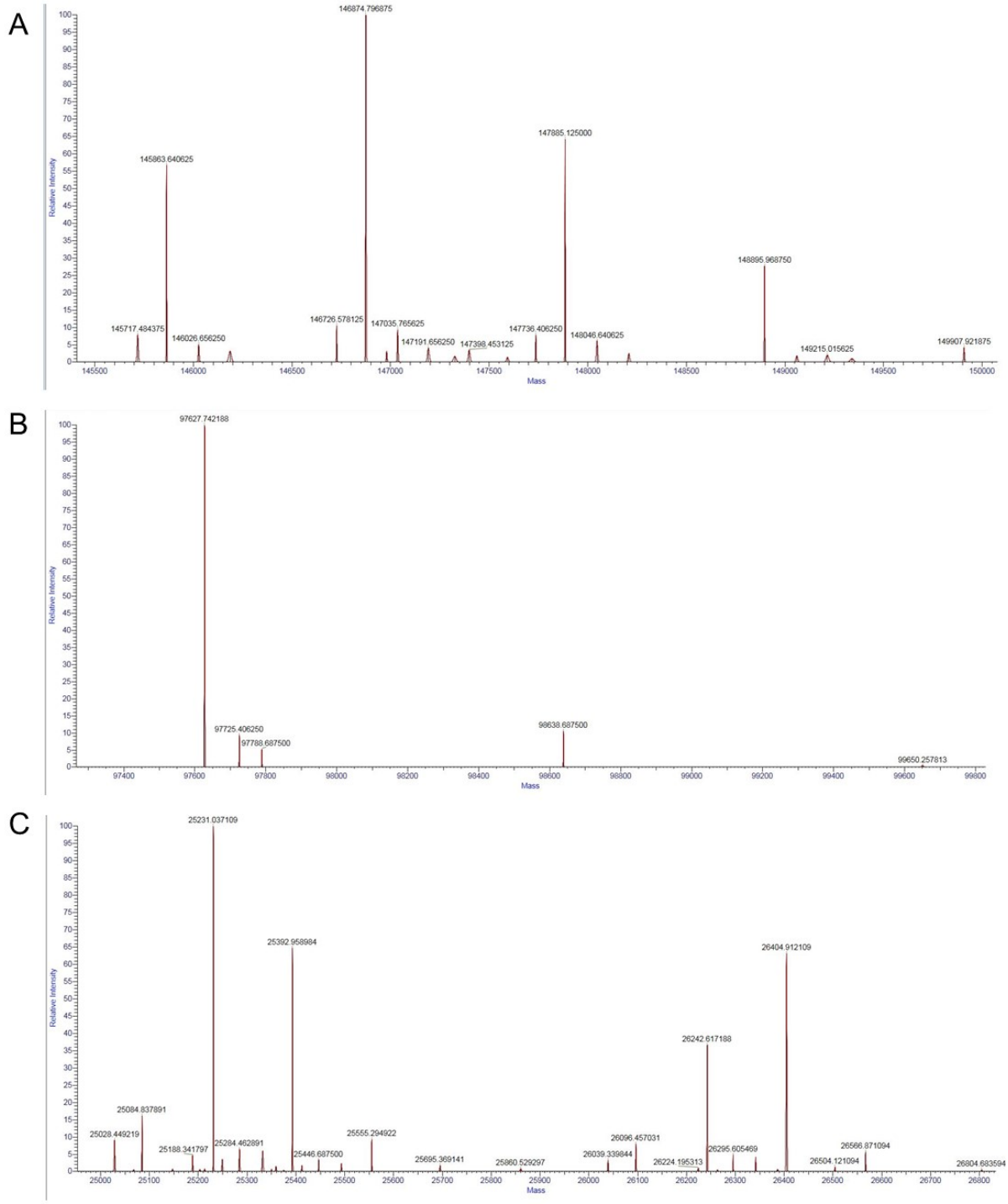

Figure S55. Deconvolved intact mass spectra of trastuzumab-DOTA (after the reaction of PEG20-Fc-III-L6Orn-DM4 with trastuzumab).
Deglycosylated intact antibody conjugate (A); antibody conjugate cleaved into Fab (B) and Fc (C) with FabRICATOR enzyme.

Figure S56. Middle-down fragmentation maps of the IgG-Fc/2 subunit after labeling with Fc-III-L6Orn-DOTA.
The main conjugation sites were identified: for one DOTA molecule being K12 (A) and for two DOTA molecules being K12 and K38 (B). Obtained sequence coverage for Fc/2-DOTA(s) subunits was 32% (A) and 30% (B), respectively. The payload conjugation site K (addition of 517.2384 Da) and glycans attachment site N (presence of 1444.5339 Da, G0F) are highlighted in yellow, identified b- and y-fragment ions – in blue. The DOTA labeling at position K12, and K38 within Fc/2 correspond to K248 and K276 in an intact Hc, respectively.

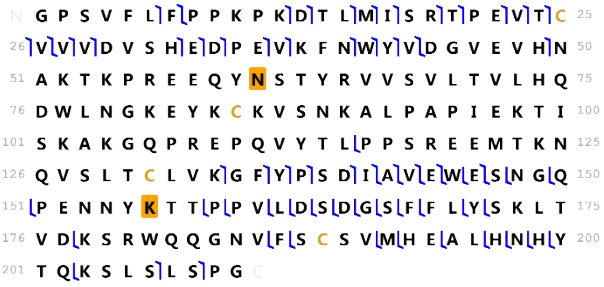

Figure S57. Middle-down fragmentation map of the IgG-Fc/2 subunit after labeling with Fc-III-L6K-DOTA.
K156 was identified as a main conjugation site. Obtained sequence coverage for Fc/2-DOTA subunit was 32%. The payload conjugation site K (addition of 517.2384 Da) and glycans attachment site N (presence of 1444.5339 Da, G0F) are highlighted in yellow, identified b- and y-fragment ions – in blue. The DOTA labeling at position K156 within Fc/2 correspond to K392 in an intact Hc.

Figure S58. Middle-down fragmentation maps of the IgG-Fc/2 subunit after labeling with Fc-III-L6Y-DOTA.
The main conjugation sites were identified: K10 (A) and K12 (B) for one DOTA and for two DOTA molecules being K12 and K38 (C). Obtained sequence coverage for Fc/2-DOTA(s) subunits was 32% (A), 32% (B) and 28% (C) respectively. The payload conjugation site K (addition of 517.2384 Da) and glycans attachment site N (presence of 1444.5339 Da, G0F) are highlighted in yellow, identified b- and y-fragment ions – in blue. The DOTA labeling at position K10, K12, and K38 within Fc/2 correspond to K246, K248 and K276 in an intact Hc, respectively.

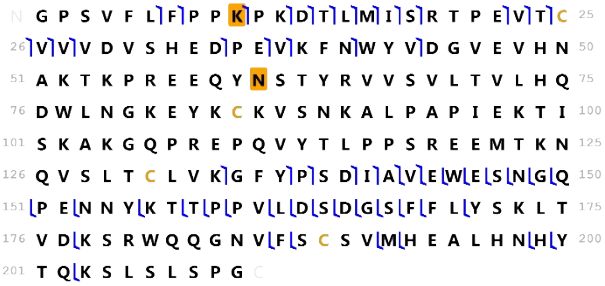

Figure S59. Middle-down fragmentation map of the IgG-Fc/2 subunit after labeling with Fc-III-E8Orn-DOTA.
K10 was identified as a main conjugation site. Obtained sequence coverage for Fc/2-DOTA subunit was 27%. The payload conjugation site K (addition of 517.2384 Da) and glycans attachment site N (presence of 1444.5339 Da, G0F) are highlighted in yellow, identified b- and y-fragment ions – in blue. The DOTA labeling at position K10 within Fc/2 correspond to K246 in an intact Hc.

Figure S60. Middle-down fragmentation maps of the IgG-Fc/2 subunit after labeling with Fc-III-A3K-DOTA.
The main conjugation sites were identified: K156 (A), K173 or K178 (B, as both are in the same fragment), and K203 (C). Obtained sequence coverage for Fc/2-DOTA(s) subunits was 24% (A), 23% (B) and 21% (C) respectively. The payload conjugation site K (addition of 517.2384 Da) and glycans attachment site N (presence of 1444.5339 Da, G0F) are highlighted in yellow, identified b- and y-fragment ions – in blue. The DOTA labeling at position K156, K173, K178, and K203 within Fc/2 correspond to K392, K409, K414 and K439 in an intact Hc, respectively.

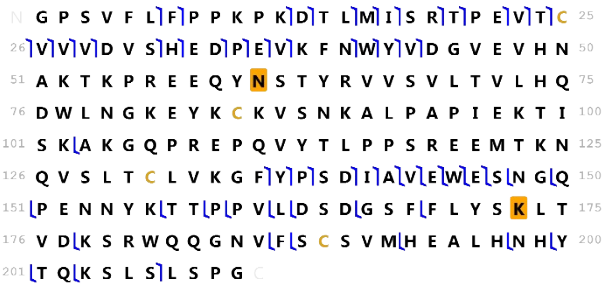

Figure S61. Middle-down fragmentation map of the IgG-Fc/2 subunit after labeling with Fc-III-A3hK-DOTA.
K173 was identified as a main conjugation site. Obtained sequence coverage for Fc/2-DOTA subunit was 28%. The payload conjugation site K (addition of 517.2384 Da) and glycans attachment site N (presence of 1444.5339 Da, G0F) are highlighted in yellow, identified b- and y-fragment ions – in blue. The DOTA labeling at position K173 within Fc/2 correspond to K409 in an intact Hc.

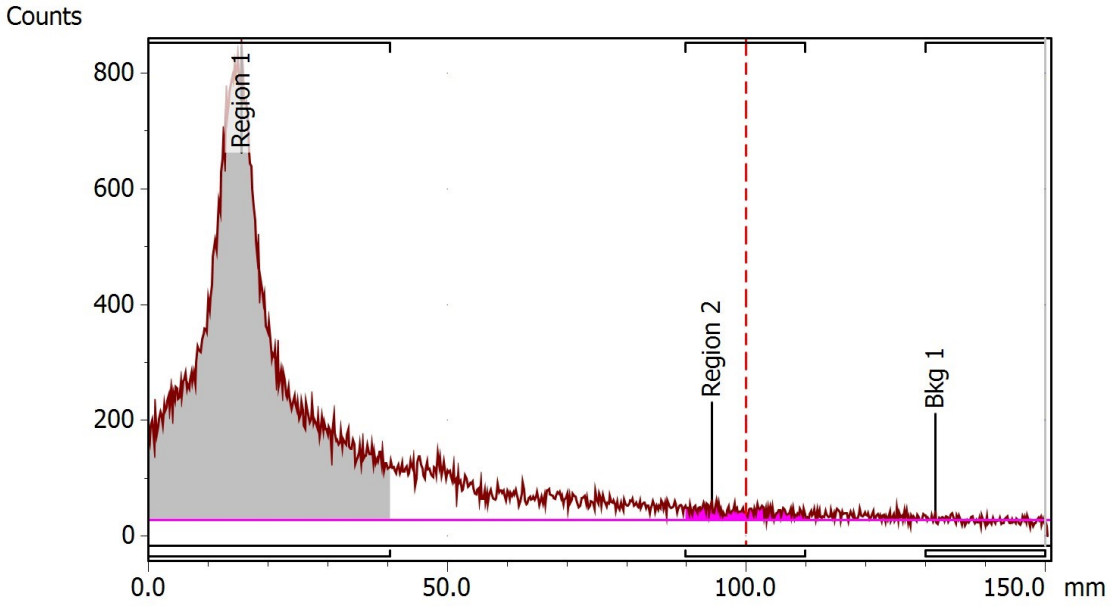

Figure S62. Example of an iTLC radio-chromatogram showing the radio-chemical purity of [^{64}Cu]Cu-NODAGA-atezolizumab after radiolabeling. Radiochemical purity was ≥ 95%. [^{64}Cu]Cu-NODAGA-AbYlink-atezolizumab remains at Rf = 0, and the unbound ^{64}Cu-EDTA migrates to the solvent front.

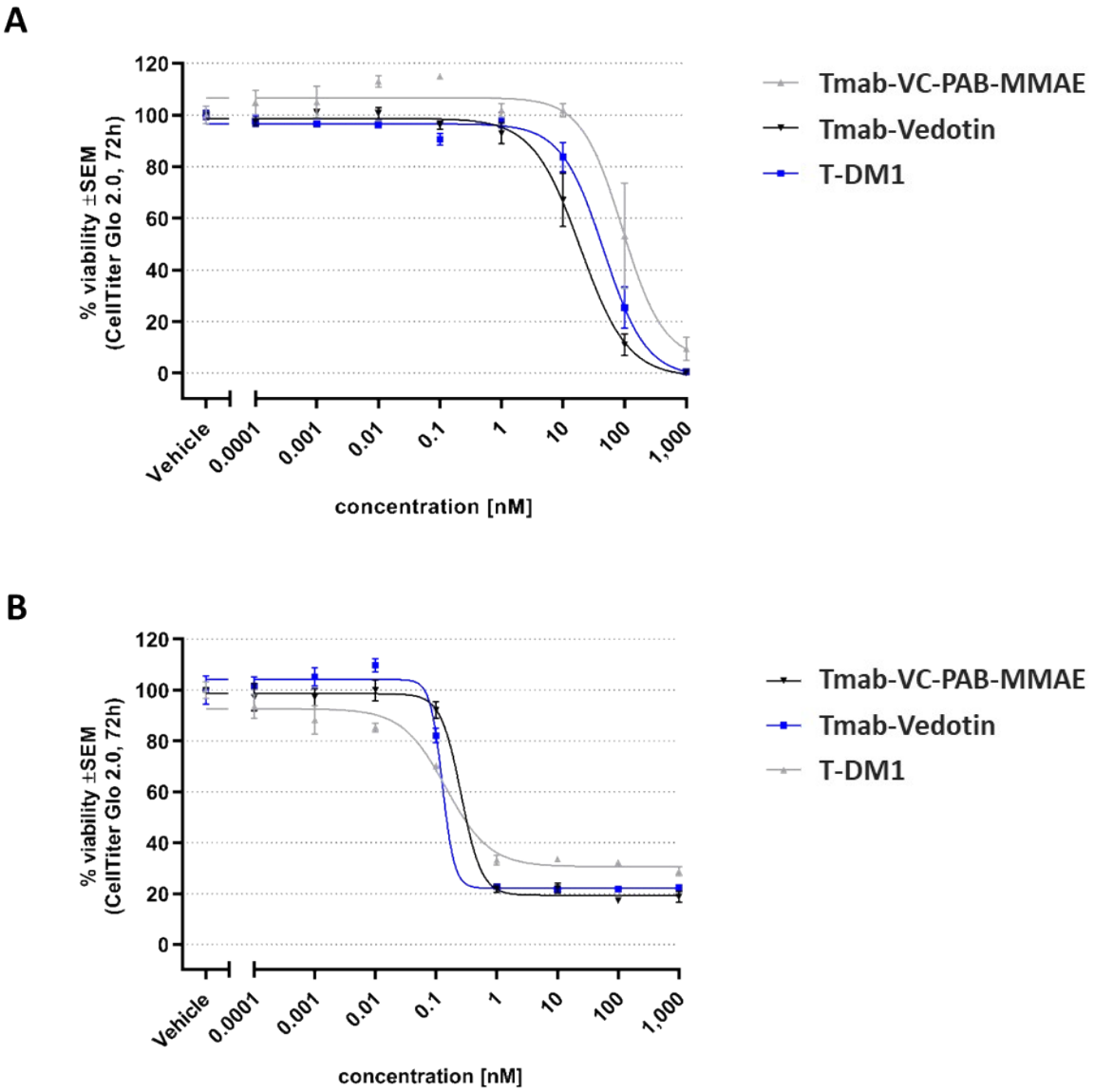

Figure S63. In vitro cytotoxicity studies of ADCs. Cytotoxicity assay results are shown as plots of relative cell viability *versus* Tmab-VC-PAB-MMAE (site-specific conjugation, DAR = 1.91), Tmab-Vedotin (conjugation *via* cysteine, DAR = 3.28) and T-DM1 (purchased from Roche); A) ADCs dose response curve in SK-BR-3 (HER-2 positive) cells after 72h of treatment; B) ADCs dose response curve in MDA-MB-231 (HER-2 negative) cancer cells after 72 h of treatment. GraphPad Prism software was used for calculation of the best-fit curves and for plotting data. The data points on each plot are generated from three replicates and are represented as mean ± standard error of the mean. The calculated IC_{50} are 0.258, 0.126 and 0.145 μM in SK-BR-3 cells and 19.13, 45.79 and 92.48 μM in in MDA-MD-231 cells for Tmab-VC-PAB-MMAE, Tmab-Vedotin and T-DM1, respectively.

[1] V. Postupalenko, L. Marx, D. Viertl, N. Gsponer, N. Gasilova, T. Denoel, N. Schaefer, J. O. Prior, G. Hagens, F. Levy, P. Garrouste, J. M. Segura, O. Nyanguile, *Chem Sci* **2022**, *13*, 3965-3976.